Summer 6-30-2012

Proceeding of International Conference on Electrical Engineering and Computer Science ICEECS 2012

Prof. Dr. Srikanta Patnaik

Editorial

Electrical engineering is a field of engineering that generally deals with the study and application of electricity, electronics and electromagnetism. The field first became an identifiable occupation in the late nineteenth century after commercialization of the electric telegraph and electrical power supply. It now covers a range of subtopics including power, electronics, control systems, signal processing and telecommunications. Electrical engineering is the study of electrical systems and their construction. Graduates of this discipline design and build systems for communications, information processing, entertainment, medical diagnosis, robotics control, navigation, and traffic control, to name a few. Cell phones, personal digital assistants, fax machines, cable and satellite television, and computers are items which are becoming essential to modern living, but would not be possible without the imagination and technical expertise of electrical engineers. Future products and systems, which will enhance our lives, will continue to require talented young people trained in electrical engineering and Computer science.

The challenges of integrating high penetrations of renewable energy technologies into the gridare less well recognized in part because they require interdisciplinary research in such areas aspower systems analysis, communications, power electronics, economics, operations research, and industrial organization. The challenges result from needed changes to achieve national and state objectives for a low carbon energy system.

Let me highlight the recent research onComputer Science & Electrical Engineering. Cloud computing is a model for enabling convenient, on-demand network access to a shared pool of configurable computing resources (e.g., networks, servers, storage, applications, and services) that can be rapidly provisioned and released with minimal management effort or service provider interaction. Cloud computing provides computation, software, data access, and storage services that do not require end-user knowledge of the physical location and configuration of the system that delivers the services. Parallels to this concept can be drawn with the electricity grid, where end-users consume power without needing to understand the component devices or infrastructure required to provide the service. Cloud computing describes a new supplement, consumption, and delivery model for IT services based on Internet protocols, and it typically involves provisioning of dynamically scalable and often virtualized resources It is a byproduct and consequence of the ease-of-access to remote computing sites provided by the Internet. This frequently takes the form of web-based tools or applications that users can access and use through a web browser as if they were programs installed locally on their own computers. Typical cloud computing providers deliver common business applications online that are accessed from another Web service or software like a Web browser, while the software and data are stored on servers. Most cloud computing infrastructures consist of services delivered through common centers and built-on servers. Clouds often appear as single points of access for consumers' computing needs. Commercial offerings are generally expected to meet quality of service (QoS) requirements of customers, and typically include service level agreements (SLAs).

The conference designed to stimulate the young minds including Research Scholars, Academicians, and Practitioners to contribute their ideas, thoughts and nobility in these disciplines of engineering. It's my pleasure to welcome all the participants, delegates and organizer to this international conference on behalf of IOAJ family members. We received a great response from all parts of country and abroad for the presentation and publication in the proceeding of the conference. I sincerely thank all the authors for their invaluable contribution to this conference. I am indebted towards the reviewers and Board of Editors for their generous gifts of time, energy and effort.

Editor-in-Chief
Dr. SrikantaPatnaik
Chairman, I.I.M.T., Bhubaneswar
Intersceince Campus,
At/Po.: Kantabada, Via-Janla, Dist-Khurda
Bhubaneswar, Pin:752054. Orissa, INDIA.

A Brief Survey on Electronic Leadership Styles Using *e*-360^o Assessment and ICT based Social Network Mining

A. Vijaya Kathiravan[1] & V. Suriya Kumari[2]

[1]Dept of ComputerApplications, Salem Govt. Arts and Science College, Salem, TN, INDIA,
[2]Periyar University, Salem, Tamilnadu, INDIA

Abstract - Organizational leadership is one of the most talked about issues in business and organizations. Human resources departments focus on the total development of human resources in organization and converges their leadership attributes relative to organizational needs. A recent study ranked the top ten issues of highest concern for human resource departments. Organizational leadership was listed as the second highest concern. Although finding and retaining the next tier of qualified leaders is a critical key to organizational success, the efforts are futile if the development of these leaders is ignored and they are inadequately prepared for their new roles. Increasing Information communication technologies (ICT) has "shrunk" the world substantially. With the advent of ICT today, organizational leadership in virtual organizations is seen as source of "competitive advantage" in a highly competitive environment such as MNCs. Complex work arrangements involving managers in one location, while their employees are dispersed around the globe as virtual teams is becoming commonplace in multiple industries especially in MNCs. Today's managers must deal with continued, rapid changes in an organizational context. Managers must count on and listen more to their employees atleast through mobile and e-mail communication in networked organizations. Consequently, new forms of organizations are becoming more common, e.g., worker-centered teams, virtual, networked, self-organizing, and self-designing teams. It is a tough task to run a community of individuals by a leader or manager in such new forms of distributed environment, where authority has to be earned from remote place. Few people do it successfully, because it demands an unusual combination of attributes such as popular powerbase, creativity, knowledge expertise, trust, professional efficiency, communication influence, group cooperation, employee service, performance towards goal, and emotional intelligence, etc. Living with these paradoxes requires great strength of character. The concept of electronic leadership assessment in virtual teams is relevant to any aspect of ensuring effectiveness in distributed-networked organizations using internet or mobile like any ICT device. This inter-disciplinary research insinuates Domain Driven Data Mining (D3M) Approach to extract leadership styles of managers in a virtual organization by studying the impact of ICT based social network mining in enhancing the traditional 360^o Leadership Assessment to be more effective.

Keywords: *Organizational leadership, Information and Communication Technologies (ICT), Social Network Mining (SNM), virtual team, Centrality, Network Role, Domain Driven Data Mining (D3M), Support Vector Machine (SVM), Leadership styles, Emotional Intelligence, Transformational leadership.*

I. INTRODUCTION

Within the next few years, many companies will face a critical shortage of senior leadership based on three issues: (a) baby boomers retiring, (b) lack of available talent, (c) difficulty in recruiting and retaining outside talent (Caudron, 1999; Grensing-Pophal, 2000). Research indicates that 66% of senior managers hired from the outside fail within the first 18 months (Callahan, 2002). Many of us have known poor leaders, who promote their own image by taking credit for work done by others, who are selfish, inconsiderate, tyrannical with followers, or who are unfair, dishonest, and threatened by competence in other people. These factors decrease our quality of life by lowering job satisfaction and commitment to organizations, while creating high levels of conflict and stress. One recent survey indicated that over 75% of employees are unhappy with their jobs. The primary reason given was that they were treated poorly by their boss. Virtual teams are an integral part of every organization and it present new challenges to identify business leaders. In fact, most teams today are a mix of indirect virtual interaction teams (mobile and e-mail) and direct Face-To-Face (FTF) interaction teams. Even co-located teams will communicate by email, mobile and phone a certain percentage of the time. Increasing diversity of workers has also brought in a wide array of differing values, perspectives and expectations among workers. Through ICT based communication technologies, the leader communicate among employees, provide follow-up comments to followers, solve crisis, make decisions, evaluate performance, inspire, develop employees, and enable the employees to identify with the organization. Organizations believe in face-to-face interaction alone for assessing organizational leadership using 360^o assessment as a tool. In this research, not only face-to-face interaction alone, but also mobile and e-mail interactions too for leadership evaluation yielding better results. Careful studies in organizations show that executive leadership can account for 45% of an organization's performance. Hundreds of studies show that Effective leadership makes difference in follower's satisfaction and performance. Leadership affects job stress and organizational change. Leadership is needed not only at the top of organizations, but at all levels. The need for good leadership is clearly ubiquitous, because it affects every aspect of employee's lives. In this research, a conventional method followed by ICT based social network monitoring is widely used as a tool for leadership development.

2.0 A BRIEF SURVEY ON LEADERSHIP

There are three popular theories for leadership: 1. Trait theory; 2. Behavioural Theory and 3. Contingency Theory. Traint theory says "Leaders are born, not made". According to Behavioural theory, "Leaders can be trained/made". The latest Contingency theory states "Leadership is situational". This research is based on contingency theory, as our main aim is virtual leadership that exists in MNCs. Leadership is a process used by an individual to influence group members toward the achievement of group goals in which the group members view the influence as legitimate (Yukl, 2002). There are extensive literature studies on measuring leadership skills and identifying leadership behavior patterns (Bass, 1990). Some of the more popular leadership methods are; MBTI - Myers-Briggs Type Indicator, LTQ – Leadership Trait Questionnaire, BARS – Behaviourally Anchored Rating Scales, LMX – Leader-Member Exchange Questionnaire, OPQ – Occupational Personality Questionnaire, FIRO - Fundamental Interpersonal Relation Orientation, and TDI – Type Differentiator Indicator. 360^o assessment using Fundamental Interpersonal Relations Orientation's (FIRO) leadership styles (Will Schutz, 1958) and Emotional Intelligence (Daniel Goleman, 2001) is surveyed in this research. A common organizational assumption is that 360º assessment should automatically lead to improved performance (London and Smither, 1995). An estimated 25% of all organizations use some type of 360º assessment for organizational leadership, and 90% of all organizations use 360º assessment as a part of performance management system (Nowack, 2005). The relationship between 360º assessment and behavior change is more complex and likely be influenced by other factors (Atwater, Waldman, and Brett, 2002). Additional research is needed to examine how different 360^o feedback approaches might influence participant, rater reactions and consequences (Waldman and Atwater, 2003). The only other study (Atwater et al., 2004) suggested that individuals prefer numeric scores and normative feedback and will be less angry, discouraged, more motivated and inspired if they receive numbers and comparative information regarding their leadership behaviors. In a research examined perceptions and consequences of 360^o feedback in a corporate leadership development program (Kenneth M. Nowack, 2005), it has been found that 69.6% reported that the results were expected to a high extent and 76.6% reported they were likely to make a change in their management behavior on job. Approximately 68% of raters reported that the 360^o feedback process led to increased trust, cooperation and communication between themselves and the recipients (Kenneth M. Nowack, 2005). Leadership can be categorized into nine types based on the interpersonal needs according to FIRO strategy of leadership styles (Will Schutz, 1958) as in Fig.1.

A strategic model of organizational performance includes the competitive position of a firm within an industry and to be competitive. Transactional leadership is based on the concept of exchange between leaders and followers by influence. Transactional leaders are responsible, communicative, and reliable. Visionary leaders are knowledgeable and they work best when the business calls for Flexibility, Rapid change, High professionalism with little supervision, Interdependent experts, Cross-disciplinary ideas, and Innovation. Charismatic leaders are defined as role model leaders, who have profound emotional effect on their followers by admiration, popularity and power base. Empowering leadership has its roots in the Japanese style of management, and the psychological concept of self-efficacy, cooperation, power sharing, and team work. Moral leadership is based on the reality that we cannot violate these natural laws with impunity. Servant leadership is a concept developed by Robert Greenleaf (1985) and is given in his book 'On becoming a Servant-Leader'. Entrepreneurial leadership insists on efficient just-in-time management, which squeezes out savings by delivering components and materials precisely and puts a high premium on planning and teamwork (Peter Drucker, 1992). Innovative leaders are typically passionate, innovative and impulsive. Each of these leadership styles has a dominant unique attitudinal parameter of its own. Emotional Intelligence is one of the newer measures that are of particular interest to leadership in organizations. The ability to manage one's emotions and to manage one's interactions with others is tantamount to effective managerial leadership (Ashkanasy 2000; Morand 2001; Michel 2004; Nardi 2002). The theory of transformational leadership has received considerable empirical support as ratings of this leadership predict both subordinate attitudes and measures of leadership effectiveness (Smith 2004). Hence this research set to address emotional intelligence also as a parameter for identifying transformational leadership using 360° assessment.

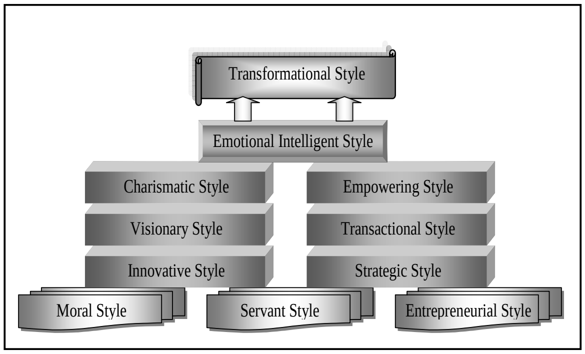

Fig 1. FIRO Leadership styles & Emotional Intelligence

Receiving 360° feedback alone, in and of itself, in MNCs does not provide sufficient support for leadership development, unless there is a communication based follow-up activity daily to support employees from remote place. Virtual managers in networked organizations strongly relied on ICT devices (such as e-mail or mobile) for communicating their employees regularly even without seeing their face. When they uses 360º feedback as a tool to develop leadership talent, it becomes failed to give accurate results. The longitudinal studies (Smither, London, Flautt, Vargas, and Kucine, 2002) suggested an enhanced 360º assessment as in Fig.2 followed by an automatic ICT based hidden pattern mining method to determine leadership effectively.

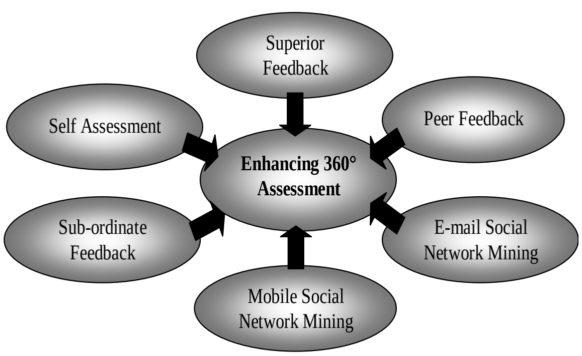

Fig. 2 Enhanced e-360º Model for Virtual Leadership

There are a number of issues that need to be further studied in the design of current SNM techniques for leadership identification. Centrality is one of the most important and frequently used leadership measurement in SNM (Carrington, 2005, Hanneman, 2005). It is a descriptive characteristic for actors or groups of actors with various structural properties and a crucial parameter for understanding and analyzing actor roles in social networks (Newman, 2005). Centrality measurement is measured mainly based on three aspects, degree, closeness, and between-ness. Degree centrality is defined as the number of ties, which are incident with a given node (Bargatti, 2005). This measurement usually reflects the popularity and relational activity of an actor (Marsden, 2002; Frank, 2002; Newman, 2005). Closeness centrality measures geodesic distances, which indicates the actor's availability, safety, and security (Frank, 2002). Between-ness centrality defines the shortest paths that represents the actor's capability to influence or control interaction between actors it links (Marsden, 2002; Frank, 2002; Newman, 2005). Ego-between-ness centrality has been verified to have high correlation with the original between-ness centrality and can be used as a good approximation for direct neighborhood relationships (Marsden, 2002; Newman, 2005; Hanneman, 2005; Marsden, 2002). Rizova (2006) distinguishes the technical-advice and organizational-advice networks as equally important. Clusters of close-by nodes reveal distinct roles within the social network (Borgatti, 2002; Gower, 1971; Hanneman and Riddle, 2005). Burt (2004) uses network constraint to measure bridging and provides substantial evidence correlating this measure to job performance. The literature on self-organizing online communities (Cheshire, 2007) are intrigued as a possible valuable addition to the dialogue on the network paradigm and collective Intelligence for social change. Nathan Eagle studied mobile communications among employees to compare organizational chart and social network graph (Nathan 2008).

3.0 ENHANCING 360º LEADERSHIP ASSESSMENT

360º assessment is a tool that provides managers with feedback in 360º angle survey about their individual's skills, performance, leadership behaviors and attributes from their supervisors, peers, subordinates, self and customers. In MNC like large scale companies, Leaders need effective and efficient ways to connect with one another to share information, get support, mobilize resources, learn, and align their visions in a strategic direction. Often mobile and e-mail communication networks form to make it easier for leaders to connect. Mobile and e-mail communication bring together diverse participants, who normally would not interact: for example, professionals, who work in different fields or sectors; or business and civic leaders in a community. In mobile and e-mail communication, they have an opportunity to get to know each other, share their experiences and perspectives, and form bonds that may endure over time. All the above reasons motivates to propose an integrated approach for understanding different types of social networks using mobile and e-mail communication for enhancing the current 360º leadership assessment method, and consider how Domain Driven Data Mining (D3M) Approach using support vector machine has been used as a tool for evaluating virtual organizational leadership. Hence the proposed e-360º model exploits ICT based social network mining and Domain Driven Data Mining (D3M) Approach as an additional support for escavating virtual leadership behavior, emotional intelligence, and leadership styles. In Fig.3, e-360˚ model assesses elctronic leadership from feedback patterns of superiors, peers, subordinates, self and customer objectively and social network patterns of mobile and e-mail communications subjectively.

Fig.3 e-360º Leadership Assessment model

By incorporating this e-360º model, virtual organizations can: (a) assess virtual talent pool in terms of social network behaviour i.e., network roles and centralities (b) determine leadership gaps, improvements, follow-up activities and negative effect behaviors periodically, (c) eliminate human bias problems such as leniency, under rating, over rating, etc,. and (d) measure transformational leadership using Electronic Leadership styles as in Fig.4 effectively aligning with key organizational priorities.

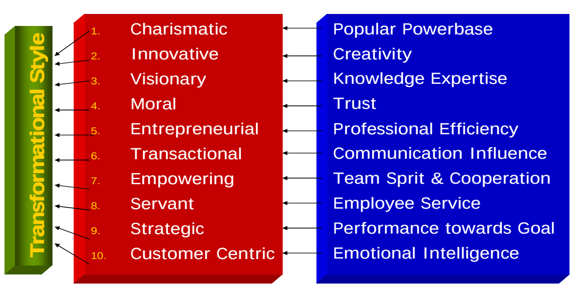

Fig.4 Leadership Styles and Attitudinal Dimensions

4.0 PROPOSED D3M APPROACH

An integrated approach as in Fig.5 using mobile and e-mail communication based social network mining and SVM based Domain Driven Data Mining (D3M) Approach is rooted in this research for identifying data, domain, human, network, social and ubiquitous intelligence. The inputs of the system are e-mail logs and mobile CDR files, pre-installed with several pieces of code that record and send the research data on servers, Bluetooth devices in proximity, cell tower IDs, application usage, and phone status.

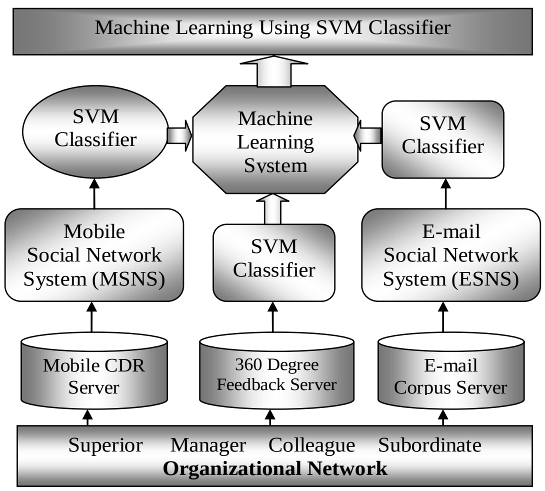

Fig. 5 Proposed D3M Approach

From the server details, the communication adjacency matrix for all the employees has been prepared in the form of excel sheet with the help of a program. The development tasks of the e-360º leadership assessment system is described as given below in Fig.6.

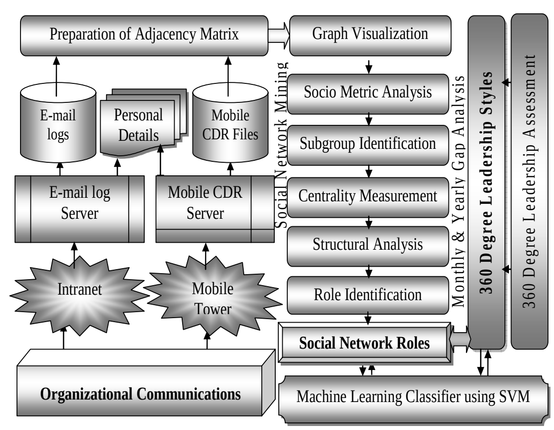

Fig.6 Architecture for e-360° Leadership Assessment

4.1 Development Process

(1) Graph Visualization. Social networks can be visualized either in ego-centered network or whole network. Employee members in different roles are granted with different views. In this research, a visualization tool called UCINet and NetDraw developed by Steve Bargatti of Analytic Technologies has been used for drawing sociogram graphs of social networks. The layout provided in this system hierarchical layout of graphs is used to make "spring" model layouts of graphs.

(3) Socio Metric Analysis. The relation between two team members may be direct or indirect. In this research, only direct relations both in direction and multiplexity have been considered. The higher the interaction in a pair, the stronger the strength in their tie is. Besides individual characteristics, the group itself can be represented by properties such as (a) the size and density of the group, (b) the number and size of the group, (c) the average reachable rate and transitive rate in the group, and (d) the bonding, bridging, connectivity and prestige of the group.

(4) Subgroup identification. Subgroup identification is used to find members with highly connected relations in a group. The method used to find subgroup in this research is Bi-partite graph.

(5) Structural Equivalence. The structural equivalence concept aims to operationalize the notion that actors may have identical or nearly identical positions in a network. It is primarily concerned with the general and abstract idea of the roles or positions that define the structure of the group.

(6) Centrality Measurement. Centrality measurement is measured mainly based on three aspects, degree, closeness, and between-ness. Degree centrality is defined as the number of ties, which are incident with a given node. Closeness centrality measurement is based on geodesic distances i.e., how far away a node is from all other nodes. Between-ness centrality of a vertex v is defined to be the fraction of shortest paths that go through v.

(7) Role Identification. The role a team member acts may demonstrate various degrees of significance in a leader's performance for identifying one's leadership styles.

(8) Social Network Mining. Based upon the size, density, total number of strong and weak ties, reciprocity, centrality, frequency, proximity, group performance, subgroup behavior, cohesion, social capital, structural equivalence, structural hole, and role, a leadership style is identified for the manager using SVM Domain Driven Data Mining (D3M) Approach classifier.

(9) Domain Driven Data Mining (D3M) Approach. This D3M phase consists of three components named as Retriever, Feature Extraction Engine, and Classifier using SVM as in Fig.9. The Retriever loads the resultant attributes from social network mining and placed in the repository. Feature Extraction Engine defines a set of parameters, which are used to distinguish ten various leadership styles based upon the role and centrality of an actor and determines the parameters for each manager individually. Classifier gets the result from Feature Extraction Engine and classifies it by using SVM classifier.

(10) 360º Feedback Assessment and Reassessment. There is a 360º tool designed using Visual Basic and Ms-Access for conducting 360º assessment and reassessment. The feedback given by superior, peer, self, customer and subordinate are collected using the tool and the results are stored in the server. The results are sent to a Domain Driven Data Mining (D3M) Approach classifier to classify leadership styles using support vector machine multiclassifier. Finally the outcomes of 360º assessment and social network mining are cross-verified. If there is a deviation in the results, a reassessment is made immediately to eliminate the human bias. After one year from 360º assessment, a 360º reassessment is made for the managers to conduct gap analysis and to check the improvement in their leadership behavior.

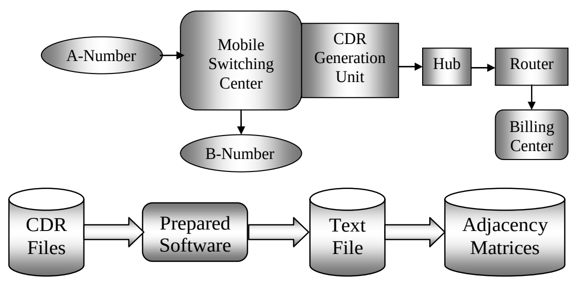

Fig. 7 Architecture of Mobile Social Network System

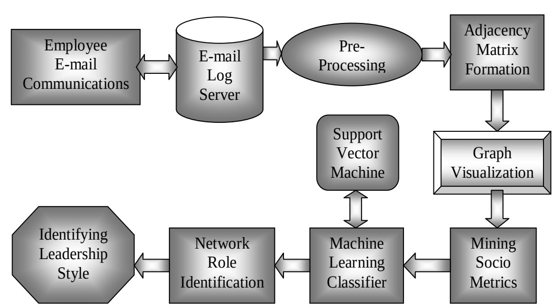

Fig. 8 Architecture of E-mail Social Network System

4.2 Variables Used

There are three categories of variables used in this research as described below in Table.1. They are (1) Attitudinal Dimensions, (2) Social network variables, and (3) Personal or Demographic variables. The Attitudinal dimensions are popular powerbase, creativity, knowledge expertise, trust, professional efficiency, communication influence, group cooperation, employee service, performance towards goal, and emotional intelligence quotient (EQ). The network dimensions are power centrality, between-ness centrality, information centrality, reach centrality, eigenvector centrality, influence centrality, group centrality, closeness-centrality, degree centrality, and contribution centrality. Demographic variables, used for the prediction of manager's performance are related to gender, age, marital status, religion, nativity, language, education, experience, working region, span of control and monthly turnover. Exemplar, Gatekeeper, Visionary, Truth Teller, Fixer, Facilitator, Enforcer, Connector, Director, and Mentor are the network roles corresponding to the ten leadership styles charismatic, innovative, visionary, moral, entrepreneurial, transactional, empowering, servant, strategic, and customer centric leadership styles respectively. The following Fig.9 represents the proposed Domain Driven Data Mining (D3M) Approach architecture using Support Vector Machine (SVM).

.

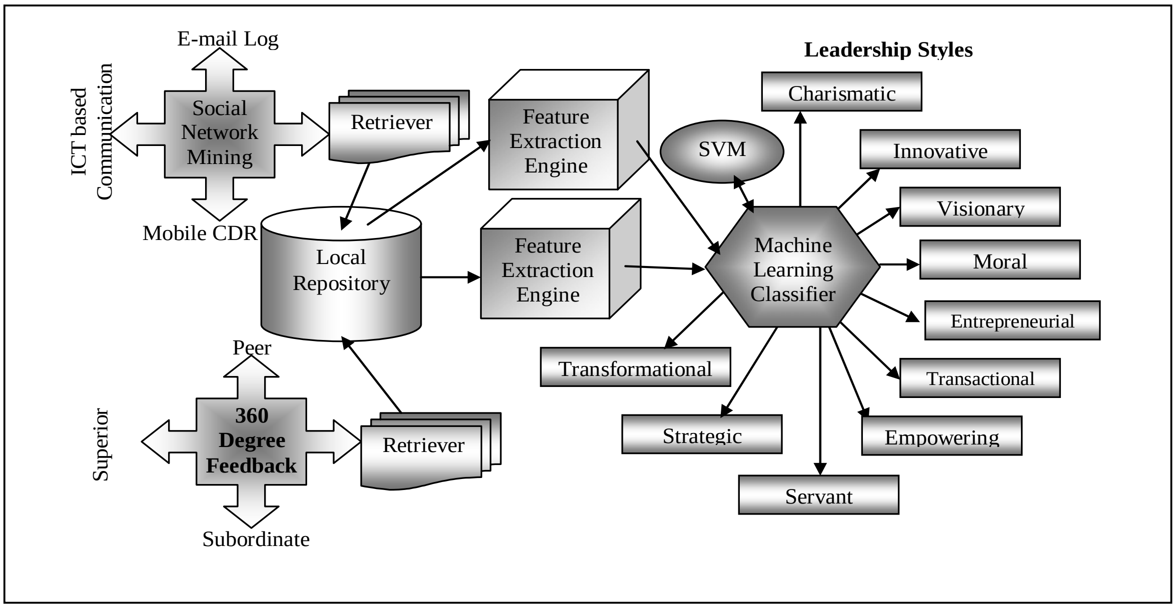

Fig. 9 Domain Driven Data Mining (D3M) Approach Using Support Vector Machine (SVM)

.V. EXPERIMENTAL RESULTS AND DISCUSSION

The experimental study aims to describe the leadership status of managers of various branches in TATA Teleservices Ltd. in all over India and the implementation of ICT based social network mining and Domain Driven Data Mining (D3M) Approach set up to enhance the existing e-360º assessment. Out of 2700 samples in India, this research focuses to conduct 235 managers. This research offers a new approach for assessing the organizational leadership behaviors using 360º assessment, social network mining in mobile Call Detail Record (CDR) files and e-mail logs generated in the company server. The program is developed using Java. ICT based SNM was conducted with a group of managers from different geographies, practices, levels of seniority, and tenure in the company.

Fig.10 Communication Matrix

Consider the following diagram in Fig 10, 11, and 12, which represents Communication Matrix, organizational chart and SNM Graph for Tiruchengode branch.

By looking at who was central in the mobile and e-mail communication networks, the company could see the various leadership styles of branch managers

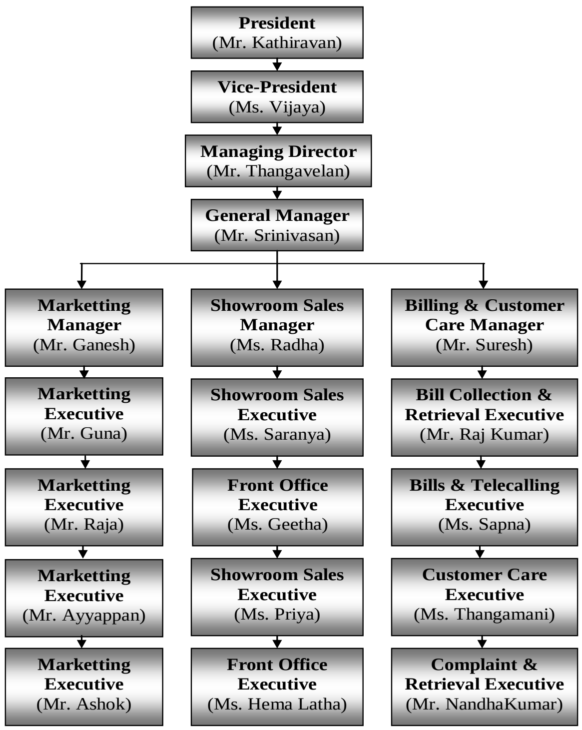

Fig.11 Organizational Chart

By looking at how often managers from each branch interacted with their employees, the SNM revealed that managers who had been with the company the longest tended to get information easier; newer get struggled.

Fig.12 Social Network Graph for SNM

The SNA and additional interviews also revealed that several leaders of the virtual team was not central in the ICT based social network and that they had become removed from many of the day-to-day workings of the group. As a result of the SNA, upper management made significant changes in the branches including formalizing leadership role. Follow-up activities revealed that time pressures using ICT based social network mining left the new managers of the branch with few opportunities to develop their leadership skills. As a result of SNA, upper management initiated a mentor system to help new managers, sponsored events several times a year that brought people together from different parts of the company, and developed an award program for leadership. In terms of employee dynamics, central network positions and links with people outside the work group are associated with power and leadership. For successful recruiting, widespread weak ties are more advantageous than strong ties; for promotions, men benefit most from weak ties and women from strong ties. Centrality, role and tie plays a vital role in identifying virtual leadership. The Table 2, Table 3 and Fig.13 shows the overall scores of the respondents for manager's leadership styles and transformational leadership style, social network roles and it also shows a significant improvement in the no. of positive respondents for all leadership styles during e-360° assessment and reassessment.

Table.2 Impact of 360° Leadership Assessment

Leadership Styles	**Before e-360°**	**After e-360°**
Charismatic	60	72
Innovative	83	89
Visionary	40	57
Moral	147	177
Entrepreneurial	126	145

Transactional	81	94
Empowering	111	133
Servant	178	217
Strategic	53	66
Customer Centric	67	92
Transformational	16	23

Table 6.4 ICT based Social Network Mining Results

Network Roles	1	2	3	4	5	6
Exemplar	60	62	66	69	70	72
Gatekeeper	83	84	86	88	88	89
Visionary	40	44	47	52	55	57
Truth Teller	147	152	153	160	171	177
Fixer	126	126	133	140	142	145
Facilitator	81	83	87	90	92	94
Enforcer	111	116	121	123	129	133
Connector	178	182	184	210	210	217
Director	53	56	59	59	63	66
Mentor	67	69	73	81	88	92

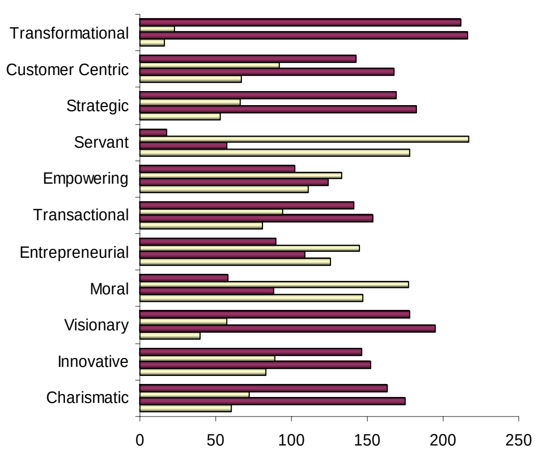

Fig.13 Improvement in the Respondents during e-360° Leadership Assessment

Research shows that network participants perform better at their jobs than "isolates."

6.0 CONCLUSION AND FUTURE DIRECTION

This research on designing a noval approach for identifying leadership behavior using social network mining and Domain Driven Data Mining (D3M) Approach presents a first step towards addressing this problem. What it provides is a look at how one could design a tool to support email and mobile, where social information brings salient employee relationships. Team members' relations are important to the leader's performance. Stronger relational links are associated with higher task performance and the effectiveness of information exchange. Therefore, this research has aimed at fulfilling such objectives as developing an online social network analysis and discovering interaction patterns of teams for organizational leadership in concerns. Generalized from various sources of relation information from teams, such as e-mail and mobile, a team member can realize his or her role within the team. The social network evolution trend thus enables the managers and participants to keep track of the team development status. After implementing the system, most people were satisfied with the system in four evaluation criteria (simplicity, utility, certainty, and novelty). Managers and employees have higher satisfaction than general team members. It implies that the system conforms to the cognition of managers, since managers interact frequently with branch members in leading the bracnch. Moreover, this work has unveiled future design possibilities for email and mobile applications that utilize social accounting meta-data. While it has been informally observed which metrics generate interesting and useful indicators for organizational leadership. Some of the limitations may be further investigated in future research. One research limitation is that this research did not identify the unnecessary communications in e-mail and mobile. It will bring richer information by analyzing the relation using content analysis in future research. Another is that this research only computed users' relations in the same branch. If they join, many teams at the same time, their intersectional relations are not considered. In future, the relation crossing different branches is an additional factor to be investigated.

REFERENCE

[1] Barry Wellman (2004), "The mobile-ized society – communication modes and social networks", Receiver Magazine, Vodafone Group, http://www.chass.utoronto.ca/ ~wellman.

[2] Brass, Daniel (2003), "A Social Network Perspective on Human Resources Management." In Rob Cross, Andrew Parker, and Lisa Sasson (eds), Networks in the Knowledge Economy, Oxford University Press, New York, p. 283-323.

[3] Carman Neustaedter, A.J. Bernheim Brush, Marc A. Smith, and Danyel Fisher (2005), "The Social Network and Relationship Finder: Social Sorting for Email Triage", Microsoft Research, Redmond, WA.

[4] Cross, R., Parker, A., Prusak, L. & Borgatti, (2001), "Knowing What We Know: Supporting Knowledge Creation and Sharing in Social

Networks", Organizational Dynamics 30(2): 100-120.

[5] Cross, Rob and Andrew Parker (2004), "The Hidden Power of Social Networks", Boston: Harvard Business School Publishing.

[6] Fu-ren Lin, Chun-hung Chen (2000), "Developing and Evaluating the Social Network Analysis System for Virtual Teams in Cyber Communities".

[7] John-Paul Hatala (2006), "Social Network Analysis in Human Resource Development: A New Methodology", Human Resource Development Review Vol. 5, No. 1, p. 45-71, DOI: 10.1177/ 1534484305284318, Sage Publications, Louisiana State University.

[8] Kathleen Marvin (2006), "Social Network Analysis -The Hidden Power of Human Networks", BAODN Newsletter, www.marvincoach.com.

[9] Knowledge@Wharton (2006), "Connecting the Corporate Dots: Social Networks Reveal How Employees and Companies Operate", PARS International, P. 212, 221-9595x407, http:// knowledge. wharton. upenn. edu.

[10] Nathan Eagle, Alex (Sandy) Pentland, David Lazer (2006), "Inferring Social Network Structure using Mobile Phone Data", MIT Design Laboratory, Massachusetts Institute of Tech., Cambridge, MA.

[11] Nina D. Ziv and Bala Mulloth (2006), "An Exploration on Mobile Social Networking: Dodgeball as a Case in Point", IEEE Conference Proceedings, MBusiness Conference, Copenhagen, Denmark.

[12] Sung Joo Bae, Peter Gloor and Sebastian Schnorf (2005), "Detection of Power User Patterns Among High School Students in a Mobile Communication Network", MIT, Cambridge, MA.

[13] Tracy Cox (2003), "Creating Business Value Through Social Network Analysis", TrainingOutsourcing. com -TI-Biz Webinar, Raytheon Professional Services' Performance Consulting Group.

[14] Tyler, J. R., Wilkinson, D. M. & Huberman, B. (2003), "EmailNet: A System for Automatically Mining Social Networks from Organizational Email Communication".

[15] Yi-Fan Chen and Katie Lever (2004), "Relationships among mobile phones, social networks, and academic achievement: A comparison of US and Taiwanese college students", The State University, New Jersey.

◈◈◈

Energy Conservation Through Energy Efficient Technologies At Thermal Power Plant

Namdeo D. Adate[1] & R. N. Awale [2]

Dept. of Electrical Engineering, VJTI, Mumbai

Abstract - Energy audit and conservation is the burning issue nowadays due to the tremendous scarcity of electricity across the county. It is specifically quantifies as optimum use of electricity available. Normally it is extended to all the sectors viz, Industrial, commercial, residential as well as agriculture. Energy efficiency is a technique which needs to be adopted seriously and religiously for effective energy conservation. Energy saved by efficient use of energy of any electrically operated device not only leads to monetary saving but is extra energy generated for the use elsewhere. Indian power sector is caught between the pressure of adding new generating capacities to match the rapid growing demand of power to achieve economic and social development and the environmental challenges which is why our per capita power consumption is still 778 KWh only.

Therefore by implementing Energy conservation in thermal power plant we try to recover the losses which go waste. By energy management, one can draw a line between the avoidable and un-avoidable losses and plan to minimize the same. So measurement Energy is a must within a plant. This paper describes basic understanding and awareness about energy conservation around the thermal power plant and also explains the energy saving measures at thermal power plant so as to minimize the auxiliary power consumption.

Keywords *— Energy efficiency, Auxiliary Power Consumption, Thermal Power Plant, Energy Management.*

I. INTRODUCTION

The energy process is an organized approach to identify energy waste in a facility, determining how this waste can be eliminated at a reasonable cost with a suitable time frame. Energy efficiency is widely used and many have different meaning depending on energy service companies. Energy audit of a building can range from a short a walkthrough of the facility to a detailed analysis. It is not only serves to identify energy use among the various services and to identify opportunities for energy conservation but it is also a crucial first step in establishing an energy management program. The efficiency will produce the data on which such a program is based. The study should reveal to the owner, manager, or management team of the building the options available for reducing energy waste, the costs involved, and the benefits achievable from implementing those energy-conserving opportunities (ECOs).

The energy efficiency discusses in this paper is carried out in aim of analyzing and identifying possible energy saving measures, which can be implemented in a factory. This effort will help the plant to reduce their monthly electrical energy consumption thus reducing the cost of production. The total energy survey is conducted by means of onsite inspections, measurements, questions and discussions with the maintenance staff.

This energy analysis contains valuable information such as energy consumption patterns of the factory and the identification of high energy intense equipments, possible energy saving measures and cost benefit analysis of energy saving measures.

II. ENERGY AUDITING PROCEDURE

Energy audit consists with several tasks which can be carried out depending on the type of the audit and the size and the function of the audited facility. Therefore an energy audit is not a linear process and is rather iterative. The efficiency describes in this paper was carried out with in four days time frame based on the following functional activities.

- Building and utility data analysis.
- Walk through survey
- Base line for building energy use.

Feasibility of energy saving measures

III. ENERGY MANAGEMENT CELL

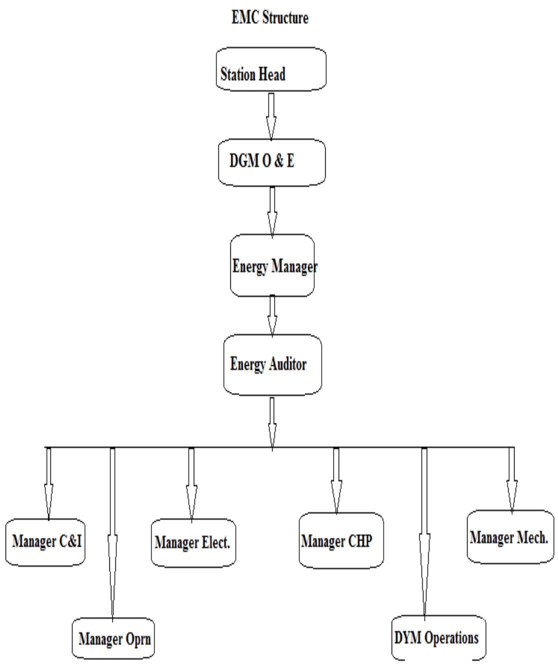

Fig 1 EMC Structure

Objectives of EMC:

- To operate the power plant at highest efficiency and optimum cost
- To create awareness about energy conservation amongst all the stakeholders.
- EMC can achieve objective of "high energy efficiency and at optimum cost" through following steps:
- Regular internal energy efficiency
- Documentation for energy management activity
- Regular energy efficiencies through accredited energy efficiency firms.
- Regular filling of energy returns to state level designated agency
- Energy conservation projects- identification, Evaluation and implementation
- Application of energy conservation techniques in the entire gamut of activities of PTPS including purchase, training, O&M, accounts, safety etc.
- Establishing energy efficiency test procedures and schedules for all equipments and systems.
- EMC can achieve objective of "Awareness Drive" through following initiatives:
- Display of posters and slogans in the plant area
- Celebration of energy conservation week
- Film show

IV. AUXILIARY POWER CONSUMPTION IN THERMAL POWER PLANT

The auxiliary power consumption plays a major role in enriching the energy efficiency of the thermal power plant. As per the norms APC should well within the 10%. Since Thermal power plant is also falls under energy intensive consumer category like railways, metal industries, port trust etc according to Electricity Act features it is paramount importance to analyze the consumption pattern of the plant and work on various areas so as to boost up the efficiency of cycles and sub-cycle.

4.1 Capacity wise APC in thermal power plant as per CEA norms

Capacity Group in MW	Auxiliary Power Consumption In %
500	6.13
250	8.80
210	8.77
195-200	7.67
100-200	10.32
<100	10.31

Table 1 Capacity wise APC in Thermal Power Plant

National Level APC = 8.32 %

Best APC is found at Sipat STPS of NTPC – 5.04 %

4.2 Elements of APC:

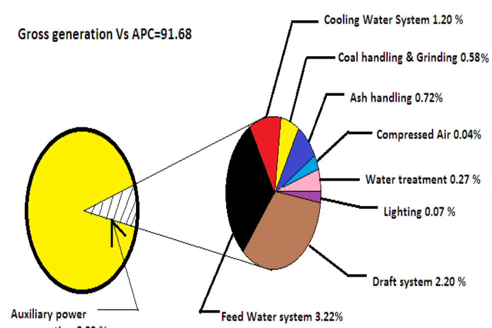

Fig 2 Tipical Breakup of APC in Thermal Power Plant

Keeping in view the typical distribution of auxiliary power in a power plant it may be observed that the total APC may reach up to 12% depending on the condition of the plant. Therefore reduction of even 0.5 to 3 % may result in huge energy saving and gives rise to additional output of few megawatts.

4.3. Factors affecting the APC

- Plant load factor = high
- Operational efficiency of the equipment = Moderate
- Startup and shutdown = low
- Age of the plant = high
- Coal quality = Moderate to high

V. ENERGY SAVING POTENTIAL AREAS

5.1 AIR & FLUE GAS CYCLE:-

a. Optimizing excess air ratio: - It reduces FD fan & ID fan loading.

b. Replacement of oversize FD and PA fan: - Many thermal power plants have oversize fan causing huge difference between design & operating point leads to lower efficiency. Hence fan efficiency can be improved by replacing correct size of fan. If replacement is not possible, Use of HT VFD for PA & ID fan can be the solution.

c. Attending the air & flue gas leakages: - Leakages in air & flue gas path increases fan loading. Use of Thermo vision monitoring can be adopted to identify leakages in flue gas path. Air pre-heater performance is one crucial factor in leakage contribution. If APH leakage exceeds design value then it requires corrective action.

5.2. STEAM, FEED WATER AND CONDENSATE CYCLE:-

a. BFP scoop operation in three element modes instead of DP mode: - In three element mode throttling losses across FRS valve reduces leads to reduction in BFP power.

b. Optimization of level set point in LP & HP heater: - Heater drip level affects TTD & DCA of heater which finally affect feed water O/L temp. Hence it requires setting of drip level set point correctly.

c. Replacement of BFP cartridge: - BFP draws more current If Cartridge is wore out, causing short circuit of feed water Flow inside the pump. It affects pump performance. Hence cartridge replacement is necessary.

d. Attending passing recirculation valve of BFP: - BFP Power consumption Increases due to passing of R/C valve. It requires corrective action.

e. Installation of HT VFD for CEP: - CEP capacity is underutilized and also there is pressure loss occurs across Deareator level control valve. There is large scope of energy saving which can be accomplished by use of HT VFD for CEP or impeller trimming.

5.3. FUEL & ASH CYCLE:-

a. Optimized ball loading in Ball tube mill: - Excessive ball loading increases mill power. Hence ball loading is to be Optimized depending upon coal fineness report.

b. Use of Wash Coal or Blending with A- grade coal: - F-grade coal has high ash content. Overall performance can be improved by using Wash coal or blending of F-grade coal with A- grade coal instead of only using F- grade coal.

c. Avoiding idle running of conveyors & crusher in CHP

d. Use of Dry ash Evacuation instead of WET deashing System: - Dry deashing system consumes less power & also minimizes waste reduction.

e. Optimize mill maintenance:- Mill corrective/preventive maintenance is to be optimized depending parameter like- running hrs, mill fineness, bottom ash unburnt particle, degree of reject pipe chocking etc.

5.4. ELECTRICAL & LIGHTING SYSTEM:-

a. Optimizing Voltage level of distribution transformer: - It is found that Operating voltage level is on higher side than required causing more losses. It is required to reduce the voltage level by tap changing.

b. Use of Auto star/delta/star converter for under loaded motor Lighting: - Use of electronic chock instead of conventional use copper Chock, Use of CFL, White LED, Replacement of mercury vapor lamp by metal Halide lamp. Use of timer for area lighting is the methods can be used. Lighting has tremendous potential of saving.

5.5. ECW & ACW SYSTEM:-

a. Isolating ECW supply of standby auxiliaries: - Many times standby coolers are kept charged from

ECW side. Also Standby equipment's auxiliaries like Lube oil system kept running for reliability. We can isolate Standby cooler from ECW system & switching of standby auxiliaries, doing tradeoff between return & reliability.

b. Improving condenser performance by condenser tube cleaning & use of highly efficient debris filter: - Tube cleaning by bullet shot method increases condenser performance, condenser tube cleaning is necessary which is to be carried out in overhaul. Also highly advanced debris filter contribute condenser performance.

c. Application of special coating on CW pump impeller: - It improves pump impeller profile condition, increasing pump performance.

5.6. COMPRESSED AIR SYSTEM:-

a. Optimizing discharge air pressure by tuning loading/unloading cycle: -It helpful to reduce sp. Power consumption.

b. Use of heat of compression air dryer instead of electrically heated air dryer: - Heat of compression air dryer use heat generated in compression cycle, thus reduces sp. Power consumption.

c. Use of screw compressor instead reciprocating compressor: - Sp. Power consumption of screw compressor is less than reciprocating air compressor leads to reduce aux. power consumption.

5.7. HVAC system

a. Cooling tower performance improvement

b. Installing absorption refrigeration system instead of vapor compression system

c. Use of wind turbo ventilators instead of conventional motor driven exhauster

VI. ENERGY EFFICIENT TECHNOLOGIES AT THERMAL POWER PLANT

6.1 Improving Power Factor using APFC

The solution to improve the power factor is to add power factor correction capacitors Fig. 3 to the plant power distribution system. They act as reactive power generators, and provide the needed reactive power to accomplish kW of work. This reduces the amount of reactive power, and thus total power, generated by the utilities using Automatic Power Factor Controller Fig-4.

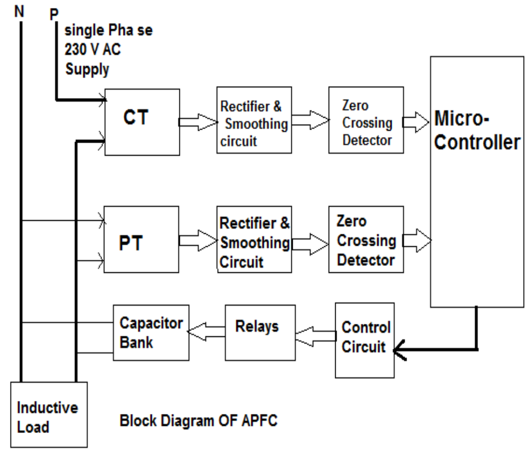

Fig-4 Automatic Power Factor Controller

Example :

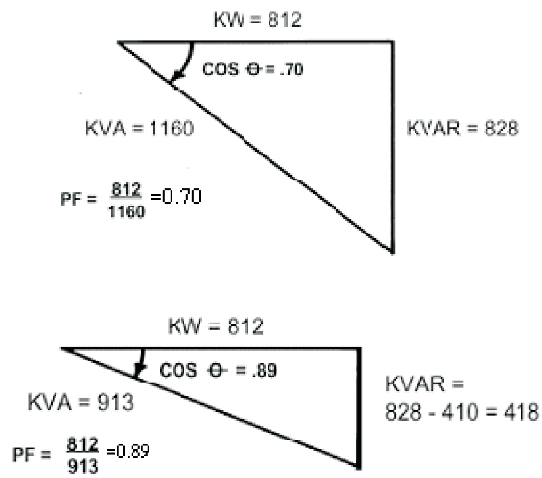

Fig 3 Power factor before and after Improvement

After improvement the plant had avoided penalty and the 1500 kVA transformer now loaded only to 60% of capacity. This will allow the addition of more loads in the future to be supplied by the transformer.

The advantages of PF improvement by capacitor addition

a) Reactive component of the network is reduced and so also the total current in the system from the source end.

b) I2R power losses are reduced in the system because of reduction in current.

c) Voltage level at the load end is increased.

d) KVA loading on the source generators as also on the transformers and lines up to the capacitors reduces giving capacity relief. A high power factor can help in utilizing the full capacity of your electrical system.

6.2 Energy Efficient Motors

Energy-efficient motors (EEM) are the ones in which, design improvements are incorporated specifically to increase operating efficiency over motors of standard design Figure 4. Design improvements focus on reducing intrinsic motor losses. Improvements include the use of lower-loss silicon steel, a longer core (to increase active material), thicker wires (to reduce resistance), thinner laminations, smaller air gap between stator and rotor, copper instead of aluminum bars in the rotor, superior bearings and a smaller fan, etc.

Energy-efficient motors now available in India operate with efficiencies that are typically to 4 percentage points higher than standard motors. In keeping with the stipulations of the BIS, energy-efficient motors are designed to operate without loss in efficiency at loads between 75 % and 100 % of rated capacity. This may result in major benefits in varying load applications. The power factor is about the same or may be higher than for standard motors. Furthermore, energy- efficient motors have lower operating temperatures and noise levels, greater ability to accelerate higher-inertia loads, and are less affected by supply voltage fluctuations.

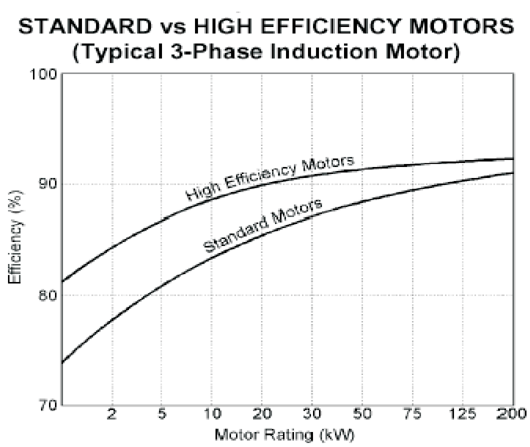

Fig 4 Comparison of standard and energy efficient motor

6.3 Soft Starters

When starting, AC Induction motor develops more torque than is required at full speed. This stress is transferred to the mechanical transmission system resulting in excessive wear and premature failure of chains, belts, gears, mechanical seals, etc. Additionally, rapid acceleration also has a massive impact on electricity supply charges with high inrush currents drawing +600% of the normal run current. The use of Star Delta only provides a partial solution to the problem. Should the motor slow down during the transition period, the high peaks can be repeated and can even exceed direct on line current.

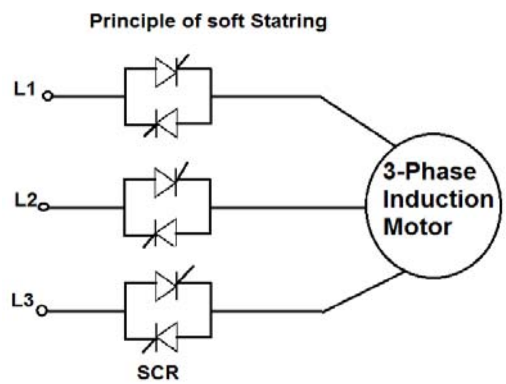

Fig 5 Principle of Soft Starter

Soft starter provides a reliable and economical solution to these problems by delivering a controlled release of power to the motor, thereby providing smooth, steeples acceleration and deceleration. Motor life will be extended as damage to windings and bearings is reduced. Soft Start & Soft Stop is built into 3 phase units, providing controlled starting and stopping with a selection of ramp times and current limit settings to suit all applications.

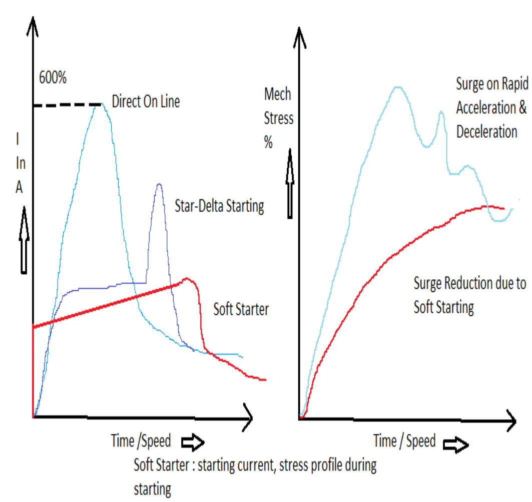

Fig 6 Comparison between direct and soft starter

Advantages of Soft Starter

- Less mechanical stress
- Improved power factor.
- Lower maximum demand.
- Less mechanical maintenance
- Reduction in current surge
- Reduction in voltage fluctuations
- Significant amount of space is saved as compared to conventional one

6.4 Variable Speed Drives

Induction motor is the workhorse of the industry. It is cheap rugged and provides high power to weight ratio. On account of high cost-implications and limitations of D.C. System, induction motors are preferred for variable speed application, the speed of which can be varied by changing the supply frequency.

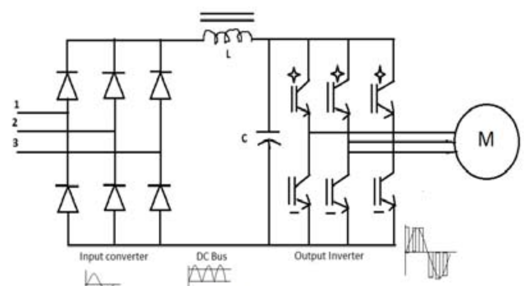

Basic Principle Of VFD

The VFD operates on a simple principle. The rotational speed of an AC induction motor depends on the number of poles in that stator and the frequency of the applied AC power. Although the number of poles in an induction motor cannot be altered easily, variable speed can be achieved through a variation in frequency. The VFD rectifies standard 50 cycle AC line power to DC, then synthesizes the DC to a variable frequency AC output. Motors connected to VFD provide variable speed mechanical output with high efficiency. These devices are capable of up to a 9:1 speed reduction ratio (11 percent of full speed), and a 3:1 speed increase (300 percent of full speed). In recent years, the technology of AC variable frequency drives (VFD) has evolved into highly sophisticated digital microprocessor control, along with high switching frequency IGBTs (Insulated Gate Bi Polar Transistors) power devices. This has led to significantly advanced capabilities from the ease of programmability to expanded diagnostics. The two most significant benefits from the evolution in technology have been that of cost and reliability, in addition to the significant reduction in physical size.

6.5 Electronic Ballast

The conventional ballasts make use of the kick caused by sudden physical disruption of current in an inductive circuit to produce the high voltage required for starting the lamp and then rely on reactive voltage drop in the ballast to reduce the voltage applied across the lamp. On account of the mechanical switch (starter) and low resistance of filament when cold the uncontrolled filament current, generally tend to go beyond the limits specified by Indian standard specifications. With high values of current and flux densities the operational losses and temperature rise are on the higher side in conventional choke.

6.6 Energy Efficient Lighting Controls

6.6.1 Occupancy Sensors

Occupancy-linked control can be achieved using infra-red, acoustic, ultrasonic or microwave sensors, which detect either movement or noise in room spaces. These sensors switch lighting on when occupancy is detected, and off again after a set time period, when no occupancy movement detected. They are designed to override manual switches and to prevent a situation where lighting is left on in unoccupied spaces. With this type of system it is important to incorporate a built-in time delay, since occupants often remain still or quiet for short periods and do not appreciate being plunged into darkness if not constantly moving around.

6.6.2 Timed Based Control

Timed-turnoff switches are the least expensive type of automatic lighting control. In some cases, their low cost and ease of installation makes it desirable to use them where more efficient controls would be too expensive.

6.6.3 Daylight Linked Control

By using an internally mounted photoelectric dimming control system, it is possible to ensure that the sum of daylight and electric lighting always reaches the design level by sensing the total light in the controlled area and adjusting the output of the electric lighting accordingly. If daylight alone is able to meet the design requirements, then the electric lighting can be turned off. The energy saving potential of dimming control is greater than a simple photoelectric switching system..

6.6.4 Localized Switching

Localized switching should be used in applications which contain large spaces. Local switches give individual occupants control over their visual environment and also facilitate energy savings. By using localized switching it is possible to turn off artificial lighting in specific areas, while still operating it in other areas where it is required, a situation which is impossible if the lighting for an entire space is controlled from a single switch.

VII. CONCLUSION

The study reveals that the plant has a considerable savings on energy in the areas of lighting, compressor, pumps units and boilers. Some of the measures need absolutely no money, some are low investment and for some huge investment is needed which may not be possible without top management support. The total energy saving is recorded to substantial having over all small simple payback period. During the study the auditors have identified the motivation of the employees is the key issue to save the energy without having a investment The possible benefits to employees from a successful EMP should addressed to improve the job security, improved working conditions & environment and incentive payments. It is important to have a well-structured employee information program regarding the energy savings and its outcomes.

The implementation of above energy saving measures at thermal power plant is solely dependent upon the decision of the management of the plant. Several energy conservation methods that are cost effective are not often implemented due to the lack of internal funding.

REFERENCES

[1] W. T. Snyder. W. Symonds, "The energy audit what it is how to conduct it , how to use the results", Proceedings of Energy Use Management International Conference, Arizona, pp. 109–115, Oct. 1977.

[2] R. L. Secor, R. S. Curl, "Energy auditing and conservation methods, management and case studies", Proceedings of Energy auditing and Conservation National Conference, Ohio , pp. 14–15, Mar. 1979.

[3] Tuluca A., and Steven Winter Associates, Energy Efficient Design and Construction for Commercial Buildings, Mc-Graw Hills, 1997

[4] V.K.Bhansali, Department of Electrical Engineering, Jodhpur explains the facts about the Indian power scenario which in turn revels that there is substantial gap between demand and supply also energy consumption pattern, etc.

[5] Yong Li, Jian-Jun Wang, Tie-Liu Jiang, Bing-Wen Zhang, China tells about the concept of energy efficiency and it's applications in coal fired power plants which was introduced firstly across the world in China.

[6] Kamalapur G. D. and Udaykumar R. Y. focuses on the scope and potential for energy conservation in developing countries like India. The paper also touch upon the approaches and challenges in implementing the ECP and the EC efforts undertaken by the Government of India.

Breast Cancer Detection Using Mammogram and Thermal Images

Sridhathan C, Ahmed M. A. Haidar and Fahmi Samsuri

Faculty of Electrical and Electronics Engineering
University Malaysia Pahang, Malaysia

Abstract - Breast cancer is one of the most important causes of death among women in world between the age of 40 and 55. Breast cancer can be treated effectively only if it is detected at a premature stage. Imaging techniques play a considerable role in assisting breast biopsies, especially of abnormal areas that cannot be felt but can be seen on a conventional mammogram or other techniques. This paper envisages the mammography and thermal based identification of breast cancer using Computer Assisted Detection System (CADS) and image processing techniques. The objective is to explore ways to extract information from images and subsequently analyse, characterize, understand and visualize the extracted information. Patient will be first screened with thermal imaging and then by using mammography technique for breast cancer. The results of these techniques will be studied and analysed.

Keywords*-cancer detection; mammography; thermal images; Computer Detection.*

I. INTRODUCTION

Cancer is a class of diseases characterized by uncontrolled proliferation of cells. Cancer cells have the ability to spread, either by invasion i.e., direct growth into adjacent tissue or by implantation into distant sites by metastasis. There are many types of cancer such as breast cancer, oral cancer, lung cancer, pancreatic cancer, bladder cancer, leukaemia (blood cancer) etc. Breast cancer is the most common form of cancer in females. Women who go through the regular breast screening have a considerable reduction in breast cancer mortality compared with women who do not. Cancer cells are classified as benign or malignant masses. Figure 1 shows the structure of benign and malignant cell. Malignant masses are radio opaque and with irregular in shapes and benign are combined with radiolucent shapes [1- 4].

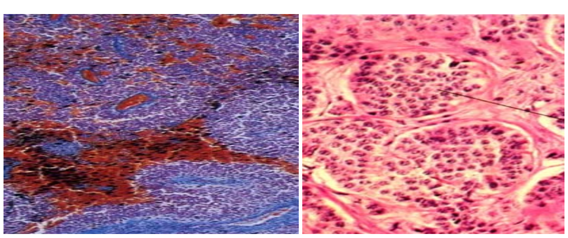

(a) (b)

Figure 1. a) Malignant Cell, b) Benign Cell (Magnification: a and b x 400) [21]

Mammographic imaging technology uses a low-dose x-ray radiation with high contrast and resolution film for breasts examination. Mammography can be classified into film and digital. Film mammography uses standard radiation rays which cannot be reduced whereas digital mammography is far advanced than film mammography with the radiation rays can be reduced half while still maintaining its capability to detect breast cancer. A mammogram rays basically has four levels of increase intensities based on several parameters such as background, fat tissue, breast parenchyma and calcifications. Mammography is a diagnostic technique that is capable of detecting not only the mass lesions but also micro-calcifications, which is the sign of early breast cancer [4]. Figure 2 shows how mammogram of breast is taken. Here the breast is pressed and flattened by the electrodes plates which can cause inconvenience to the patients.

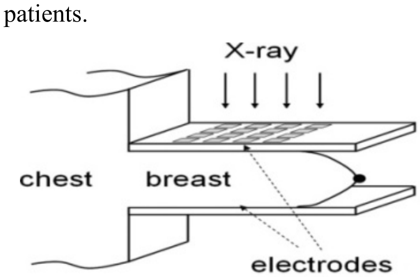

Figure 2. Breast is flattened by the plates for Mammography [6]

However the accuracy in detecting the cancer based on the mammogram images with only bare eyes by qualified personnel (radiologist) can be affected by poor mammographic image quality. Radiologist misdiagnose between 10 to 35% of the malignant cases due to the difficulty in maintaining required attention level while screening and analysing large number of mammograms [5].

Human body whose temperature is above zero Kelvin has the ability to emit infra-red radiations as an exponential function of temperature. Black body is an object which absorbs all radiations incident on it and emits them back. Hence it is called as the ideal body. The wavelength of emission is dependent on temperature and spectral emissivity, ε (λ). For black body ε =1, grey objects ε < 1. The spectral emissivity of any objects will be in the range of 0 ≤ ε ≤ 1. According to Planks radiation law, the radiation power and its wavelength distribution is given as,

$$w(\lambda, T) = \frac{2\,\pi hc^2}{\lambda^4}\left[exp\left(\frac{hc}{\lambda kt}\right) - 1\right]^{-1} W cm^{-2}\, \mu m^{-1} \quad (1)$$

where,

h (Planck's constant)	=	$6.6256\ X10^{-34}$ J s
c (velocity of light)	=	$2.9979\ X10^{8}\ ms^{-1}$
k (Boltzmann's Constant)	=	$1.38054X10^{-23}\ WsK^{-1}$
λ (wavelength) in μm		
T (Temperature) in K		

Thermograph's measurement of heat emission from the tissues was investigated in the 1970s and 1980s but abandoned when it was found to be of low specificity and selectivity. Heat transfer may be due to conduction in the tissues layers, convention by vascular system and radiation because of environment. Thermography is an imaging technique which shows temperature patterns at the surface of an object. The breast heat patterns indicate the metabolic activity, sweating and blood circulation in breast tissue. Temperature will be high at the region of the cancerous tissue compared to normal tissues [7]. However as the image only shows the surface temperature, clinician find problems in specifying the location, shape and type of the cancer cell which directly affect the decision for further therapy [8]. Figure 3 shows how the thermal image of breast is taken using the infrared camera.

Figure 3. Infrared Camera used for taking Thermography

Thermal images can be used to pre-screen the patient. Mammography is the best method to detect early signs of breast cancer such as masses, calcifications, bilateral asymmetry and architectural distortion. However, due to human limitation computer system has to take the major role in detecting abnormal tissue. The challenges faced by the system are the wide range of abnormalities features and the indistinguishable from surrounding cell [9]. Due to the need of overcoming the problem that cause high rate of false positive and false negative detection, a CADS was developed to provide assistant for clinician to identify cancerous tissue in mammogram and thermogram images. The system will be designed based on image processing technique on MATLAB platform. CADS and diagnosis method for breast cancer is presented in this paper. The paper is organized in the following manner: Section 1 gives brief introduction into mammography and thermal imaging techniques. Section 2 deals with the CADS for thermal and mammogram based image processing. Performance and Results are discussed in Section 3, and then followed by a conclusion

II. COMPUTER ASSISTED DETECTION SYSTEM

CADS based image processing has been used in many applications. Here, it is used to detect cancer cell based on the obtained images. It involves filling gaps, dilating gaps, removing border, smoothing the objects, finding structures, extracting large objects and identify the required region of interest [10]. The feature extractions in mammogram are based on three main categories; geometric, texture and gradient which may be used for breast cancer detection [4]. An interpretation system must be able to characterize thermography image as normal or otherwise, as required by the clinician. It was reported that Infrared Thermography Based Image Construction (ITBIC) interpreter system was used to characterize and match the result of a number of clinical findings. The system is interfaced with graphical user interface (GUI) to allow easier thermogram analysis by the radiologist or clinician [11]. Edge detection, Hough transform, segmented classification and diagnostic based on asymmetric analysis of image with automatic approach may improve the accuracy in earlier detection schemes of breast cancer for thermography image technique [12]. In this system, patients are asked to fill up the following questionnaire for medical records: Name, Age, Height, Weight, Family history of breast cancer, Hormone replacement therapy, Age of menarche patient, Presence of palpable lump, Previous breast surgery/ biopsy, Presence of nipple discharge, Pain in the breast, Menopause at the age of > 50years old, First child at the age of >30.

A. Thermogram Image Processing

While capturing the thermal image, the room temperature must be kept stable at approximately 22 to 24°C, so that the patient feels comfortable, and not sweating nor shivering. Fluorescent ceiling lights are used and very far away from the scanned area. Patients are asked to remove their dress from their waist upwards and left to equilibrate with the ambient surroundings for 10 to 20 minutes. Patient is later instructed to sit in the middle of a rotation stool without a back rest, positioned at approximately 100 cm from the thermal camera [13]. Patients are asked to keep their hands on their head and remain at rest. Three images are captured from each patient: one face (0 degree) and one oblique on each side at 45 degree angle from middle line for optimal exposure of all aspects of the breasts. Images are then appropriately labelled and stored. These colour images (thermogram) comprise colour pixels, each one reflecting a single temperature measurement.

Diagnostic criteria for breast cancer by thermography are as follows [14, 15]:

- An asymmetric hot spot
- Asymmetric abnormal exaggeration of vascular patterns
- Significant temperature differences in heat pattern - a high thermal index
- Positive heat patterns in sequential thermography
- Existence of a hot spot in subtraction thermography

The major difficulty in the interpretation of breast thermography is the complexities of the vascular patterns (false negatives and false positives), and a secondary problem is the existence of cold tumours (false negatives). The digital mammography images are found from online mammogram database (MAIS database) [16, 17, 18, 19]. Here thermal images are segmented using 3 methods based on grey threshold, RGB and K-mean technique. In threshold based image segmentation cut off value is selected by trial and error methods and an optimal value is selected as the threshold. In RGB the images are segmented by the colour function. In k-mean the images are segmented using the k-means algorithm. K-mean thermogram image analysis detects the masses by using image segmentation technique and asymmetry analysis. It is the fastest unsupervised learning technique for image clustering. The process and steps are demonstrated in flow chart as shown in Figure 4. In this work, the K-mean colour segmentation is used for identifying the high temperature region on the breast. Based on this technique the images are segmented into many clusters i.e., small regions based on the colours. K-mean divides the M data points to K disjoint subsets Si where i = 1, 2, 3...K. It is based on the objective minimization function as given by,

$$I = \sum_{i=1}^{K} \sum_{m \in S_i} \left\| x_n - \mu_i \right\|^2 \qquad (2)$$

where x_n : a vector representing n^{th} data point in S_i

μ_i : geometric centre of data points

In threshold based image segmentation, the green, blue and red threshold values are obtained by trial and error method. An optimal threshold value is chosen and based on that, the image is separated. The optimal threshold value will be calculated for all the primary colours red, green and blue. RGB based segmentation colours are grouped as Red, Green and Blue. All fades of red comes under Red, fades of green under Green and so on. Whereas detecting Red regions, all fades are grouped together and other colours are separated similarly.

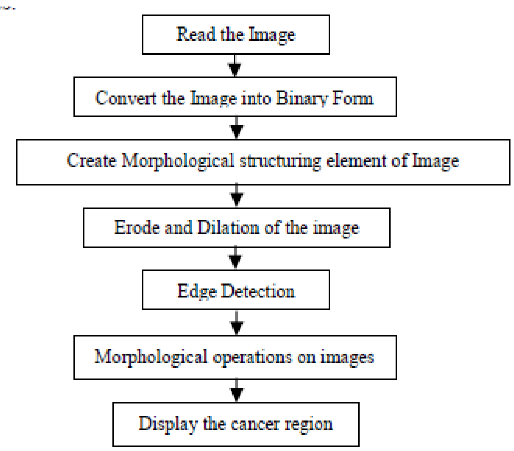

Figure 4. The steps involved in K-mean clustering of Thermal images

B. *Mammogram Image Processing*

For mammography image analysis, the proposed method uses edge detection and morphological techniques to detect the masses. The mammograms are pre-processed using erode, dilation methods. The edge detection and morphological processing are used to identify the cancer regions. The steps are shown in Figure 5. The Canny method is used to find the edges by looking for local maxima of the gradient of image. The gradient is calculated using the derivative of a Gaussian filter. The method uses two thresholds, to detect strong and weak edges, and includes the weak edges in the output only if they are connected to strong edges. This method is therefore less likely than the others to be fooled by noise, and more likely to detect true weak edges.

Read the Image

Convert the Image into Binary Form

Create Morphological structuring element of Image

Erode and Dilation of the image

Edge Detection

Morphological operations on images

Display the cancer region

Figure 5. The steps involved in Mammographic images processing

III. RESULT

Thermal image of a patient is shown in Figure 6 with its grey scale and histogram. The temperature of right side breast is higher than the left side which indicates there are abnormal blood circulations and metabolism.

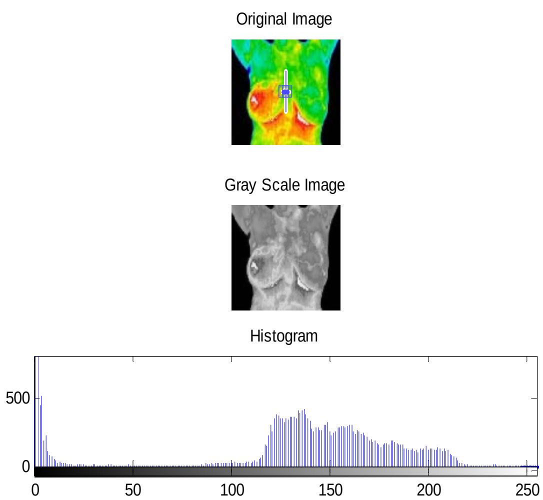

Figure 6 : Thermal Image of breast with gray scale and histogram [7]

This indicates that the right side breast might have a higher probability of having cancerous tumours. It was later found that the mean temperature difference between the tumours and the normal region was in the range of 0.40°C to 1.4 °C. In Figure 7 the thermal image is segmented based on the threshold values. It can be clearly seen here that the regions are divided into high, low, mid temperature regions based on thresholds. The high temperature region is indicated by fades of red colour. Green and blue colour fades indicate normal and low temperature regions.

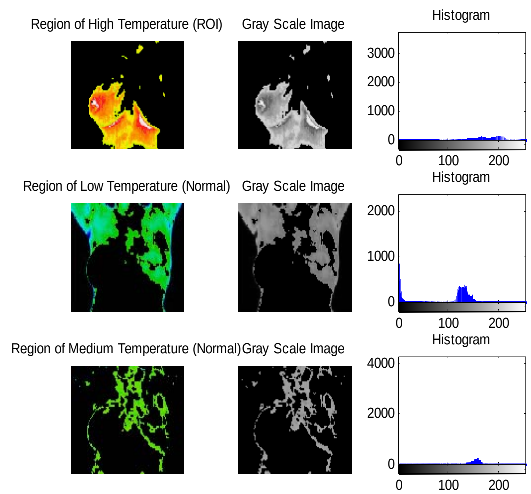

Figure 7 : Threshold based Colour segmented thermal image with histogram

In Figure 8 the images are segmented using RGB filters. However this segmentation is not very effective since it transforms the fades of red into single red colour as marked as RED region in the image. The same thing with the green and blue fades. When the threshold and filter based segmented images are added, the original image can be retrieved from RGB filter based segmentation. But in threshold of images, it was found that some regions were missing as shown in Figure 8 (bottom row). This missing region indicates that the few pixel values were omitted in the original image while calculating the threshold values.

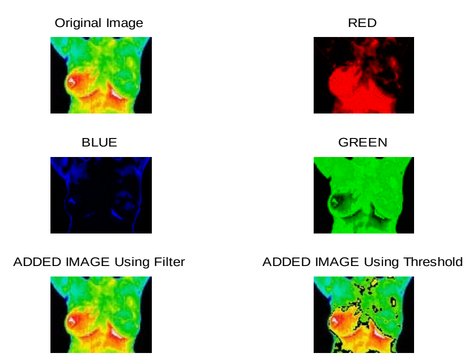

Figure 8 : RGB based Colour segmented thermal image [7]

Figure 9 shows the segmented thermal images using K-mean. Since the number of clusters used for segmentation is five, so the produced segmented coloured images will be five.

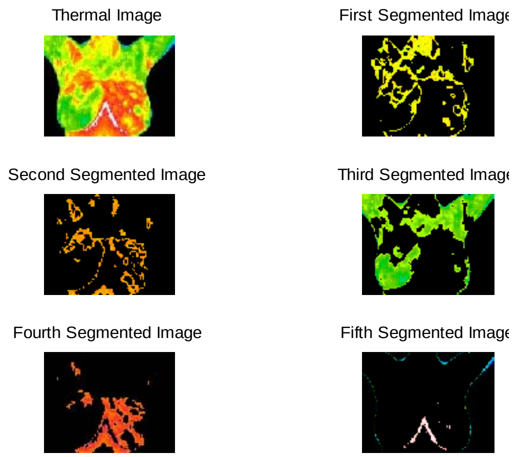

Figure 9 : K-Mean based Colour segmented thermal image [7]

Red colour in the thermal image shows the region of high temperature. Referring to Figure 9, the fourth segmented image is red in colour. This represents the region of high temperature. From this we can obviously determine the region of the cancer tumours by using thermal images. In Figures 7, 8 the left side breast is in lower temperature region compared to the right breast. The hotter spots are more pronounced in the right breast which indicates the possibility of cancer. In Figure 9, the right side breast is in lower temperature compared to the left breast. The hotter spots are more pronounced in the left breast. Thus we can conclude that the probability of the left breast to have cancerous tumours is very high.

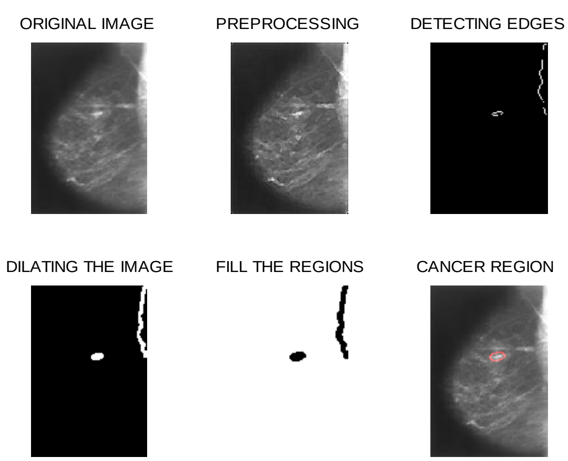

Figure 10 : Detection of cancer from Mammography Sample 1

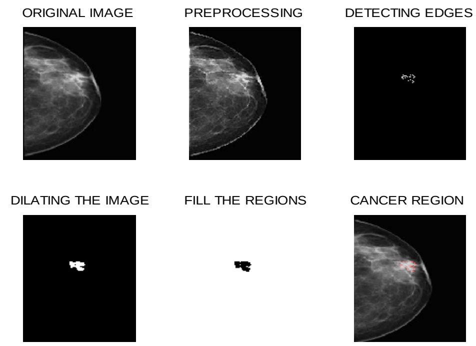

Figure 11 : Detection of cancer from Mammography Sample 2

Figures 10, 11 show the mammogram and the cancer region detected by Mammogram Image Processing techniques. In Figure 10, the high intensity region can be found at the centre of the breast which corresponds extensively to cancerous region, while in Figure 11 the cancer region can be located on the edge of the right side of the breast.

IV. CONCLUSION

CADS based image processing system helps the clinician to identifying the cancer regions. Cancer identification can be done by using mammogram or thermal images or by both. The patients might feel discomfort during the mammogram session since the breast will be pressed by the plates while taking the image. In thermal image the patient would feel more comfortable since there is no such painful procedure like mammogram. It can be concluded that the thermal images can be used effectively to detect cancer cells. This would help physician especially pathologist to diagnosis cancer at earlier stage and be able to propose adequate and effective treatment for the patients.

REFERENCES

[1] Greenlee RT, Hill-Harmon MB, Murray T, Thun M. “Cancer statistics”, 2001. CA Cancer J Clin 2001; 51: pp. 15–36.

[2] Sandra Y. Moody-Ayers, Carolyn K. Wells and Alvan R. Feinstein, ‘Benign” Tumours and “Early Detection” in Mammography-Screened Patients of a Natural Cohort with Breast Cancer’, ARCH INTERN MED/VOL 160, APR 24, 2000, pp. 1109–1115.

[3] Nicholas Petrick, Berkman Sahiner, Heang-Ping Chan, Mark A. Helvie, Sophie Paquerault and Lubomir M. Hadjiiski, “Breast cancer detection: Evaluation of a Mass-detection algorithm for

Computer-aided diagnosis – Experience in 263 patients", Radiology July 2002, pp. 217–224,

[4] Hala Al-Shamlan and Ali El-Zaart. "Feature Extraction Values for Breast Cancer Mammography Images" 2010 International Conference on Bioinformatics and Biomedical Technology, pp. 335–340.

[5] Gulzar A. Khuwaja, "Breast cancer detection using mammography," Proceedings of the 5th WSEAS International Conference on Signal Processing, May 2006, pp. 20–23.

[6] Myoung Hwan Choi, Tzu-Jen Kao, David Isaacson, Gary J. Saulnier, and Jonathan C. Newell, "A Reconstruction Algorithm for Breast Cancer Imaging With Electrical Impedance Tomography in Mammography Geometry", IEEE transactions on biomedical engineering, VOL. 54, NO. 4, 2007, pp. 700–710.

[7] http://www.breastthermography.com

[8] Haifeng Zhang, Liqun He, Liang Zhu, "Critical Conditions for the Thermal Diagnosis of the Breast Cancer," IEEE 2009.

[9] Jelena Bozek, Kresimir Delac, Mislav Grgic, "Computer-Aided Detection and Diagnosis of Breast Abnormalities in Digital Mammography," Proceed of 50th International Symposium ELMAR-2008, pp 45 – 52.

[10] Ranjeet Singh Tomar, Tripty Singh, Sulochana Wadhwani, Sarita Singh Bhadoria, "Analysis of Breast Cancer Using Image Processing Techniques," 2009 Third UKSim European Symposium on Computer Modelling and Simulation, IEEE press 2009, pp. 251 – 256.

[11] V. Umadevi, S. V. Raghavan and Sandeep Jaipurkar, "Interpreter for Breast Thermogram Characterization," IEEE EMBS Conference on Biomedical Engineering and Sciences, IEEE press 2010. pp.150-154

[12] Pragati Kapoor, S. V. A. V. Prasad, "Image Processing for Early Diagnosis of Breast Cancer Using Infrared Images," 2nd International Conference on Computer and Automation Engineering, IEEE press 2010. Vol3, pp 564-566

[13] M. Kontos, R. Wilson, I. Fentiman "Digital infrared thermal imaging (DITI) of breast lesions: sensitivity and specificity of detection of primary breast cancers" www.elsevierhealth.com/journals/crad, Clinical Radiology 66 (2011) 536 to 539.

[14] E.Y.-K. Ng "A review of thermography as promising non-invasive detection modality for breast tumour" International Journal of Thermal Sciences 48 (2009) 849–859.

[15] EtehadTavakol & S. Sadri & E. Y. K. Ng "Application of K- and Fuzzy c-Means for Color Segmentation of Thermal Infrared Breast Images" Springer – J Med Syst (2010) 34:pp.35–42.

[16] Poulami Das, Debnath Bhattacharyya, Samir K. Bandyopadhyay and Tai-hoon Kim "Analysis and Diagnosis of Breast Cancer" International Journal of u- and e- Service, Science and Technology Vol. 2, No. 3, September, 2009.

[17] http://peipa.essex.ac.uk/ipa/pix/mias/.

[18] Yasuhiko Ohashi and lsao Uchida, "Applying Dynamic Thermography in the Diagnosis of Breast Cancer – Techniques for Improving Sensitivity of Breast Thermography" IEEE Engineering in Medicine and Biology. pp 42–51

[19] E.Y.K. Ng, E.C. Kee, Rajendra Acharya U, "Advanced Technique in Breast Thermography Analysis" , Proceedings of the 2005 IEEE, Engineering in Medicine and Biology 27th Annual Conference, Shanghai, China, September, 2005; pp.710–713

[20] Tabar L, Fagerberg C, Gad A, et al. "Reduction in mortality from breast cancer after mass screening with mammography". Lancet 1985; 1:pp. 829–832.

[21] http://treatment-of-mesothelioma.co.cc

◈◈◈

Overview of Band Stop Filtering Approach For Moving Acoustic Source

M. Mayilvaganan [1] & M. Devaki[2]

P.S.G College of Arts and science, Coimbatore-14, India.

Abstract - Traditional moving acoustic source monitoring and direction of arrival in a multipath propagation environment has been an emerging technology and challenging research goal for many years. Using the array of sensors under multipath propagation area the direction of arrival estimation is computed. This paper presents the overall system architecture of an acoustic source noise monitoring and noise mitigation (filtering) under reverberant environment using band stop filters. We have conducted real time experiments to monitoring and recording the noise in acoustic archieves and tested the internal/ external factors that affect the sound in different environments. Furthermore, the simulation results shows the acoustic absorbtion under highly applicable for reverberant areas.

Keywords: *Direction of arrival; noise mitigation; band stop filter; acoustic achieves; sensor array.*

I. INTRODUCTION

The problem of moving acoustic source locating and tracking in a multipath propagation environment is one of the emerging technology and challenging research area including sonar, seismology, video conferencing, speech recognition[1]. In this paper we focus on moving acoustic source noise monitoring and mitigation (filtering) recorded in acoustic achieves using circular sensor array in reverberant areas. Traditional approach to this problem collect the acoustic source signal using Digital Audiotape(DAT) and estimate the current location of the moving source[2].

Traditional approach can be divided into two categories: (i) time-delay estimation (TDE)method such as generalized cross-correlation function(GCC) which estimate the time delay arrival of signals between microphones; and (ii) steered beamforming in which the microphone placed near to the source is called acoustic holography and microphone placed far to the field is called acoustic beamforming[3]. This paper we focus on overview of moving acoustic source sound mitigation and external factors using bandstop filter[3][4]. We assume the following factors, (i)the single acoustic source in multipath environment ii)propagation speed of wave and iii) sensor position. In this paper, the moving acoustic source achieves are collected using following methods.

Real Time Acoustic Source Data Acquisition

1. Traditional or manual recording on Digital AudioTape (DAT) using directional microphones.
2. Circular microphone array connected to a laptop where sound is recorded,
3. Circular microphone array connected to a sensor node to process data in real-time

The paper is organized as follows. Section 2 focus on moving acoustic source system architecture and sound mitigation. Section 3 describes proposed mitigation filtering algorithm. Section 4 reveals internal and external factors affecting the sound propagation. Section 5 shows the simulation results. Section 6 concludes the paper and future trends.

II. MOVING ACOUSTIC SOURCE SYSTEM ARCHITECTURE

In this section, we describe the system architecture for moving acoustic source noise monitoring and mitigation under highly reverberant areas. Figure 1. Shows the system architecture and it components.

Sensor nodes: The sensor nodes are placed in linear array of known positions with necessary hardware configuration to capture and collect the different types of acoustic source signal archeives (database).

After collecting the sound or noise in archives and detect the noise mitigation using the filtering algorithm and determines the direction of arrival of a moving acoustic source signal[1]. When a sensor node captures the sound, it transmits the essential information regarding timestamp, direction, time and time difference of arrival of the sound to the special node.

Sink node : Sink node collects the data from the sensor node and transmit to the server.

Server : After retrieving the information from the sink node the server determines the acoustic source direction of arrival, time of arrival, time difference of arrival using the Asymptotic log likelihood Gaussian process.

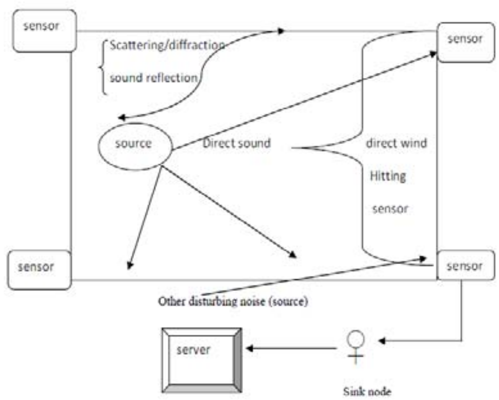

Figure 1 : Shows the system architecture and it components

III. PROPOSED SYSTEM (SOUND MITIGATION ALGORTIHM)

The band pass filter is designed to pass a desired band of frequencies that lie between two cut-offf frequencies called, respectively, the upper and lower cut off frequencies[2][4]. Tuned amplifiers are called band-pass filters (BPFs) in that they permit only a certain range of frequencies to pass through them; all other frequencies, which lie outside this range, are attenuated.

The normalized low pass filter is transformed to desired band pass filter using the following relation. For band pass filter, let us define center frequency Ω0 and the quality factor Q as below

$$Q = \frac{\Omega 0}{\Omega 2 - \Omega 1} \quad ; \Omega 0 = \sqrt{\Omega 1\, \Omega 2} \qquad (1)$$

Where Ω2= upper cut-off frequency, Ω1=lower cut off frequency

The transformation relation is

$$S = \frac{Q(s^2 + \Omega 0^2)}{s\, \Omega_0} \qquad (2)$$

Low pass to desired Band Pass Filter Transformation

The desired low pass filter is transformed to the desired digital band pass filter using the relation

$$Z\text{-}1 \text{-----}> \left[\frac{Z^{-2} - \frac{(2\alpha k)}{K+1} Z^{-1} + \frac{k-1}{k+1}}{\frac{(1-k)}{1+k} Z^{-2} \frac{(2\alpha)}{K+1} Z^{-1} + 1} \right] \qquad (3)$$

$$\text{where } \alpha = \frac{\cos \frac{(\acute{\omega}2 + \acute{\omega}1)}{2}}{\cos \frac{(\acute{\omega}2 - \acute{\omega}1)}{2}} \qquad (4)$$

$$k = \tan \frac{(\acute{\omega}2 - \acute{\omega}1)}{2} \tan \frac{(\acute{\omega}^1 c)}{2} \qquad (5)$$

IV. ERROR ANALYSIS - INTERNAL/ EXTERNAL FACTOR

Depending upon the environment there are some internal or external factors that affects the sound absorption property. We have conducted real time experiments for monitoring and recording the moving acoustic source and collected it on acoustic archieves. We have listed the few error analysis factors that affect the acoustic source. Sound energy is dissipated in air by two major mechanisms:

Viscous losses due to friction between air molecules, which result in heat generation, called “classical absorption“.

Relaxation processes: acoustic source energy is absorbed in the air molecules and causes to vibrate and rotate. When a sound wave penetrates through a medium such as air ,water, colder air, or a solid object, fog and grass part of the sound is reflected or scattered or diffracted or refraction back from the object in a manner similar to a beam of light. The balance of the sound passes into and is transmitted by the second medium.

Reflection or diffraction: when sound reflects off a special curved surface called a **parabola**, it will bounce out in a straight line no matter where it originally hits. If the parabola is closed off by another curved surface, it is called an **ellipse**. **Echoes** are the sound of your own voice reflecting back to your ears[2][3].

Refraction : When sound penetrates at an direction of arrival at 90degree, it is bent from its original direction. This change in angle of direction is called **refraction**. Because of the direction of arrival, the wave penetrates the new medium first and changes speed. The difference in speeds causes the wave to bend. The angle of refraction depends on the angle that the waves has when it enters the new medium and the velocities of the waves in the two materials.

Snell's Law describes the relationship between the angles and the velocities of the waves. Snell's law equates the ratio of material velocities $\mathbf{V_1}$ and $\mathbf{V_2}$ to the ratio of the **sine's** of incident (θ_1) and refracted (θ_2) angles, as shown in the following equation[2].

$$\frac{\sin\theta 1}{VL_1} = \frac{\sin\theta 2}{VL_2}$$

Where, VL1 is the longitudinal wave velocity in material 1, VL2 is the longitudinal wave velocity in material 2.

Scattering is a physical process in which some forms of radiation, such as light, sound, or moving acoustic source are forced to deviate from a straight trajectory by one or more localized non-uniformities in the medium through which they pass.

Sound speed & equation

A sound wave is a pressure disturbance that travels through a medium by means of particle-to-particle interaction. As one particle becomes disturbed, it exerts a force on the next adjacent particle, thus disturbing that particle from rest and transporting the energy through the medium.

Speed = distance / time

Like any wave, a sound wave has a speed that is mathematically related to the frequency and the wavelength of the wave.

Speed = wavelength (f). Frequency (λ)

V. SIMULATION RESULTS OF ACOUSTIC ABSORBTION

The sound absorption properties of a material are quantified by its sound absorption Coefficient. The sound absorption coefficient of a material can have a value between 0 and 1, with 0 representing no absorption and total reflection, and 1 representing total absorption of all the incident sound. The sound absorption coefficient varies with the frequency of sound. The following table 1 & chart shows the results of acoustic absorption in different materials. Figure 2 Geometry for reflection of sound from ground level.

Table 1 : Internal / External Acoustic absorption materials.

0.1	CONCRETE	125HZ
0.2	BRICK	250HZ
0.3	WOOD	500HZ
0.4	GLASS	1HZ
0.5	WOOD WITH AIR BEHIND	2HZ

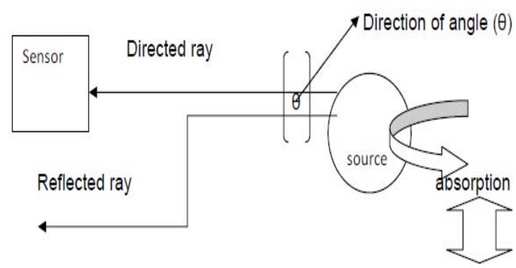

Figure 2 Geometry for reflection of sound from ground level.

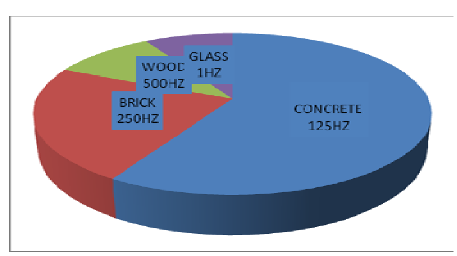

Pie chart of different absorption coefficients in different materials

VI. CONCLUSION & FUTURE TRENDS

We presented a acoustic source noise monitoring in archives and noise mitigation (filtering) under reverberant environment using band stop filters. We discuss band stop filtering approach algorithm that can be accomplish within the multipath propagation area. While we have not tested the full system yet, but we have tested to recording the noise in acoustic archieves and tested the internal/ external factors that affect the sound in different environments. Furthermore, the simulation results show the band stop filtering approach is highly applicable for reverberant areas. In future we plan to implement the moving multi source direction of arrival and filtering in multipath propagation environment. These ideas will be strongly implement in the future.

REFERENCES

[1]. M. Brandstein and D. Ward, Eds., *Microphone Arrays: Signal Processing Techniques and Applications*, Springer, 2001.

[2]. B.Somanathan Nair., Digital Signal Processing Theory, Analysis and digital Filter Design(textbook) prentice hall of india private limited.

[3]. D.B.Ward and R.C.Williamson, “Particle filter beamforming for acoustic source localization in a reverberant environment,”in *Proc. IEEE ICASSP*, Orlando, FL, USA, May 2002.

[4]. D. B. Ward, E. A. Lehmann, R. C. Williamson, ”Particle filtering algorithms for tracking an acoustic source in a reverberant environment”, *IEEE Trans. Speech Audio Processing*, vol. 11, pp. 826-836, 2003

◈◈◈

Analysis of Converters
For Switched Reluctance Generator

K. Poojitha
Power Electronics and Drives Department, RMK Engineering College, Chennai.

Abstract - This paper presents the analysis of performance of switched reluctance generator (SRG) for various types of converter. The converters used for analysis are Asymmetric half bridge converter (AHBC), New converter and Miller converter. The simulation process is carried out between AHBC and New converter for SRG of these three converters by using MATLAB. On the basis of the analysis of simulation results, the performance of SRG is better with New converter when compared with the AHBC and it suits best for better performance of SRG.

Keywords*: SRG, AHBC, Miller, New converter.*

I. INTRODUCTION

The SRG is an attractive solution to the increasing worldwide demand of electrical energy. In these machines phase coils are concentrated windings in the stator poles. There are no windings in its rotor. The doubly salient poles structure is a characteristic inherent to these machines. Therefore, there is minimal thermal loss in the rotor. A SRG is easy to construct and to maintain. Its commonly quoted advantages are the absence of permanent magnets, a low manufacturing costs with a rugged structure, fault tolerant, reliability, robustness and operates with high efficiency over a wide speed range. The operational speed range is very wide. Though these advantages have already been confirming, some aspects of these machines must be mentioning here: there is a strong magnetic discontinuity providing current, voltage and torque ripples that should be properly controlling. The power electronics requirements to control a SRG are sometimes quoting as a disadvantage of this kind of machine. Furthermore, they are a little noisy. Due to its advantages, SRG are considering as a special electrical generator for wind power. In many applications, size and weight are the main criteria in selecting the generator. Hence, in design and control of the generator, system designers always strive for increasing power density, or in other words, maximizing the output power for a given size. The generator performance, including output power, torque ripple, and copper losses are determined by simulation in terms of turn-on and turn-off angles for different speeds while the dc bus voltage is maintained at a constant value. The currents in the SRG phases are limited to a maximum admissible value. Recently, switched reluctance motor drives have been finding their applications in the variable speed drives due to their relatively low cost, simple and robust structure, high ratio of torque to rotor volume, reliability, controllability and high efficiency.

The necessity for a converter to drive the machine and position sensor limit the general use of SRM drives. Requirements of converter to increase the performance and efficiency of the switched reluctance machine are (a) Fast magnetization and demagnetization capability. (b) Fault tolerance capability. (c) High di/dt at turn on and turn off instances for phase current should be achieved.

II. MATLAB BASED MODELING

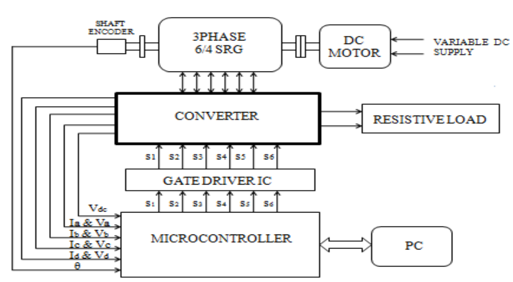

Fig.1 Schematic representation to analyze the converters for .switched reluctance generator

SRG modeling:

Output power of SRG depend on various variables such as: excitation current, excitation voltage, rotor position and also rotor speed. The parameters above can be controlled to achieve high efficiency of the SRG. However the challenge lies on how to determine the best parameters that will produce the optimum performance. Based on that, the modeling of the SRG is proposed using MATLAB/SIMULINK. The software has all the tools to model the dynamics of electrical machines. The simulations are performed using block diagrams and special MATLAB functions. At this stage of research a simulation model of the SRG comprising of the converter, controller and genera-tor operating at steady state is proposed. Assuming that there is no mutual interaction between phases and neglecting flux linkage the representation of SRG is performed for one phase. Electromagnetic characteristics and torque can be calculated individually for each phase hence additional phases can be added. At a later stage the model will then be subject to testing with a prototype for practical implementation. The SRG is modelled as an inductor and a resistor in series. The simulation model of the SRG is shown in the fig 8. In order to maximize switched-reluctance generator (SRG) efficiency, we seek to maximize the ratio of the average output power to given input average mechanical power, ${P_{out}}/{P_{mech}}$. This ratio captures our intended goal of providing the required electrical output with the minimum electromechanical input.

Corresponding equations of the SRG modeling are

$$T_m - T_e = J\frac{d\omega}{dt} + B\omega \qquad (1)$$

$$\omega = \int \frac{1}{J}(T_m - T_e - B\omega) \qquad (2)$$

$$\omega = \frac{\partial\theta}{\partial t} \qquad (3)$$

$$V_j = Ri + \frac{d\lambda}{dt} \qquad (4)$$

The torque equation of the switched reluctance machine is shown in the equ 5. And it is negative.

$$T = \frac{1}{2} i^2 \frac{\partial L}{\partial \theta} \qquad (5)$$

Inductance profile:

The operation of Switched Reluctance Generator (SRG) is similar to Switched Reluctance Motor (SRM). However, for SRG the excitation of stator phase must be made when rotor is moving pass the stator when inductance is decreasing as shown in Figure 2.(ii) and (3) whereas for motoring the excitation is on the increasing inductance region. Movement of rotor in an out of alignment with the stator poles creates variation of reluctance flux path. It can be seen that this variation creates con-version of energy. Hence in every cycle the flux must be established and returned to zero before excitation of the next phase.

The torque (*T*) is produced by the tendency of the rotor moving to the excited stator phase winding where minimum reluctance occurs independent of direction of current (*i*) flow as shown by equation [5]

The phase of the stator must be excited in synchronism with rotor position to produce continuous torque. If the phase is excited when the poles are unaligned as in Figure 2.(iii), no torque will be produced since is $dL/d\theta$ zero. However, if the stator phase is excited as rotor is moving pass the stator pole as in Figure 2.(ii) there will be a braking torque trying to realign the poles back together creating negative torque extracting energy from prime mover during generating mode. A controller with position feedback must be developed so that pulses of phase current can be synchronized according to the appropriate rotor position.

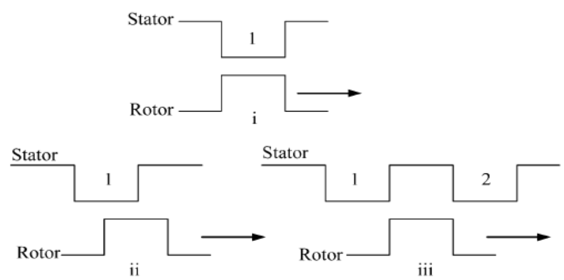

Fig 2: Variation of inductance with respect to movement of rotor. (a) Rotor movement with respect to stator i) Maximum inductance, minimum reluctance (full alignment) ii) Inductance decreasing linearly; iii) Minimum inductance (misalignment)

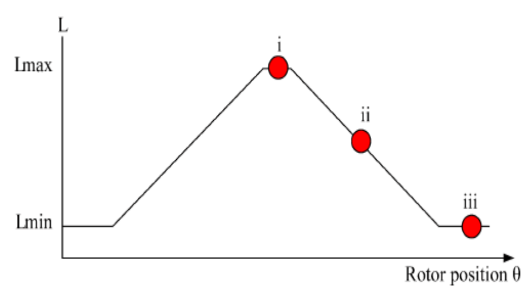

Fig 3: Inductance profile with respect to rotor position

The converters used for switched reluctance drive are

A .Asymmetric half bridge converter (AHBC)

B .New converter

C. Miller converter

In designing of converter the switches used are IGBT switches and the gate pulses of pulse generation is giving by writing the program in embedded Matlab function and the corresponding signals are given to their corresponding switches. All the components are user defines functions of Matlab/Simulink.

D. Simulation model

A. ASYMMETRIC HALF BRIDGE CONVERTER

This converter circuit shown in the fig. 4 is the standard topology for switched reluctance machine drives, as it undergoes provides the most control flexibility and fault tolerance**.**

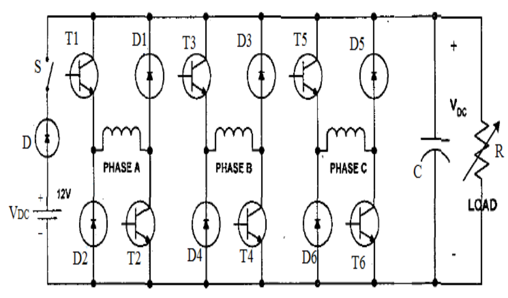

Fig 4: Asymmetric half bridge converter for SRG drive.

The following switching strategy will be available in every phase.

Magnetization: Both switches in a phase leg are on, and phase is energized from power supply (Excitation).

De magnetization: Both switches in a phase leg are off. Phase current commutates to the diodes and decays rapidly (Generation).

Freewheeling mode: Only one of the switches is off. The voltage across winding is near zero and phase current decays slowly (freewheeling).

B. Miller converter

In order to reduce the number of switches and therefore bring down the converter cost, Miller converter was proposed and the circuit diagram of the miller converter is shown in the figure 5. Here in this converter the numbers of switches used are four so the switching losses also getting reduced compare to the other converter circuits. The following switching strategy will be available in every phase.

Magnetization: Both IGBT1 and switch in any phase leg (phase A or B or C) are in ON position (excitation)

De magnetization: Both IGBT1 and switch in any phase leg (phase A or B or C) are in OFF position (De Magnetization mode) phase current flows through the diode and diode in the corresponding phase leg and phase current decays very rapidly.

Freewheeling mode: When IGBT1 is OFF and the corresponding phase switch is in ON position (freewheeling mode) then the voltage across phase winding is near zero and decays very fastly.

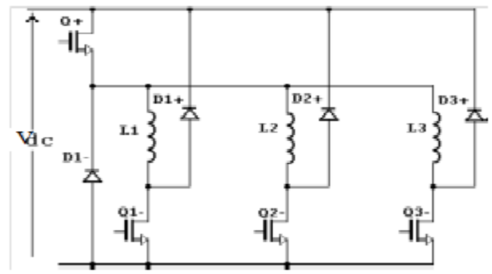

Fig 5: Miller converter for switched reluctance drive.

C. New converter

Asymmetric half bridge converter has been considered as a benchmark topology for driving the switched reluctance machine (SRM). However the lack of its commercialization in the form of a single module makes this converter to suffer from higher cost, lower speed and lesser efficiency. This research paper presents a new converter which uses the standard full bridge inverter along with one extra leg for star connected phases. The new converter circuit is shown in the fig6.

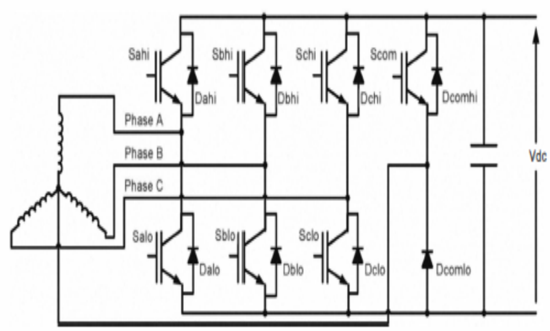

Fig 6: New reduced switch converter for SRG.

This converter proposes a reduced switch converter topology driven by a very efficient switching algorithm to control the torque ripple. In this switching strtagy the common converter is always in ON postion. The following switching strategy will be available in every phase.

Magnetization: Sahi and Scom will be in ON for one time and during this time the positive flux will be generated. Salo and Scom for one time and in this case the negative flux will be generates.

De magnetization: The common switch will be in on position for all time and the switches in off-going phase leg are off. Phase current commutates to diodes and decays rapidly.

Freewheeling mode: The winding can be short-circuited by ei turning off switches in the corresponding phase leg as high or low and the Scom will be in ON position in any mode of operation. Phase current decays slowly.

The operation characteristics of new reduced switch converter are shown in the figure 7.

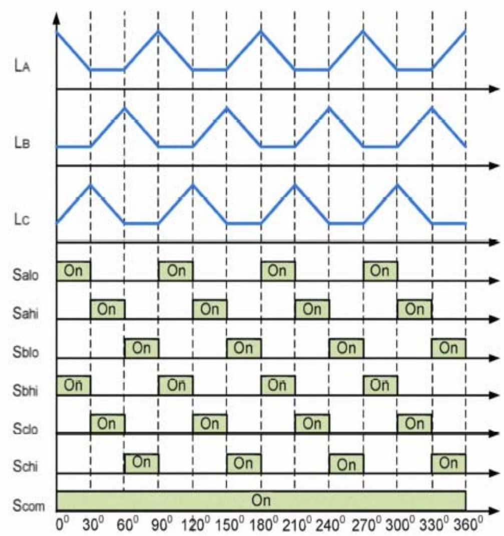

Fig 7: Basic switching for the new reduced switch converter.

D. SIMULATION MODEL:

Here in this models the input dc voltage is 240V, negative torque is -20, moment of inertia in SRG modeling is 0.0028 and friction coefficient is 0.026, number of turns per phase is 50, the switches used for the converter are IGBT switches and the switching frequency is 50Hz

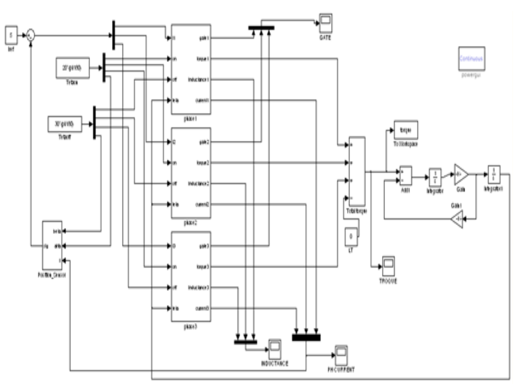

Fig 8: Simulation model of SRG

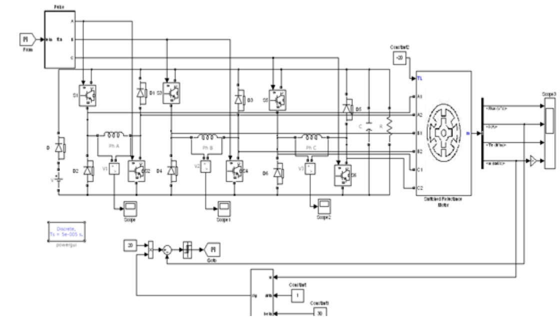

Fig 9: Simulation diagram SRG drive using AHBC

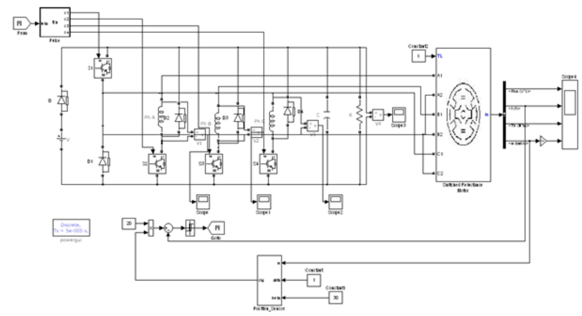

Fig 10: Simulation diagram SRG drive using Miller converter

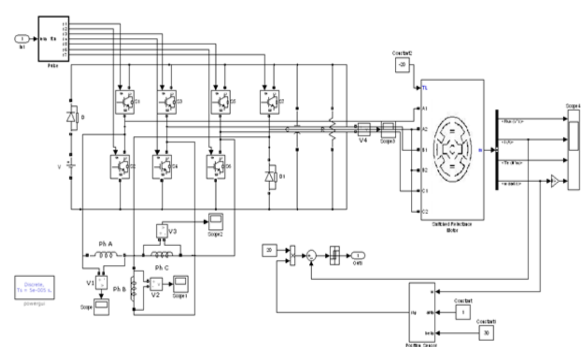

Fig 11: Simulation diagram SRG drive using New converter

III. SIMULATIONS RESULTS

The proposed model is implemented into MATLAB software and simulated for analysis of converters for switched reluctance generator. Figures 9, 10 and 11 show the three converter simulation model for SRG. Here in this models the input dc voltage is 240V, negative torque is -20, moment of inertia in SRG modeling is 0.0028 and friction coefficient is 0.026, number of turns per phase is 50. The gate signals of the three converters given to the SRG machine is shown in the figure 12, 13 and 14 simulation output of the AHBC for SRG is shown in the fig 15,Miller converter shown in the fig 16 and the simulation output of the new converter for SRG is shown in the fig 17.

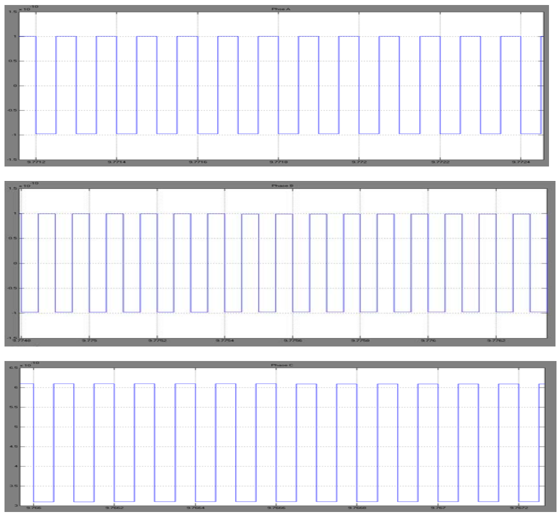

Fig 12: Gate signals output of the AHBC.

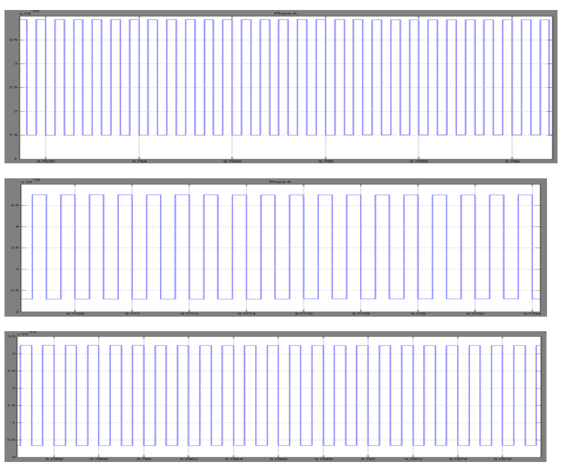

Fig 13: Gate signals output of the Miller converter.

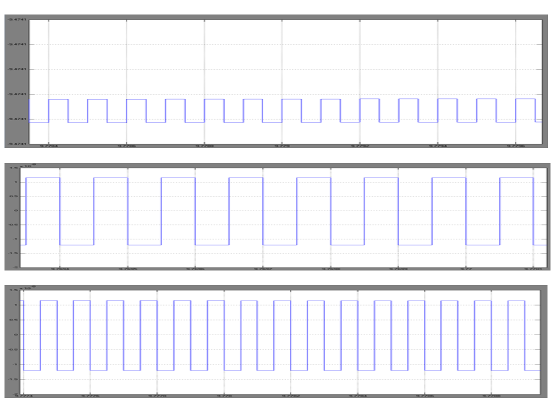

Fig 14: Gate signals output of the New converter.

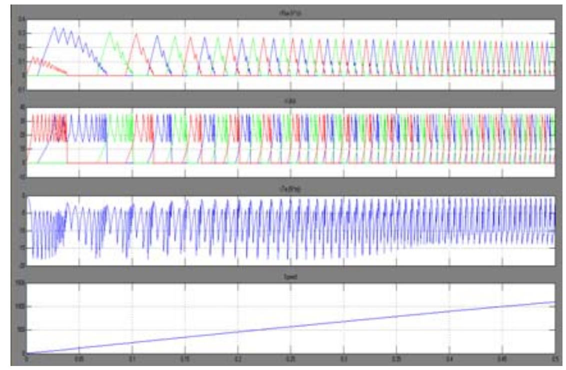

Fig 15: Simulation Output of the SRG Driver Using Asymmetrical Half Bridge Converter.

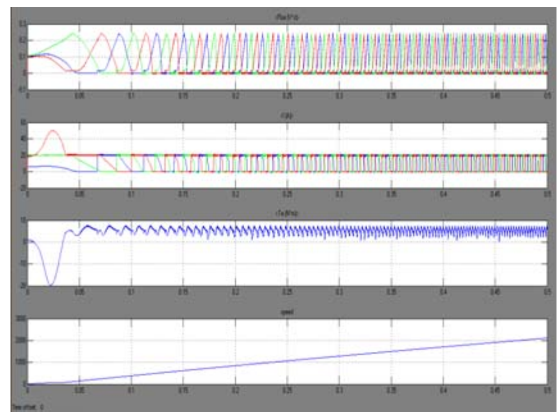

Fig 16: Simulation Output of the SRG Driver Using Miller converter.

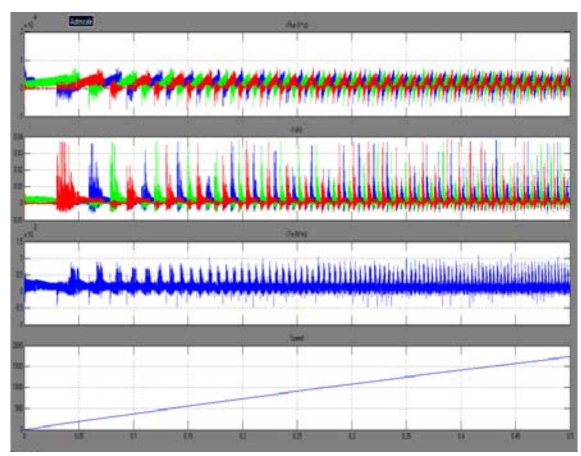

Fig 17: Simulation Output of the SRG Driver Using New converter.

On by comparing the simulation results of AHBC, Miller and New converter analysis for SRG, the Miller converter is performing its operation above the rated speeds also and the switching losses are less compare to the other converters . So, the Miller converter is best suitable for SRG drive system.

IV. CONCLUSIONS

The simulation process is carried out between AHBC and New converter for SRG of these three converters by using MATLAB. On the basis of the analysis of simulation results, the performance of SRG is better with Miller converter when compared with the AHBC and New converter and it is analyzed by comparing the speeds of the simulation output and the switching losses and is depends on the number of switches used for the corresponding converter simulation. From simulation output the Miller converter is working above the base speeds also where AHBC is operating with the rated speed and the New converter is operating just across the rated speed for same rating of the generator.

REFERENCES

[1]. A Modified Switching Strategy For Asymmetric Half-Bridge Converters For Switched Reluctance Motor Drives.P. Chancharoensook and M.F. Rahman

[2]. A New Converter Topology and Control Scheme for Switched Reluctance Machines in application to Wind Energy Conversion System. Erkan Sunal, Kazmi Syed Muhammad Raza, Hiraki Goto, Hai-Jiao Guo, Osamu Ichinokura.

[3]. A Novel Power Inverter for Switched Reluctance Motor Drives. zeIjkoGrbo, Slobodan Vukosavic, and Levi

[4]. Switched Reluctance Generator for Variable Speed Wind Energy Applications. Amissa Arifin, Ibrahim Al-Bahadly.

[5]. Dynamic Simulation Model of Switched Reluctance Generator.Osamu Ichinokura, Member, *IEEE*, Tsukasa Kikuchi, Kenji Nakamura, Member, *IEEE*,

[6]. Design and Control Characterization of Switched Reluctance Generator for Maximum Output Power. P. Asadi, M. Ehsani, B. Fahimi.

[7]. Study on an Alternative Converter Performance for Switched Reluctance Generator. Fleury, A.(1), Andrade, D.(2), Oliveira, E. S. L.(3), Fleury-Neto, G. A.(3), Oliveira, T. F.(3), Dias, R. J.(3) , A. W. F. V. Silveira.

◈◈◈

Design And Analysis of Single Stage Buck-Boost PFC With Flyback Converter To Drive Leds For Lightening Applications

Laxmikant Reddi [1], Manish.G.Rathi[2] & PavanKumar[3]

Dept of Electrical & Electronics Engg, Poojya Doddappa Appa College of Engg, Gulbarga. INDIA

Abstract- Due to the enormous progress recently achieved in the technology of light emitting diodes (LEDs) it can be expected that LEDs lighting will replace incandescent and halogen bulbs in general illumination in the near future. A LED light source typically consists of a series connection of single LED cells.The conventional driver stage approach employs two stages: the first stage is using a non-isolated boost converter to perform input-current shaping and universal input voltage handling and the second stage is using an isolated flyback converter to subsequently step down the boosted voltage to a desirable load-regulated output voltage.The drawbacks of two-stage topology are lower efficiency due to twice processing of the input power, larger control circuits, higher cost and lower reliability. This paper develops a single-stage power driver for high-power LEDs with high power factor, high efficiency, reduced voltage stress on the power switch, cost-effectiveness, ability to be dimmed, and constant voltage control scheme. The presented circuit combines a buck-boost PFC converter with a flyback converter into a single-stage power-conversion circuit. MATLAB is applied to execute whole circuit simulations. Finally, a prototype driver is developed and tested in order to supply 100W LEDs with universal utility-line input voltages.

Keywords *- LED lamps, driver circuit, Power Factor Correction, Single Stage PFC, Flyback.*

I. INTRODUCTION

About one-fifth of the electric power is used for residential, commercial and industrial lighting applications world-wide. The commonly employed lighting sources include incandescent bulbs and fluorescent lamps [1]-[4].Incandescent bulbs and florescent lamps generate light via two physical mechanisms for converting electrical energy. Incandescent bulbs exploit Joule-heating by the electrical heating of a highly-resistant tungsten filaments to intense brightness. The electrical behavior is simple. The lamp current is determined by the applied voltage and the resistance of the tungsten filament, whose v-i characteristic is close to that of a linear resistor. However, only about 10% of the electricity flowing through incandescent bulbs is converted to light, so the luminous efficiency of incandescent bulbs is very low. Fluorescent lamps convert electrical energy into light by transforming electrical energy into the kinetic energy of moving electrons, which in turn generate radiation when they collide. Modifying the composition of the gas can considerably alter the luminous efficiency. Although fluorescent lamp offers high luminous efficiency at a low cost, its mercury content is harmful to both the health and the environment. Besides, the fluorescent lamps require high striking voltage for starting and limiting currents after ignition because they have negative incremental impedance characteristics. Traditional electromagnetic ballasts, operating at line frequency, have been used to solve these problems. In spite of their low cost, these ballasts present flicking, large size, heavy weight, and hum. Compared with the traditional commonly used lighting sources, LED has 30% efficiency and much room to improve [5]-[6]. Unlike the fluorescent lamp, it contains no mercury, and is not easy to break. It is compact and can be installed on printed circuit board (PCB). It has very long lifetime (100,000 hours which is more than 10 times of a fluorescent lamp), and high turn on/off times. In addition, it is easy to drive compared with the traditional sources. Therefore, LEDs for lighting sources have received great attention in recent years owing to their merits of light weight, small size, energy saving, high luminous efficiency, long lifetime and environmental friendliness. Obviously, LED lighting application is more suitable as the lighting source for general lighting applications in the future.

Typically, the lighting fixture with LEDs commonly uses a full-bridge rectifier and a high-frequency inverter with an isolated transformer that converts the switching converter output characteristic from a voltage source into a current source, thus ensuring stable driving current for LED devices [7]-[10]. Because the full-bridge rectifier absorbs energy from the AC power line only when the input voltage is higher than the dc-link voltage, the input line current contains rich harmonics, which pollute the power system and interfere with other electronic equipment. The power factor (PF) is typically less than 0.6 and the total harmonic distortion (THD) can be greater than 100%. In order to improve the consumption of electrical energy and meet the power quality standards, the LED lighting fixtures must incorporate power factor correction (PFC) techniques. Usually, PFC circuits present better results related to PF and THD in the input current. Then, the AC power line can be utilized more efficiently.

Basically, these techniques can be realized in two forms, i.e. two-stage topology and single-stage topology [11]-[14]. In two-stage topology, an ac/dc converter with PFC is connected to the AC power line, followed by a dc/dc converter. These two power stages can be controlled separately, and thus it makes both converters possible to be optimized. Another advantage of two-stage topology is that the bulk capacitor of the PFC circuit is located at the high voltage side, resulting in more energy stored in the capacitor and hence a longer hold-up time. The drawbacks of this topology are lower efficiency due to twice processing of the input power, larger control circuits, higher cost and lower reliability. On the other hand, single-stage topology combines the PFC circuit and power conversion circuit in one stage. Due to its simplified power stage and control circuit, this topology is potentially more efficient. The underline strategy of this scheme is to design the circuit in a certain way that allows its PFC circuit and power conversion circuit to share the same power switch. Despite of the increased popularity of this single-stage approach, the conventional two-stage approach still dominates the commercial ac/dc power adapter in LED lighting applications. The two-stage approach employs two stages: the first stage is using a non-isolated boost converter to perform input-current shaping and universal input voltage handling and the second stage is using an isolated flyback converter to subsequently step down the boosted voltage to a desirable load-regulated output voltage. Although the two-stage solution has drawbacks of high cost and large size, it is still commonly used due to its relatively simple and viable operation in wide power range and universal line range application.

A string of LED in series and/or parallel needs proper voltage and current to drive. A more efficient method of providing proper voltage level and electrical isolation between input AC power line and output driver circuit of the LED lighting fixture is to adopt a high-frequency isolated transformer. A number of isolated power conversion topologies can be used as both LED driver and PFC stage.Generally, the isolated switching-mode converter, which is fundamentally classified into three types of flyback converter, forward converter and push-pull converter, has been developed in the use of both LED driver and PFC stage [15]-[18]. Comparing the three different isolated dc/dc converter topologies, it appears that the flyback converter is the best topology for this application because of its many merits. In addition, for single-phase lighting applications, the flyback converter is generally recommended as high power factor (HPF) input rectifying stage, especially for low power levels (as in this application, feeding multiple LEDs), due to its simple circuitry and typical input characteristics. Therefore, a two-stage approach, i.e., a PFC stage followed by a LED driver stage, is utilized. The two-stage approach has good performances such as a near unity power factor and wide range of line input voltage variation. Besides, the design procedure is relatively easy. The main problem of the two stage approach is that it has more components and, thus, a higher cost, which is a drawback for cost-sensitive products. Several single-stage PFC LEDs driver circuit, aimed at reducing the cost, have been proposed previously. In the single-stage approach, the PFC stage is combined with the LED driver stage into one stage; thus one or more active power switches and its controller can be saved, and consequently the cost is reduced. Although both boost and flyback converters are capable for single-stage PFC applications, the boost converter finds more usage than the flyback converter, partly because the existing control methods make it easier to control the average inductor current than the average switch current. For low power applications, the flyback converter is more attractive than the boost converter because of its simplicity. It provides the isolation, start-up, and short-circuit protection with a single switch. Besides, the input line voltage is not necessarily lower than the output voltage, as in the boost converter case. Then, a high power factor can be achieved by deliberately operating the flyback converter in the discontinuous conduction mode (DCM) with constant frequency control scheme. As a consequence, the flyback converter provides simultaneously a unity power factor to the utility line and appropriate output voltage to the LED strings, as well as offers small size, low cost and high reliability compared to conventional two-stage high-power-factor LEDs driver circuit The gate drive signal of the active power switch of the flyback converter is generated by comparing the saw-tooth carrier signal of the PWM controller with the output voltage feedback signal. This circuit has the advantages of one stage of power conversion, no need to sense the input voltage, simple feedback control, high power factor and dimmable LED current. It is particular suitable for the LED lighting applications. The critical design constraints and equations for both the power stage and control loop are highlighted and detailed.

II. ANALYSIS OF THE PRESENTED LED DRIVER

The proposed power driver for high-power LEDs, along with a control integrated-circuit (IC) that uses a peak-current control scheme for achieving input current shaping and constant output voltage control, is shown in Fig1; the driver integrates a buck-boost PFC converter with a flyback converter into a single-stage power converter and includes an inductor Lin and a magnetic inductor Lm, four capacitors Cin, Crec, Cf and Cb, a power switch Sb, six diodes D1, D2, D3, D4, Df and Db, a transformer Tr, and the LEDs.

The proposed LED driver, shown in Fig. 1, consists of a buck-boost-flyback converter and it is composed of transformer T_r with two windings, power switch S_b, two diodes D_b and Df, and two dc-linked capacitors C_b and C_f. The input utility-line voltage V_{ac} is defined as

$$V_{ac} = V_m \sin 2\pi ft \tag{1}$$

Where V_m is the input peak voltage, f is the utility-line frequency. In order to simplify analysis, it is considered that the switching frequency is much higher than line frequency. Thus, the sinusoidal input voltage can be considered constant for each switching period. The operational principals of the proposed circuit are described as followings.

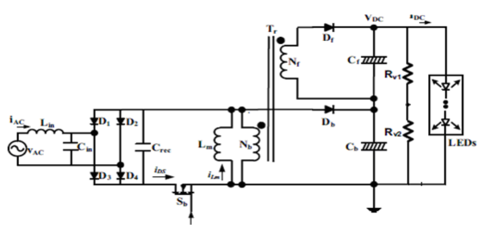

Fig1

The proposed single-stage power driver for LEDs.

Operation of Buck-Boost-Flyback Converter

The operation modes and key switching waveforms of the two-output buck-boost-flyback converter are shown in Fig. 2.Mode 1 (t0, t1) - When the switch Sb is turned on at t0, the absolute value of the average rectified voltage $|V_{rec}|$ is applied to the magnetic inductor L_m, and the magnetizing current I_{Lm} linearly increases. Since the buck-boost-flyback converter is designed to operate in boundary-conduction-mode (BCM) for achieving high-power-factor (HPF), the magnetizing current linearly increases from zero, and can be expressed as

$$I_{Lm}(t) = \frac{|V_{rec}|}{L_m}(t_1 - t_0) \tag{2}$$

where $V_{rec}=2V_m/\pi$- average value of input rectified voltage .The diodes D_b and D_f are off due to reverse biased therefore, no current flows through the windings N_b and N_f. The current I_{Lm} increases linearly to its peak value according to the following equation

$$I_{Lm,pk} = \frac{|V_{rec}|}{L_m} DT_s \tag{3}$$

Where D - duty cycle of the switch S_b ,T_s- switching period This mode finishes with the switch S_b turning off.

Mode 2 (t1, t2) - [Fig. 2)]: When S_b is turned off at t1, D_b and D_f turn on due to forward biased. Specifying the number of primary and secondary turns is identical, which means $N_b=N_f$ and$V_{Cb}=V_{Cf}=V_{DC}/2$. Thus, the drain-to-source voltage V_{DS} is given by

$$V_{DS} = |V_{rec}| + \frac{V_{DC}}{2} \tag{4}$$

The magnetizing current i_{Lm} linearly decreases with a down-slope of $V_{DC}/2Lm$, and can be expressed

$$I_{Lm}(t) = \frac{V_{DC}}{2L_m}(t_2 - t_1) \tag{5}$$

The diode currents i_{Db} and i_{Df} deliver energy to the capacitors C_b and C_f as well as LEDs during the off-time interval. This mode finishes when power switch S_b turns on again at time interval t_2.

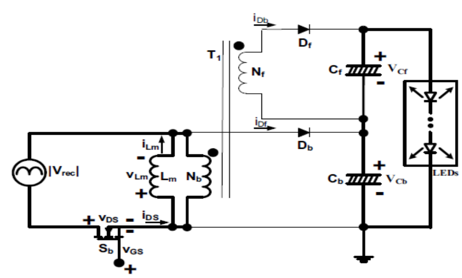

(a) Mode 1

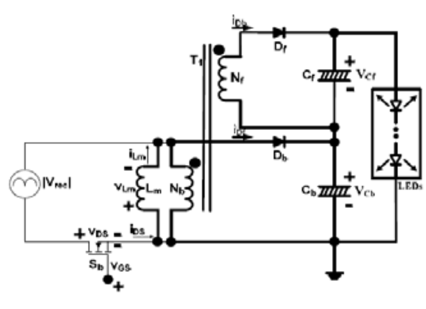

(b) Mode 2

Fig.2 Operation modes of the proposed LEDs driver.

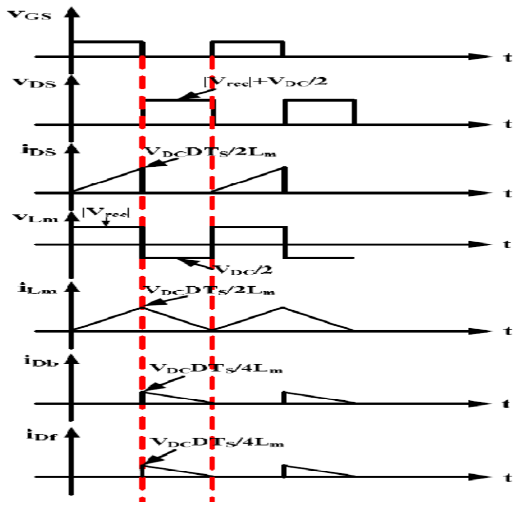

Fig 3 The buck boost-flyback converter switching waveforms

III. DESIGN GUIDELINES OF KEY COMPONENTS

A. Design Equation of Magnetic Inductor Lm

Fig. 3 shows the illustrated waveform for the magnetic inductor current i_{Lm} under the control scheme that has constant T_{on} and variable T_S. The peak value of input current is given by

$$I_{AC-PK} = \frac{\sqrt{2}P_{in}}{V_{AC-rms,\min}} = \frac{\sqrt{2}P_{out}}{\eta V_{AC-rms,\min}} \qquad (6)$$

Where $V_{AC\text{-}rms,min}$ is the minimum value of the input utility-line rms voltage; η is the estimated circuit efficiency, and the relationship between input power P_{in} and output power P_{out} is $P_{out}=\eta P_{in}$.

The peak value of magnetic inductor current can be expressed by

$$I_{Lm-pk} = 2I_{Ac-pk} = \frac{2\sqrt{2}P_{out}}{\eta V_{Ac-rms,\min}} \qquad (7)$$

Where ΔI is the difference in amplitude between peak and low levels of current, and T_{on} and T_{off} are turn-on and turn-off time of the power switch, respectively.

$$\Delta I = \frac{V_{Ac}}{L_m}T_{on} = \frac{2\sqrt{2}V_{AC-rms} - V_{DC}}{2L_m}T_{off}$$

In order to design the magnetic inductor under BCM, the turn-on time of the power switch can be expressed by

$$T_{on}(2\pi f_{AC}t) = \frac{L_m I_{Lm-pk}\sin(2\pi f_{AC}t)}{\sqrt{2}V_{AC-rms,\min}\sin(2\pi f_{AC}t)} \qquad (8)$$

While sin($2\pi f_{AC}t$) is equal to unity, the maximum level of T_{on} is given by

$$T_{on} = \frac{L_m I_{Lm-pk}}{\sqrt{2}V_{AC-rms,\min}} \qquad (9)$$

The turn-off time of the power switch can be expressed as

$$T_{off}(2\pi f_{AC}t) = \frac{2L_m I_{Lm-pk}\sin(2\pi f_{AC}t)}{2\sqrt{2}V_{AC-rms,\min}\sin(2\pi f_{AC}t) - V_{DC}} \qquad (10)$$

the magnetic inductor Lm operated in BCM can be expressed as

$$L_m = \frac{V_{AC-rms,\min}^{2}(2\sqrt{2}V_{AC-rms,\min}\sin(2\pi f_{AC}t) - V_{DC})}{2f_{sw-\min}P_{in}(4\sqrt{2}V_{AC-rms,\min} - V_{DC})} \qquad (11)$$

where $f_{sw\text{-}min}$ is the minimum switching frequency of the power switch.

B. Description of DC Output Voltage V_{DC}

The DC output voltage VDC can be expressed as

$$V_{DC} = (1+\frac{N_f}{N_b})\frac{\sqrt{2}V_{AC-rms,\min}D_{\max}}{1-D_{\max}} \qquad (12)$$

Where N_b and N_f, respectively, are the primary-side and secondary-side windings of the transformer T_r, and D_{max} is the maximum duty cycle of the power switch S_b.

C. Design Equation for Turns-Ratio n

From (14), the definition of turns-ratio n of transformer T_r can be determined by dividing windings N_f by N_b, and can be expressed as

$$n = \frac{N_f}{N_b} = \frac{(1-D_{\max})V_{DC}}{\sqrt{2}V_{AC-rms,\min}D_{\max}} - 1 \qquad (13)$$

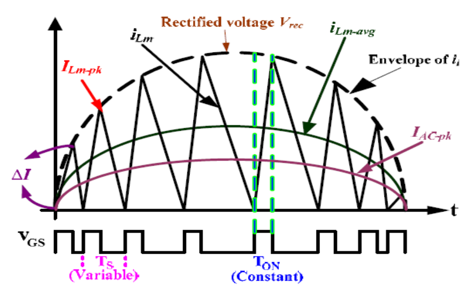

Fig. 4. Illustrated waveform of magnetic inductor current iLm under constant Ton and variable TS control scheme.

IV. DESIGN EXAMPLE

A. Input Specifications

1) input utility-line voltage: $V_{AC\text{-}rms} = 230V$

2) input utility-line frequency: f_{AC}=50Hz

3) minimum input voltage: $V_{AC\text{-}rms,min} = 85V$

4) output power: $P_{out} = 100W$

5) output voltage: V_{DC}= 100V

6)output current: $I_{DC} = 1A$

7) minimum switching frequency $f_{sw\text{-}min}$: 10 kHz

8) maximum duty cycle D_{max}: 0.5

9) estimated efficiency η : 90%

B. Determining Peak Value of Input Current and Inductor Current

According to (5.6) and (5.7), the peak value of input current Iin-pk and magnetic inductor current ILm-pk are respectively given by

$$I_{AC-PK} = \frac{\sqrt{2}P_{in}}{V_{AC-rms,\min}} = \frac{\sqrt{2}P_{out}}{\eta V_{AC-rms,\min}}$$

$$I_{AC-PK} = \frac{\sqrt{2}100}{0.9 * 230} = 0.683\ A$$

C. Determining the Magnetic Inductor Lm

From (27), the magnetic inductor Lm can be determined by

$$L_m = \frac{V_{AC-rms,\min}{}^2 (2\sqrt{2}V_{AC-rms,\min}\sin(2\pi f_{AC}t) - V_{DC})}{2 f_{sw-\min} P_{in}(4\sqrt{2}V_{AC} - rms,\min - V_{DC})}$$

$$= \frac{230^2(2\sqrt{2} * 230 - 100)}{2 * 10K \cdot (\frac{100}{9})(4\sqrt{2} * 230 - 100)} = 0.001mH$$

D. Determining the Turns-Ratio n

Referring to (15), the turns-ratio n is given by

$$n = \frac{N_f}{N_b} = \frac{(1 - D_{\max})V_{DC}}{\sqrt{2}V_{AC-rms,\min} D_{\max}} - 1$$

In addition, the turns-ratio n is selected as 1.

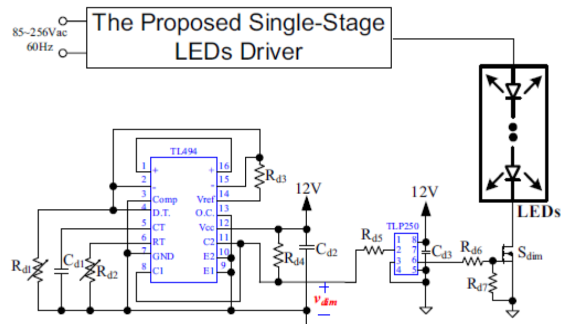

Fig. 5. The dimming control circuit utilized in the presented single-stage LEDs driver.

Fig. 5 shows the dimming control circuit utilized in the presented single-stage LED driver; it is composed of a pulse-width-modulation (PWM) IC (TL494), an optical coupler (TLP250), and a power switch S_{dim} in series connection with the LEDs. The duty cycle and switching frequency of the dimming control voltage signal v_{dim} from the PWM IC are respectively determined by the resistor R_{d1} and the resistor R_{d2} along with the capacitor Cd1. By altering the resistor Rd1, the dimming signal v_{dim} feeds into the power switch S_{dim} through the optical coupler and changes the duty cycle of S_{dim}, and thus the dimming function is achieved for the LEDs.

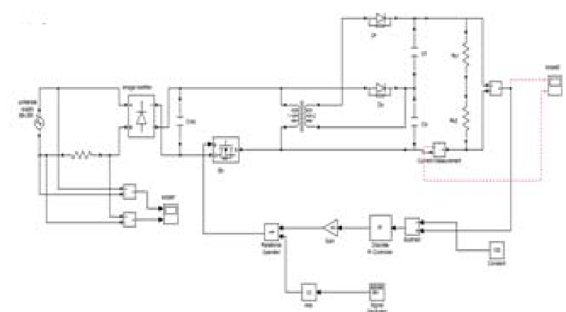

Fig 6 Simulation model of LED driver. A 230v 50 Hz input supply

Fig 6 Shows the simulation model of LED driver. A 230v 50 Hz input supply is fed to an bridge rectifier and the corresponding dc out-put is obtained. The filtered dc is then fed to a flyback converter where it is boosted. A closed loop feedback control is used in the circuit to maintain constant output. The output of the flyback is given to a summer where it is compared to a 100v constant and the error signal (if any) is fed to the PWM modulation block. In PWM modulation where the gating pulses for the MOSFET switch of flyback converter is generated. Hence the feedback control ensures a constant dc. This dc is then finally connected to the load.

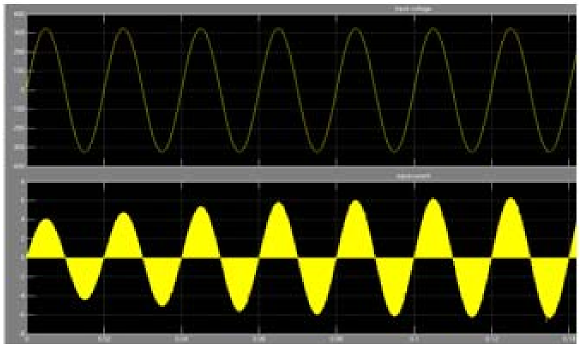

Fig 7 input voltage and input current waveform shows high power factor

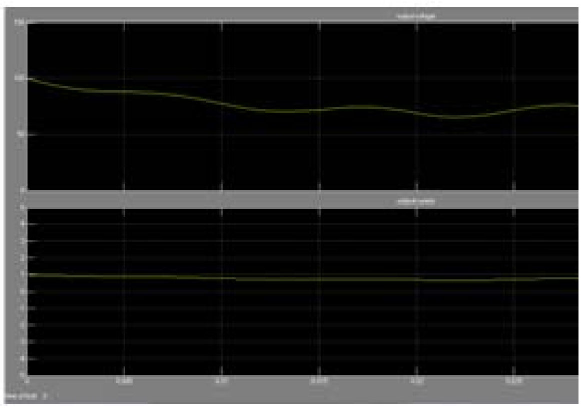

Fig 8 output voltage and output current waveform

V. EXPERIMENTAL RESULTS

A prototype driver for supplying 100W LEDs (ten high-power-rated LEDs in series connection and rated power of 10 W for each LED) has been built and tested in this paper, and Table I displays the specifications of the utilized high-power-rated LEDs. The key parameters in the proposed driver for high-power LEDs are presented in Table II.

Fig. 9 depicts the measured output voltage VDC (approximately 100 V) and current IDC (about 1 A). The measured input utility-line voltage (from 230 V-rms) and current are shown in Fig. 10. Table III lists the measured input utility-line current harmonics, and compares them with the IEC 61000-3-2 Class C standards. The measured power factor and total harmonic distortion (THD) are 0.98 and 15%, respectively, as determined by utilizing a power analyzer.

The measured output voltage, current waveforms are shown in Fig. 10, Fig. 11 respectively.

Fig.11 shows measured power factor and efficiency under input utility-line voltage .The measured efficiency of the presented ballast is approximately 90% at a utility-line voltage of 85 V. Moreover, the measured highest efficiency of 91% along with lowest power factor of 0.91 occurred at maximum utility-line voltage of 230V; the measured lowest efficiency of 89.2% along with highest power factor of 0.95 occurred at minimum utility-line voltage of 85V.

Fig. 12 depicts the digital photos of the prototype LED driver along with ten high-power-rated LEDs. The photos before lighting and after lighting the eight LEDs are shown in Fig. 13(a) and Fig. 13(b), respectively.

TABLE I.

SPECIFICATIONS OF THE UTILIZED HIGH-POWER-RATED LEDS

Items	Values
Each LED Rated Voltage	10 V
Each LED Rated Current	1 A
Each LED Rated Power	10 W
Output Voltage of 8 LEDs in Series Connection	100 V
Output Current of 8 LEDs in Series Connection	1 A
Output Power of 8 LEDs in Series Connection	100 W

TABLE II.

KEY PARAMETERS IN THE PROPOSED HIGH-POWER LED DRIVER

Parameters	Values
Filter Inductor (Lin)	3Mh
Filter Capacitor (Cin)	100nF/630V
Magnetic Inductor (Lm)	0.001Mh
Power Switch (Sb)	SPP20N60S5
Power Diode (Df , Db)	BYT56M
Capacitors (Cf , Cb)	470µF/250V

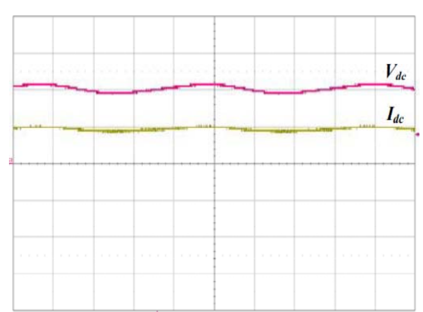

Fig 9 . Measured output voltage V_{dc} (100V/div) and current I_{dc} (0.5A/div); Time: 2ms/div.

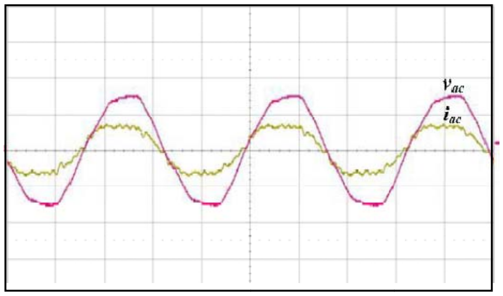

Fig. 10. Measured input utility-line voltage v_{ac} (100V/div) and current i_{ac} (2A/div); Time: 5ms/div.

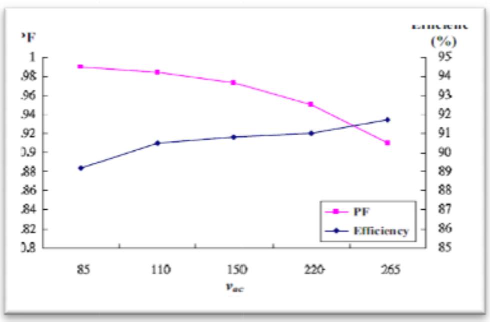

Fig. 11. Measured power factor and efficiency of the presented driver under universal input utility-line voltage.

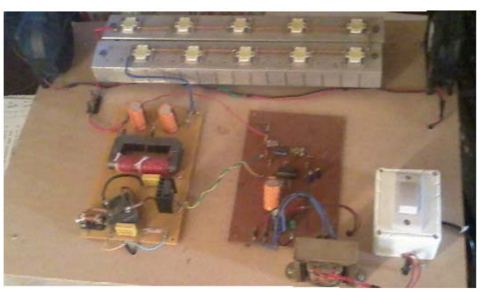

(a)

(b)

Fig. 12. Photos of the prototype LED driver along with 10 high-power-rated LEDs, taken with a digital camera (a) before lighting 8 LEDs, and (b) after lighting 8 LEDs.

TABLE III.

MEASURED INPUT UTILITY-LINE CURRENT HARMONICS COMPARED WITH IEC 61000-3-2 CLASS C STANDARDS.

Order(n)	IEC 61000-3-2 Class C Standards (%)	Measured (%)
2	2	0.8
3	30× Power Factor	13.6
5	10	5.3
7	7	3.3
9	5	2.4
11≤n≤39	3	1.9

VI . CONCLUSION

The analysis and design of the presented high power led driver is done. Simulation is done using MATLAB and results shows that high input power factor, high efficiency and low total harmonic distortion. The proposed single-stage dimmable power driver consists of constant output voltage control scheme for supplying LEDs. The proposed driver, integrates a buck-boost PFC converter with a flyback converter into single stage conversion and it offers fewer power switches and greater cost-effectiveness than the conventional version.buck-boost converter is used for power factor correction and flyback is used for supplying power to the load. A prototype circuit has been built in order to provide 100W LEDs with 110V-rms utility-line input voltage. The experimental results have demonstrated high power factor (>0.95), high efficiency (>0.9), low THD (<15%), and constant output voltage for supplying LEDs; these results verify the functionality of the proposed LED driver triangle wave, and sine wave respectively.

REFERENCES

[1] A.Zukauskas, Introduction to solid-state lighting, Wiley 2002.

[2] E. F. Schubert, Light-emitting diodes, Cambridge University Press, 2006.

[3] ON Semiconductor, “LED lighiting solutions”, Feb. 2010, pp. 1-36.

[4] S. Y. R. Hui, S. N. Li, X. H. Tao, W. Chen and W. M. Ng,”A novel passive off-line light-emitting-doide (LED) driver with long lifetime,” in Proc. of IEEE APEC’10, pp. 594-600, 2010.

[5] J. Sebastian, D. G. Lamar, M. Arias, M. Rodriguez, and M. M. Hernando,” A very simple control strategy for power factor correctors driving high-brigtness LEDs,” in Proc. of IEEE APEC’08, pp 537-543, 2008.

[6] H. J. Chiu, Y. K. Lo, J. T. Chen, S. J. Cheng, C. Y. Lin and S. C. Mou, “A high-efficiency dimmable

LED driver for low-power lighting applications", IEEE Trans. Ind. Electron., vol. 57, no. 2, Feb. 2010, pp.735-743.

[7] H. Broeck, G. Sauerlander and M. Vendt, "Power driver topologies and control schemes for LEDs," in Proc. of IEEE APEC'07, pp. 1319-1325, 2007.

[8] D. Gacio, J. M. Alonso, A. J. Calleja, J. Garcia and M. Rico-Secades, "A universal-input single-stage high-power-factor power supply for HB-LEDs based on integrated buck-flyback converter, in Proc. Of IEEE APEC'09, pp. 570-576, 2009

Virtual Mouse by Motion Recognition Using Template Matching

Balaji Thiruppathi[1], **Subramanian Alagappan**[2] **& T. E. Raja**[3]
1. Amritha school of engineering,coimbatore
2. P.B College of engineering, Chennai
SRM University, Chennai

Abstract - Mouse is one of the most commonly used Input devices. But this is in use for more than two decades. We need more intuitive computer interface. In this paper I am proposing to use the camera as mouse by processing the image captured by the camera and tracking the motion of specific objects in the image and determine the X, Y coordinates of the mouse. This will make the computing interface more intuitive and fun to use. OpenCV library is integrated with VisualC++ for computer vision functions.

Keywords: *Human Computer Interaction, Image processing, Gesture recognition, Object detection.*

I. INTRODUCTION

In the last decade the computing technology has improved a lot but, the interface devices are still the same old keyboard and mouse. These devices make computing bounded to limits so; we need more intuitive computer interface. Now a days we have some great technology such as surface computer, Next generation tablets, etc. But these devices are of high cost. We need more intuitive and cost effective computing interfaces. The best solution for this problem is using the webcam in the computer as input device.

Gestures are one of the important and inevitable activities we do in our day to day life. So, using these gestures to interact with the computer would be much easier, intuitive and fun to use. In this paper I am proposing a new way to interact with the computer using gesture and motion recognition. I have used OpenCV library integrated with VisualC++ for object detection, gesture recognition and motion tracking.

This Kind of method is already available but the method used is less efficient than the proposed method. In the existing method a technique called corner detection is used where most recognizable corners are chosen and tracked but when there is some sudden physical changes such as light change then this becomes inefficient but in the proposed system template matching method is used where a user selected area is saved as a separate image and used as a template to run through the image and matched with the next frame of the video input to detect the part in the image so, that we can track the area to use as mouse.

II. THE METHOD

A. Object Detection

Object detection is the first and foremost step in motion tracking. To track an object in a live video feed, we first need to identify the object to track. To track an object we follow many methods. They are:

1.) Background subtraction.

2.) Watershed algorithm.

3.) Mean-Shift segmentation

4.) Delaunay triangulation, Voronoi tesselation

B. Motion Tracking

When an object to be tracked is detected its motion is tracked using many methods. Some of the methods are:

1.) Template matching

2.) Corner finding

3.) Optical flow

4.) Mean-Shift and CamShift tracking

5.) Motion Templates

C. Gesture Recognition

Motion templates were invented in the MIT Media Lab by Bobick and Davis [Bobick96; Davis97] and were further developed jointly with one of the authors [Davis99; Bradski00].

Motion templates are an effective way to track general movement and are especially applicable to gesture recognition. Using motion templates requires a silhouette (or part of a silhouette) of an object. Object silhouettes can be obtained in a number of ways.

1.) The simplest method of obtaining object silhouettes is to use a reasonably stationary camera and then employ frame-to-frame differencing. This will give you the moving edges of objects, which is enough to make motion templates work.

2.) You can use Chroma keying. For example, if you have a known background color such as bright green, you can simply take as foreground anything that is not bright green.

3.) Another way is to learn a background model from which you can isolate new foreground objects/people as silhouettes.

4.) You can use active silhouetting techniques—for example, creating a wall of near infrared light and having a near-infrared-sensitive camera look at the wall. Any intervening object will show up as a silhouette.

5.) You can use thermal imagers; then any hot object (such as a face) can be taken as foreground.

6.) Finally, you can generate silhouettes by using the segmentation techniques (e.g., pyramid segmentation or mean-shift segmentation).

III. THE EXISTING SYSTEM

The Existing method of motion tracking involves two main methods Template matching, ROI (Region of Interest) in Corner finding.

Template matching involves two images target image and template. The target image is obtained from the live webcam, template image is preset and used to match with the target image.

The algorithm for template matching is as follows:

```
IplImage *res=cvCreateImage(size,IPL_DEPTH_32F,1);
cvMatchTemplate(tgt,tml,res,CV_TM_SQDIFF);
cvMinMaxLoc(res,&minval,&maxval,&minloc,&maxloc,0);
```

Figure 1: Template Matching is done by running template image into target image in hoizontal and vertical direction

ROI method involves selecting the particular Region of Interest. Usually ROI is selected by the user using mouse event handling. The algorithm for ROI is as follows:

```
void mouseHandler(int event, int x, int y, int flags, void* param)
{
/* user press left button */
if (event == CV_EVENT_LBUTTONDOWN && !drag)
{
point = cvPoint(x, y);
drag = 1;
}
/* user drag the mouse */
if (event == CV_EVENT_MOUSEMOVE && drag)
{
img1 = cvCloneImage(frame);
cvRectangle(img1, point, cvPoint(x, y), CV_RGB(255,0,0),
1, 8, 0);
cvCopy(img1,frame, NULL);
cvShowImage("result", img1);
}
```

```
/* user release left button */
if (event == CV_EVENT_LBUTTONUP && drag)
{
img1 = cvCloneImage(frame);
cvSetImageROI(img1, cvRect( point.x, point.y, x - point.x          point.y));
cvNot(img1, img1); // or do whatever with the ROI
cvResetImageROI(img1);
cvCopy(img1,frame, NULL);
cvShowImage("result", img1);
drag = 0;
}
/* user click right button: reset all */
if (event == CV_EVENT_RBUTTONUP)
{
cvShowImage("result", frame);
drag = 0;
}
```

This algorithm allows the user to select a particular region which is then tracked by corner tracking by finding the best parts.

Figure 2 : ROI is selected by the user.

Both these methods have some drawbacks. The template matching method fails because of the different lighting conditions where the user is and ROI corner finding fails due to laggy images and a lot of other factors.

IV. THE PROPOSED SYSTEM

I propose a new method to track the objects using both ROI and Template matching method. In this method the user selects an ROI and this ROI is saved as a new image and used as a template and template matching technique is used to find out the position of the object in each frame live from the webcam.

The algorithm for this technique is the combination of the two algorithms mentioned above.

```
void mouseHandler(int event, int x, int y, int flags, void* param)
{
/* user press left button */
if (event == CV_EVENT_LBUTTONDOWN && !drag)
{
point = cvPoint(x, y);
drag = 1;
}
/* user drag the mouse */
if (event == CV_EVENT_MOUSEMOVE && drag)
{
img1 = cvCloneImage(frame);
cvRectangle(img1, point, cvPoint(x, y), CV_RGB(255,0,0),
1, 8, 0);
cvCopy(img1,frame, NULL);
cvShowImage("result", img1);
}
/* user release left button */
if (event == CV_EVENT_LBUTTONUP && drag)
{
img1 = cvCloneImage(frame);
cvSetImageROI(img1, cvRect( point.x, point.y, x - point.x          point.y));
cvNot(img1, img1); // or do whatever with the ROI
cvResetImageROI(img1);
cvCopy(img1,frame, NULL);
cvShowImage("result", img1);
drag = 0;
}
/* user click right button: reset all */
if (event == CV_EVENT_RBUTTONUP)
{
IplImage *tml=cvLoadImage("tml.jpg",frame);
drag = 0;
```

```
}
cvMatchTemplate(tgt,tml,res,CV_TM_SQDIFF);
    cvMinMaxLoc(res,&minval,&maxval,&minloc,&maxloc,0);
```

In this algorithm when the user presses and drags the left mouse button the ROI is selected and when he releases the left mouse button the ROI is saved in a new image "tml.jpg" as a new image and used as the template for template matching algorithm. This template can be later destroyed or saved for further use.

V. ADVANTAGES

In the Template matching method the surrounding conditions and lighting differ from one user to another so most of the time this technique fails but when the template is part of the original image then this technique works the best.

In the ROI corner finding method the best pixels to be tracked must be found out, if such kind of pixels is not present in the ROI this method fails.

In the proposed method the template is obtained from the target image by the user so the template matching method works best when the ROI is selected by the user so, this method is very much effective in this way.

VI. CONCLUSION

In this modern world computers have become one of the most inevitable device. While computing has become one of our most important day to day need computing interfaces must be intuitive. These intuitive computing interfaces take computing to the next level. These cost effective interfaces change the way we compute.

This will avoid the humans being machines sitting in front of another machine.

REFERENCES

[1] "The Camera Mouse: Visual tracking of body fetures to provide computer access for people with severe disabilities" Betke,M. ; Gips.J ; Fleming.P;

[2] "Learning OpenCV" by Bradski, Gray and Kaehler, Adrian

[3] "OpenCV 2 Computer Vision Application Programming Cookbook" by laganiere, Robert.

Reduction of Distortion for Induction Motor Drives Using Multilevel Inverter

Vasantha kumar c, Rudranna Nandihalli

Department of Electrical and Electronics Engineering, RVCE Bangalore, India

Abstract - Electrical drives plays main role in industries like spinning mills, thread mills and tractions. Induction motor drives are driven by Multilevel inverters. These drives have to maintain constant speed under fluctuation of loads. In this paper, a new multilevel inverter using reverse voltage topology is proposed to achieve constant speed of induction motor. Also in this technique the harmonics are reduced and hence losses are reduced as compared to convention multi level inverter. Using matlab simulink ,the simulation is carried out to show the performance .(seven voltage level with reduced TDH)

Keywords*—THD, Reverse Voltage topology, Multilevel inverter.*

I. INTRODUCTION

In drives, the induction motor plays a vital role and requires constant speed during variation of load torque. More losses are occurring due to increase in distortion of motor current. Hence it is required to reduce the distortion and also maintaining constant speed. The distortion is reduced by increased levels of voltage of inverter. A scheme is also presented to regulate the voltage levels of the multilevel inverter so that it operates in an optimum amplitude modulation index regime [1]**.**

Multilevel converters offer high power capability, associated with lower output harmonics and lower commutation losses. Their main disadvantage is their complexity, requiring a great number of power devices and passive components, and a rather complex control circuitry. This work reports a new multilevel inverter topology using an H-bridge output stage with a bidirectional auxiliary switch. The new topology produces a significant reduction in the number of power devices and capacitors required to implement a multilevel output. The new topology is used in the design of a five-level inverter; only five controlled switches, eight diodes, and two capacitors are required to implement the five-level inverter using the proposed topology. In this new topology, the total number of components is reduced has compared to convectional multilevel inverter.

A cascaded H-bridge multilevel boost inverter for electric vehicle (EV) and hybrid EV (HEV) applications implemented without the use of inductors. Currently available power inverter systems for HEVs use a dc–dc boost converter to boost the battery voltage for a traditional three-phase inverter. The present HEV traction drive inverters have low power density, are expensive, and have low efficiency because they need a bulky inductor. A cascaded H-bridge multilevel boost inverter design for EV and HEV applications implemented. Traditionally, each H-bridge needs a dc power supply. A fundamental switching scheme is used to do modulation control and to produce a five-level phase voltage. Experiments show that the proposed dc–ac cascaded H-bridge multilevel boost inverter can output a boosted ac voltage without the use of inductors [3].

The Reversing Voltage topology that was previously Proposed [6] is implemented here in single-phase and three-Phase five-level inverter to improve the multi-level performance by compensating the disadvantages already mentioned. Especially at higher levels this topology requires less number of components as compared to available inverters. This topology requires less carrier signals and does not need balancing of the voltages [6].

In case of multi-level inverters with dual inverter fed open end winding induction motor, the open-end winding induction motor structure is achieved by opening the neutral connections of the conventional induction motor without any other structural changes. Different multi-level structures can be realized by feeding an open end winding induction motor from both the ends. This type of configuration increases the redundancy of switching states to generate same number of voltage vectors turns out to be a very useful feature for achieving common-mode voltage elimination and dc-link capacitor voltage balancing in multi-level inverter fed drives with higher number of levels [3].

II. NEW MULTI-LEVEL TOPOLOGY

The block schematic of Reversing Voltage topology for multi-level inverter is depicted in fig.1. The principle of this topology for single phase is as shown in fig. 2. The positive level generator block generates the positive level voltage and the full bridge converter reverses the voltage direction when the voltage polarity requires to be changed for negative polarity (negative half cycle of the fundamental output voltage) [6].

DC supply

Multi-level Inverter

Motor

Load

TTL Driver

Micro-Controller

fig.1. Block Diagram of the setup

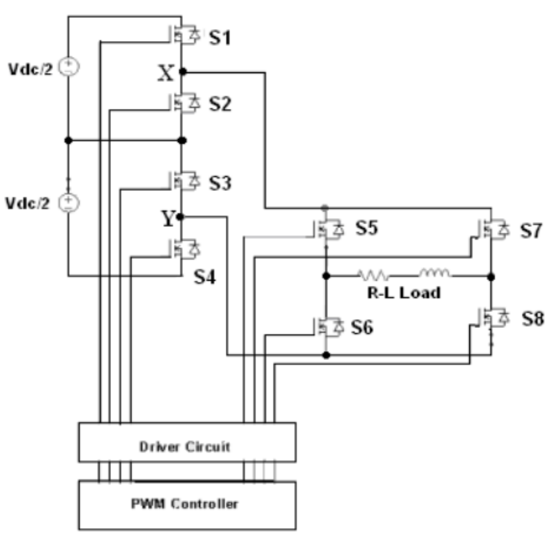

Fig 2: Circuit diagram of single phase system

OPERATION OF SINGLE-PHASE & THREE-PHASE FIVE-LEVEL INVERTER USING REVERSING VOLTAGE TOPOLOGY:

Operation of the topology is explained with the help of Table I. When S1 and S4 are turned "on" the output voltage V_{XY} is V_{dc}. when switches S2 and S4 are turned "on" the output voltage is $V_{dc/2}$ .Thus by proper switching combinations of S1, S2, S3 and S4, the positive half cycles are generated. Switches S5 and S6 are complementary, similarly S7 and S8 also for a complementary pair. When S5 and S8 are switched "on" together (for duration 10 ms or half cycle duration of fundamental output voltage), positive half cycle can be generated and when S6 and S7 are switched "on" together (for duration 10 ms) negative half cycle can be generated across load. The voltage blocking capacity of each switch is $V_{dc}/2$. . This topology requires half of the carriers for PWM controller because it is sufficient to produce pulses only for positive half cycles of the fundamental output whereas output for negative half cycle is automatically generated by switching of full bridge converter (by reversing the voltage generated for positive half cycle).

In fig.2 the switches S5, S6, S7 and S8 are switched at very low frequency (i.e. 50 Hz fundamental frequency of output).

Output voltage V_{XY}	S_1	S_2	S_3	S_4
0	0	1	1	0
$V_{dc}/2$	0	1	0	1
V_{dc}	1	0	0	1

Table I

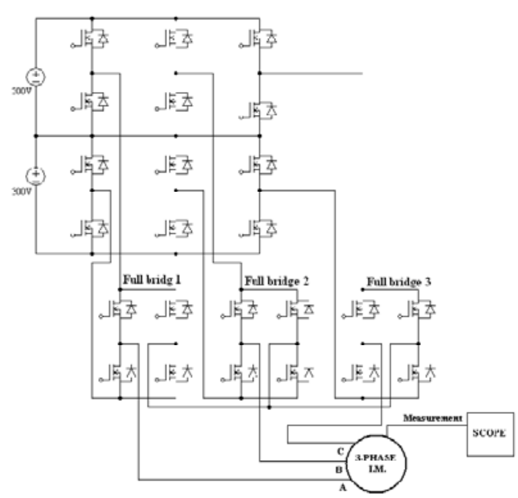

Fig.3.Schematic diagram of three-phase five-level inverter with induction motor load

According to MIL-HDBK-217F (Military Handbook) standard, the reliability of the system is indirectly proportional to the number of its components [6]. Hence, the reliability of the converter is decreased with increase of number of high frequency switches. In the this converter, as can be seen, half of the switches in full bridge inverter will not require to be quickly switched "on", since they are just required to be switched in zero crossings whose frequency is very low (i.e., 50 Hz even at the rated speed of the induction motor). So in this case the reliability of the converter is improved

The number of required three-phase components according to output voltage levels (N) is illustrated in Table II [6]. Analysis from Table II clearly shows that the number of components in new topology is lower than any other topologies especially at higher voltage levels. Table II shows the comparison between different topologies [6].

This topology requires fewer components. As it requires fewer high frequency switches, in addition to high power induction motor drives, it also deserves to find widespread applications in medium-voltage level high-power applications like FACTS and HVDC.

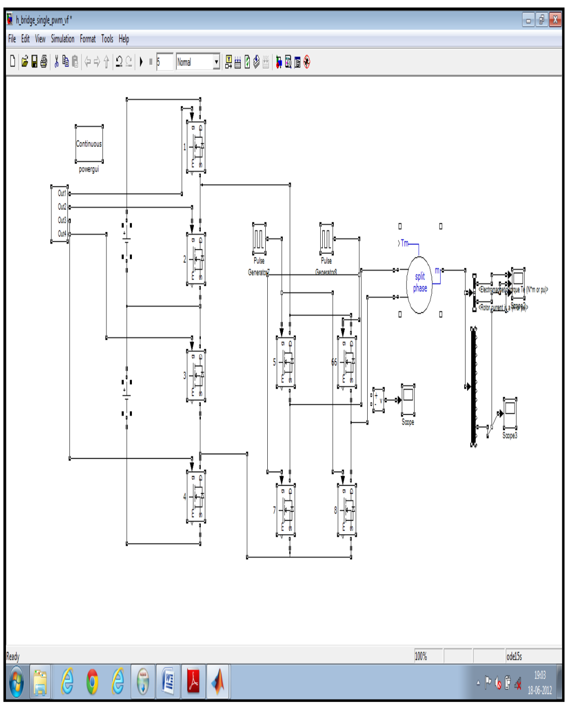

Fig.4. shows the simulated circuit diagram of single phase multilevel inverter with motor load.

NUMBER OF COMPONENTS FOR THREE-PHASE INVERTER

Table II

Inverter Type	NPC	Flying Capacitor	Cascaded H-bridge	Reversing Voltage
Main switches	6(N-1)	6(N-1)	6(N-1)	3((N-1)+4)
Main diodes	6(N-1)	6(N-1)	6(N-1)	3((N-1)+4)
Clamping diodes	3(N-1)(N-2)	0	0	0
DC bus capacitors/ isolated supplies	3(N-1)	3(N-1)	3(N-1)/2	(N-1)/2
Flying capacitors	0	3/2(N-1)(N-2)	0	0
Total numbers	$3(N^2+2N-3)$	3/2(N-1)(N+8)	27/2(N-1)	(13N+35)/2

III. SIMULATION AND RESULTS

The simulation results for five-level inverter using Reversing Voltage topology are demonstrated by MATLAB simulink module. The dc source voltage is 300 V. Frequency of carrier signal is 4.5 kHz. In this topology, in the carrier based implementation, the phase disposition PWM scheme is used. In phase disposition technique the carrier waveforms are in phase with the reference waveform.

Fig.6 ,8,&14 shows the simulated with various voltage levels, Fig, 7,10,12,15 shows the simulation result of winding current, torque and speed of single phase and three with phase motor load. Fig.9, 11, 13, 16 shows the reduced THD in single phase and three phase with motor load, Here the phase disposition PWM scheme is used .

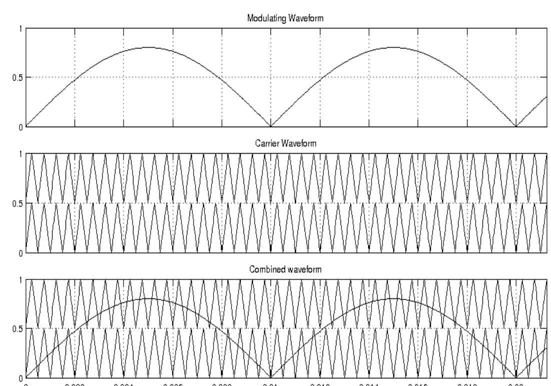

Fig.5. Phase disposition SPWM modulation waveform

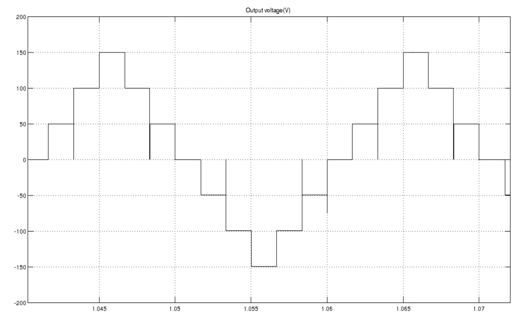

Fig: 6 Seven level output waveform with 100V and 50V input.

The output waveform of the multi-level inverter shows that the seven level output 0, +dc, +dc/2, +3dc/2, -dc, -dc/2, -3dc/2 is the output voltages of the inverter. The switches are switched accordingly.

TABLE III

Type of machine	Split-phase-induction motor
Power rating	.25 HP
Voltage	220V
Frequency	50hz
Poles	2

MOTOR NAME-PLATE DETAILS

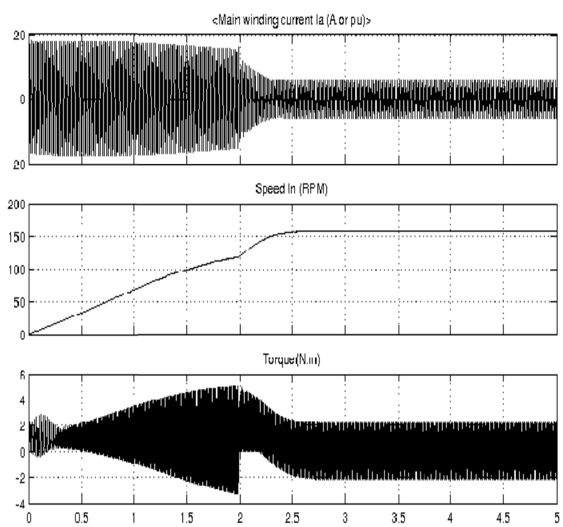

Fig: 7 main winding current, speed and Torque waveforms of the seven level inverter

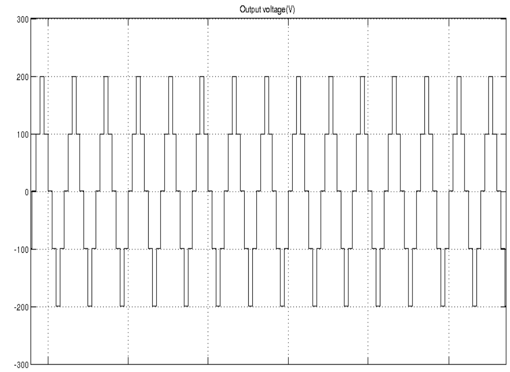

Fig: 8 output of five level inverter with motor load

Fig: 9 Harmonic spectrums of harmonics in 7-level inverter

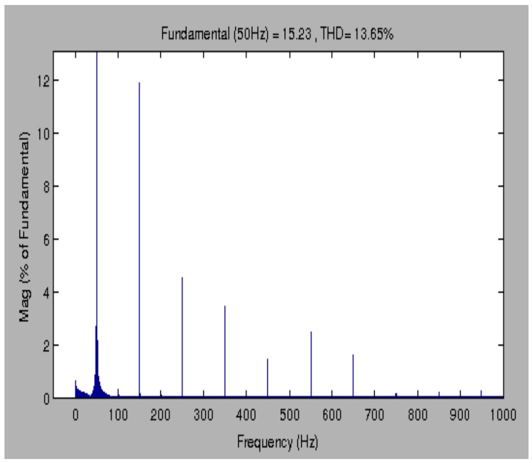

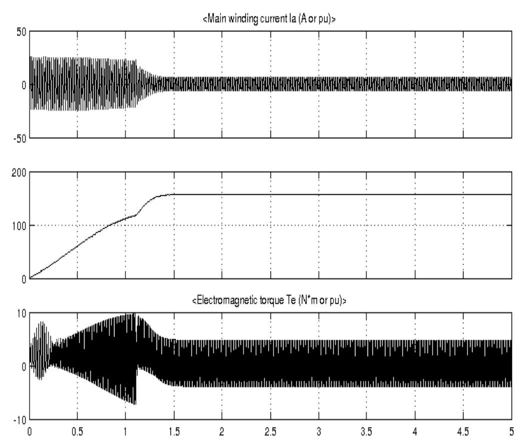

Fig: 10 Main winding current, Speed and Torque Waveforms of five-level inverter

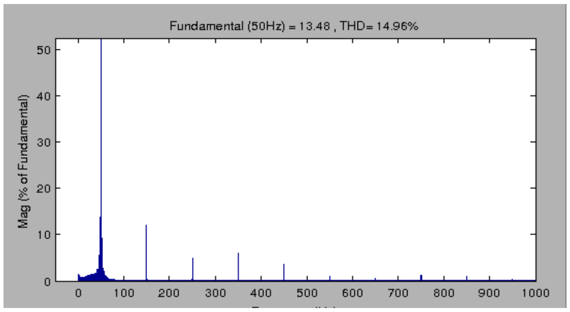

Fig:11 Harmonic spectrum of harmonics in 5-level inverter

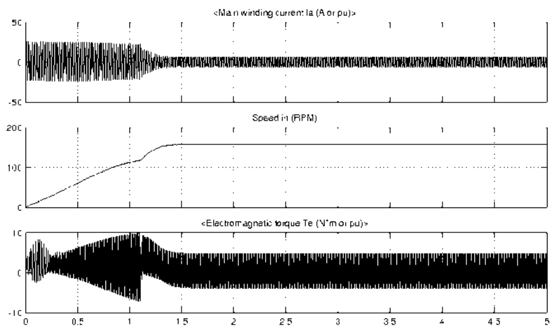

Fig: 12 Main winding current, Speed and Torque Waveforms of five-level inverter using phase disposition SPWM technique

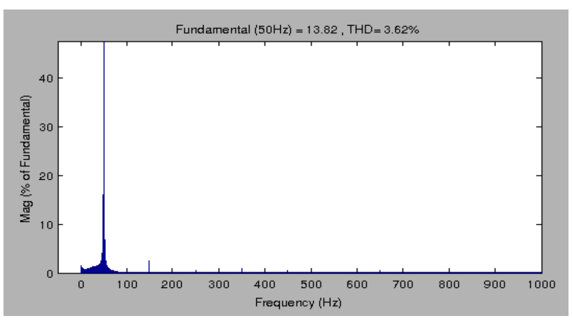

Fig: 13 Harmonic spectrum of five-level inverter using Phase disposition SPWM technique

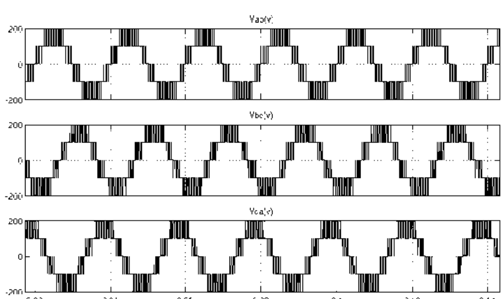

Fig: 14 Reverse voltage topology based Multi-level inverter in three- phase

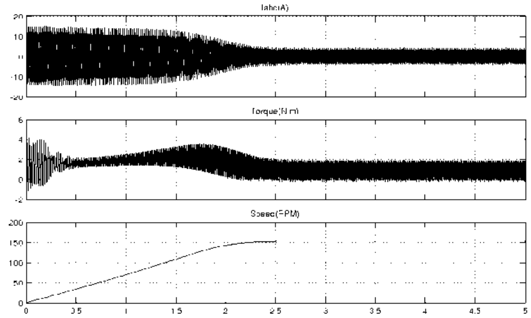

Fig: 15 Stator Current (Iabc), Torque(N-.m), Speed(RPM) in Multi-level inverter using reverse voltage topology

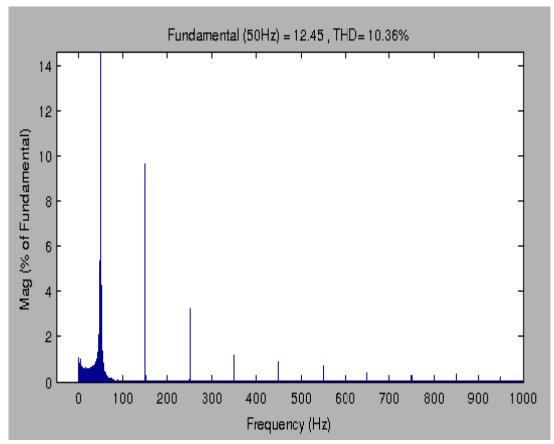

Fig: 16 Harmonic spectrum of five-level inverter using Phase disposition SPWM technique in three-phase inverter

TABLE- IV

THD ANALYSIS OF THE MULTI-LEVEL INVERTER WITH MOTOR-LOAD

Topology	**Modulation Technique**	**%THD**
Single phase 5-level inverter	Basic PWM	14.98
Single phase inverter 7-level inverter	Basic PWM	13.65
Single phase 5-level inverter	Phase disposition SPWM technique	3.62
Three-phase Multi-level inverter	Phase disposition SPWM technique	10.36

IV. CONCLUSIONS

In this paper, a Reversing Voltage topology is implemented which has superior characteristics over traditional topologies in terms of required components as switches, control requirements and reliability. In order to cover strict voltage harmonic standards in a STATCOM this inverter has good potential for such applications as it requires fewer components. Here SPWM controller has less complexity. Having lesser number of switches and higher reliability, this three-phase five-level inverter has good potential for medium voltage applications like FACTS and HVDC. Switches of full bridge converter are switched at 50 Hz, so total switching loss of the inverter reduces. GTO can be used instead of IGBT for such low switching operation in high power induction motor drive. Simulation results illustrate the performance and effectiveness of the five-level inverter for R-L load, single-phase and three-phase induction motor loads. The three-phase five-level inverter is tested on different types of load and found to work satisfactorily. The inverter also works satisfactorily as variable voltage variable frequency drive. In this topology less high frequency switches are used compared to any other topology so reliability of induction motor drive increases.

Advantages of SPWM scheme and Reversing Voltage topology in multi level inverter:

- In conventional inverter the number of carriers used is N-1, so four carrier waveforms are needed to design a five level inverter.
- However five-level inverter using this will require (N-1)/2 carriers, i.e. only two carriers.
- So this topology just requires half of the carriers compared to that of a traditional multi-level inverter.
- As shown in fig. 8, the carriers are just positive and half the number of required carriers in a traditional multi-level inverter. So the control signals are easily generated and it requires simple controller.
- Especially at higher levels this topology requires less number of components as compared to available inverters. This topology requires less carrier signals and does not need balancing of the voltages

ACKNOWLEDGEMENT

I wish to express my deep sense of gratitude to my Internal Guide, Dr.Rudranna Nandihalli Associate Professor, EEE dept ,RV college of engineering Bangalore, for his able guidance and useful suggestions, which helped me in completing the paper presentation, in time. I take immense pleasure in thanking RV college of engineering for having permitted me to carry out this paper presentation.

REFERENCES

[1] Leon M. Tolbert, "Modulation Index Regulation of a Multilevel Inverter for Static Var Compensation " Senior Member IEEE, John N. Chiasson, Member, IEEE.

[2] Gerardo Ceglia, A New Simplified Multilevel Inverter Topology for DC–AC Conversion" IEEE transactions on power electronics

[3] Zhong Du, "DC–AC Cascaded H-Bridge Multilevel Boost Inverter With No Inductors for Electric/Hybrid Electric Vehicle Applications" IEEE transactions on industry applications,.

[4] Jose Rodriguez, Jih-Sheng Lai and Fang Zheng Peng. "Multilevel Inverters: A survey of topologies, controls and applications." IEEE Trans. Ind.Electronics.vol-49 no.4 pp 724-738, Aug. 2002.

[5] A. Nabe , I. Takahashi and H. Akagi. "A new neutral point clamped PWM inverter." IEEE Trans. Ind. Applicat. vol. 1A-17, pp 518-523,sep./oct. 1981.

[6] P.N.Tekwani, R.S.Kanchan and K.Gopakumar, "A dual five-level inverter-fed induction motor drive with common-mode voltage elimination and DC link capacitor voltage balancing using only the switching-state redundancy---- Part I" IEEE Trans. Ind. Applicat.vol,-vol.54, no. 5, pp 2600-2608, October 2007

[7] Jose Rodriguez, Leopoldo G. Frequelo, Samir Kouro, Jose I. Leon, Ramon C. Portillo, Ma Angeles Martin Prats and Marcelo Perez. "Multilevel Converters: An Enabling Technology for High-power Applications" IEEE Proceedings, vol. 97, no. 11, pp1786-1817,Nov 2009.

[8] Madhav D. Manjrekar, Peter K. Steimer, and Thomas A. Lipo. "Hybrid Multilevel Power Conversion System:A Competitive Solution for High-Power Applications" IEEE Trans. ON Industry applications,VOL. 36, NO. 3, pp 834-841 May/June 2000.

[9] E.Najafi, A.H.M.Yatim and A.S. Samosir. "A new topology-reversing voltage (RV) for multi-level inverters." 2nd International conference on power and energy (PECon 08),pp 604-608, December 2008 Malaysia. S. M. Metev and V. P. Veiko, *Laser Assisted Microtechnology*, 2nd ed., R. M. Osgood, Jr., Ed. Berlin, Germany: Springer-Verlag, 1998

◈◈◈

Analysis of Fault on 1.5 MW Wind Power Plants

Manonmani .N, Divya. K & Loganathan. R

Electricals and Electronics Engineering, Sri Krishna College of Engineering & Technology, Coimbatore-641008, India.

Abstract - Large size wind farms are booming day by day. As wind energy generated is highly dynamic and dependent on only wind, the overall system's performance is important for profitable operation. Faults produced by wind turbine generator systems will impact not only the wind farms but also the interconnected system including the grid if proper protection is not ensured. In this paper it is proposed to model a 1.5MW wind farm using doubly fed induction generator and study the effects of phase to ground faults under various load conditions. For the study the vector control of the Doubly Fed Induction Generator is used.

Keywords: *DFIG, Wind farm, Phase to ground error, Simulation*.

I. INTRODUCTION

The current electrical energy are mainly depends in fossil fuels like coal, natural gas, petroleum. These fossil fuels took several years to form and the base material for the fossil fuels were organic substances. (Hence fossil fuels can be described as biomass stored for a long period). A huge amount of the fossil fuels is already depleted in the 20th century. But due to the increasing demand, the extraction of fossil fuels will become more risky and expensive at present. If the consumption of fossil fuels continues as now, all available resources of natural gas and petroleum will be exploited by 21st century. Suggests that renewable energy sources are a better alternative to foster to the increasing energy demand. Renewable energy sources are the only way by which the Earth's energy demand can be met without affecting the climatic conditions.

The conventional energy sources are limited and have pollutions to the environment. So more attention have paid to utilize the renewable energy sources such as wind, fuel cells and solar. Wind energy is the fastest growing and most promising renewable energy sources among them because it is abundant, cheap, inexhaustible, widely distributed, clean and climate benign. The environmental concerns associated with the wind power generation are noise, aesthetic impact and bird mortality. These problems can be solved by proper choice of site for wind plants. The major challenge associated with the wind power generation is due to the intermittent nature of the wind. Challenges using wind energy include that wind cannot be stored and all the energy in the wind cannot be harnessed during the time of demand. Also another issue is that the wind power plants are located in remote areas far away from the consumer ends. The major part of wind power generation is the induction generators. The different types of generators used are squirrel cage induction generators, wound rotor induction generators, permanent magnet and synchronous generators. Among the variable speed generators the doubly fed induction generator is commonly preferred for reasons such as

- Improved efficiency under light load conditions
- Acoustic noise reduction
- Possible to control Active and Reactive Power
- Improved stability when connected to grid
- Low cost of the converters.

In this paper the dynamic behavior of a 1.5 MW wind farm is modeled using MATLAB. The behavior of the system for a single line to ground fault is analyzed

II. DOUBLY FED INDUCTION GENERATOR

Fig.1. shows a doubly fed induction generator connected to grid. Doubly fed induction generator is basically a wound rotor induction machine with multi phase wound rotor with multiphase slip rings assembly and brushes enabling access to the rotor. The rotor windings are connected to the grid through a AC-DC-AC converter. The rotor and the grid currents are controlled by controlling the converter. This enables the control of the active power and reactive power flow to the grid from the stator independent of the generator's speed. The number of turns on the rotor of a doubly fed induction generator is 2 to 3 times that of the stator. This means that the rotor voltages are higher and the currents are lower. Therefore in the typical operational speed

range of $\pm$ 30% of the synchronous speed, the converter has to handle lower currents thus reducing the cost of the converter. But the disadvantage is that outside the operational speed range it is impossible to control as the rotor voltages higher. Under grid disturbances, the transient voltages and currents are also magnified. To prevent the high transients from destroying the power electronic devices a crowbar circuit is provided. The rotor windings are short circuited through a small resistance by the crow bar circuit when excessive current flows through the rotor windings. A doubly fed induction generator has the advantage that power can be imported from or exported to the grid through the power electronics converter. This allows the system to support the grid during severe voltage disturbances thus improving the system stability. By controlling the rotor voltages and currents the synchronization of the machine with the grid is maintained even when the wind speed varies. Under light load conditions, the wind energy is utilized more efficiently than a fixed speed wind turbine. Only 25 – 30 % of the power is fed to the grid through the converter while the remaining is fed directly to the grid. Due to this reason, the cost of the converter is low and the efficiency of the doubly fed induction generator is good.

Figure 1: DOUBLY Fed Induction Generator

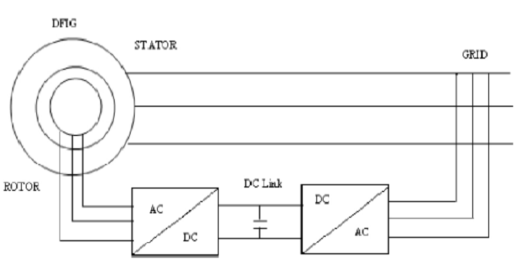

III. VECTOR CONTROL OF DFIG

Fig.2. shows a wind turbine connected to a DFIG. The AC/DC/AC converter used has two parts namely the rotor side converter and the grid side converter implemented using IGBT's to synthesize the required AC voltage from a DC voltage source. The source of the DC component is achieved using a capacitor connected to the DC side. From figure 1 it can be observed that the stator winding is directly connected to the grid whereas the rotor winding is connected to the rotor side of the AC/DC/AC converter using slip rings and brushes. The energy generated by the wind turbine is converted to electrical energy by the DFIG and is transferred to the grid by the stator and rotor windings. Rotor speed for the experimental setup implemented runs at sub synchronous speed for wind speeds lower than 10 m/s. For sub-synchronous speed operation, *rotor electrical power. output* is taken out of DC bus capacitor and tends to decrease the DC voltage. Grid side converter is used to generate or absorb the grid side converter electrical power output in order to keep the DC voltage constant.

The rotor-side converter is used to control the wind turbine output power. The power control is shown in figure 3. As shown in the figure the actual output power, measured at the grid terminals of the wind turbine, is added to the mechanical power loss and the electrical power loss. This is compared with the reference power obtained from the tracking characteristic. A Proportional-Integral (PI) regulator is used to reduce the power error to zero. The output of this regulator is the reference rotor current Iqr_ref that must be injected in the rotor by converter C_{rotor}. This is the current component that produces the electromagnetic torque $T_{em.}$

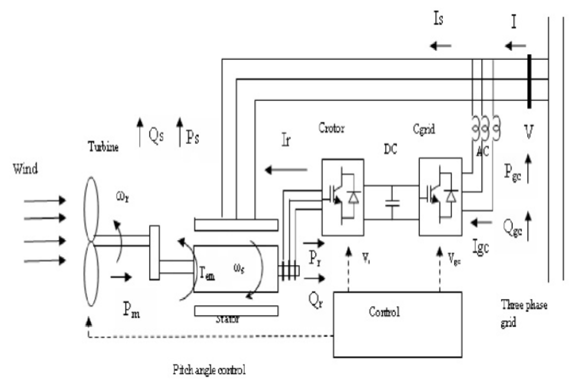

Figure 2: Wind Turbine Connected to DFIG

P_m - Mechanical power captured by the wind turbine and transmitted to the rotor P_s - Stator electrical power output

P_r - Rotor electrical power output P_{gc} - C_{grid} electrical power output Q_s - Stator reactive power output Q_r - Rotor reactive power output Q_{gc} - C_{grid} reactive power output

T_m - Mechanical torque applied to rotor

T_{em} - Electromagnetic torque applied to the rotor by the generator ω_r - Rotational speed of rotor

ω_s - Rotational speed of the magnetic flux in the air-gap of the generator, this speed is named synchronous speed. It is proportional to the frequency of the grid voltage and to the number of generator poles.

J - Combined rotor and wind turbine inertia coefficient

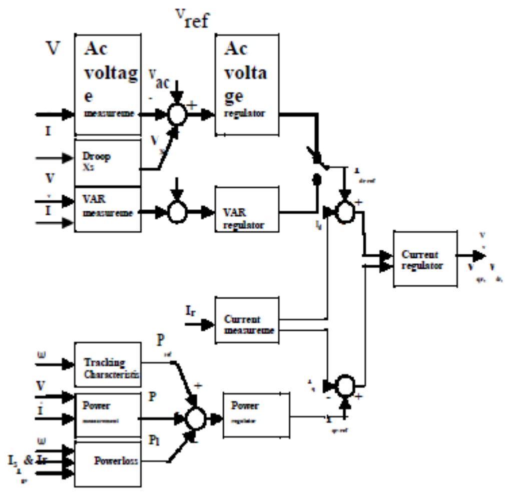

Figure 3: Rotor side converter control system

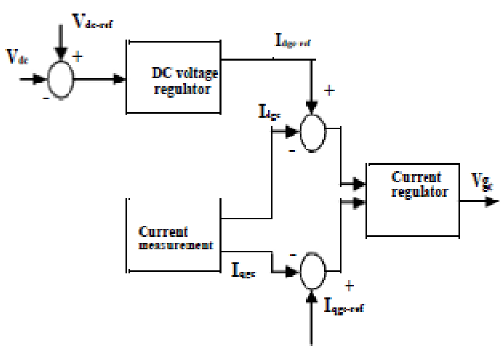

Figure 4: Grid side converter control system.

The converter C_{grid} is used to regulate the voltage of the DC bus capacitor. In addition, this model allows using C_{grid} converter to generate or absorb reactive power. The system consists of an outer regulation loop consisting of a DC voltage regulator. The output of the DC voltage regulator is the reference current Idgc_ref for the current regulator. The inner current regulation loop consists of a current regulator. The current regulator controls the magnitude and phase of the voltage generated by converter C_{grid} (Vgc) from the Idgc_ref produced by the DC voltage regulator and specified Iq_ref reference. The current regulator is assisted by feed forward terms which predict the C_{grid} output voltage.

IV. EXPERIMENTAL SETUP

Matlab Simulink was used to model a 1.5-MW wind farm connected to a 11-kV distribution system. The power generated is exported to a 120-kV grid through a 15-km, 11-kV feeder. The designed system consists of a 2-MVA plant consisting of a 1.68MW induction motor load along with a 100-kW resistive load at bus B25. To implement the line fault a single phase to ground fault is implemented on the 11 KV line. The fault occurs for a period of 9 cycles at t=5 seconds. The results obtained is shown in figure 5 and figure 6.

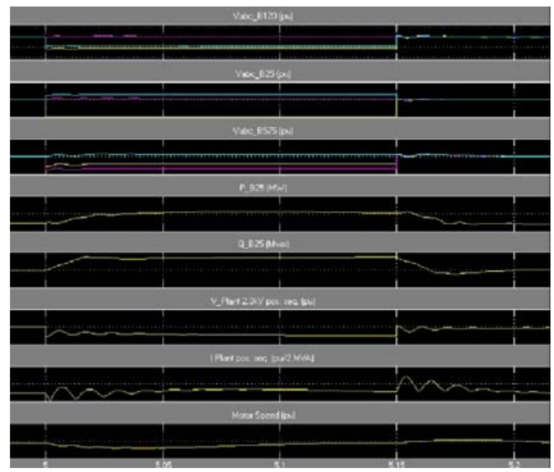

Figure 5: Graphs of measured parameters on the grid side for a fault in phase A

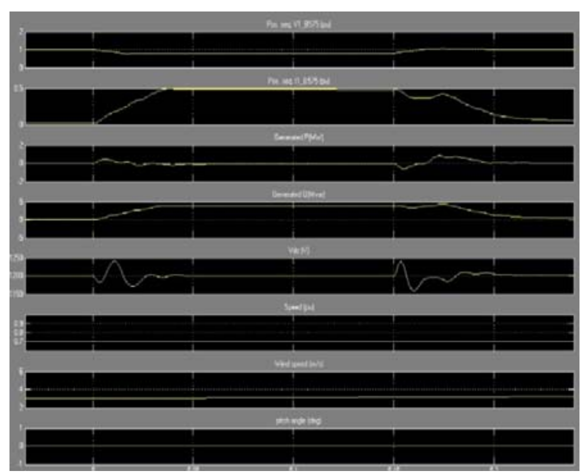

Figure 6: Graphs of measured parameters in the wind turbine side for a fault in phase A

From figure 5 it is observed that the positive-sequence voltage at wind-turbine terminals (First graph in figure 4) drops to 0.8 pu during the fault whereas the positive sequence current increases. The real power generation has flickers at the fault instant and the generated reactive power increases. The Dc voltage has spikes both at the instant of fault and at the instant of fault recovery.

For a fault in phase A, on the grid side, the voltage of one phase is maintained whereas the voltage of the other two phases drops. At B17, the voltage of phase A is zero and the voltage of the phase B is maintained and the voltage of phases C increases to 1.3 p.u. At B234, the voltage of phase C increase to 1.06 p.u, the voltage of phases a increases to 0.75 p.u and the voltage of phase B decreases to 0.65 p.u. There is an increase in both real and reactive power.

If phase A and B has line to line fault the positive sequence at wind turbine terminals (first graph in figure 7) drops to 0.35 pu and the system trips.

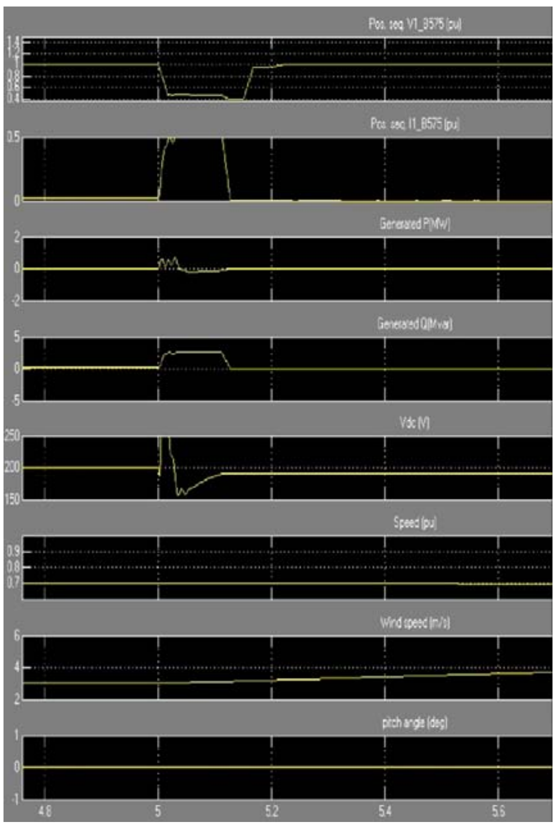

Figure 7: Graphs of measured parameters in the wind turbine side for a line to line fault in phase A and phase B

V. CONCLUSION

In this paper 1.5 MW wind farm is modeled using MATLAB. The effect of Phase to Ground Fault in phase A is analyzed for the 1.5 MW doubly fed Induction Generator wind farm unit. Even though the per unit value fells the system will recover it. In case Line to Line fault occurs the system will recover it up to 0.35 p.u voltage drop (drips it) and increases the Active power and decrease the reactive power. This gives the profitable operation and the interconnected systems are protected.

REFERENCES

[1] R.Datta and v.t.ranganathan, sep.2002, "*variable speed wind power generation using doubly fed wound rotor induction machine-a comparisition with alternate schemes",* IEEE Trans.Energy convers.,vol.17,no.3,pp.414-421.

[2] Hoboken, NJ: Wiley T.Ackermann, 2005,"*wind power in power systems*

[3] S. Muller, M. Deicke, and R. W. D. Doncker,"Doubly fed inductiongenerator systems for wind turbine," *IEEE Ind. Appl. Mag.*, vol. 8, no. 3,pp.26–33, May/Jun. 2002.

[4] Mick Sagrillo&LAN Woodened, June/July2009 "*How to buy a wind Generator*", home power magazine

[5] Peng Zhou, Yikang He, and Dan Sun, Nov2009, "*Improved Direct Power Control of a DFIG-based Wind turbine during Network unbalance*", IEEE Trans. Power Electronics, vol.24, no.11.

[6] Schauder.C and Mehta.H,Jul 1993"*Vector analysis and control of advanced static VAR compensators*

[7] V. Galdia, A. Piccoloa and P. Siano "Exploiting maximum energy from variable speed wind power generation systems by using an adaptive Takagi–Sugeno–Kang fuzzy model " Journal of Energy Conversion and Management Volume 50, Issue 2, February 2009, Pages 413-421

[8] Lubosny Z.,"Wind turbine operation in electric power systems", Chapter 5, page 87-92, Springer

[9] J.Tamura, T.Yamazaki, R.Takahashi, S.Yonaga, H.Kubo, Y.Matsumura, "Analysis of Transient Stability of Wind Generators", Conference Record ofICEM 2002, No. 148, 2002.

[10] Salman K. Salman, Anita L. J. Teo. "Windmill modeling consideration and factors influencing the stability of a grid-connected wind power based embedded generator", IEEE Transactions on Power Systems, vol. 18, no.2, pp. 793-802, 2003.

[11] Holdsworth L., Wu X. G., Ekanayake J. B., Jenkins N.. "Comparison of fixed speed and doubly-fed induction wind turbines during power system disturbances". IEE Proc. Generation, Transmission and Distribution, vol.150, no. 3, pp. 343-352, 2003.

[12] Castro, R.M.G., Ferreira de Jesus, J.M.,"A wind park reduced-order model using Singular Perturbation Theory", Energy Conversion, IEEE Transaction on Volume 11, Issue 4, Dec. 1996 Page(s):735 - 741 .

Feed Forward Control of 3ф Squirrel Cage Induction Motor by Using Fuzzy Logic Controller

N.Satyavani, B.Chandrasekhar & K. Dinesh Kumar Reddy.

Abstract - This paper presents a feed forward control of 3ф Squirrel cage Induction motor by using fuzzy logic controller to achieve high performance. The analysis, design and simulation of the fuzzy logic controller for 3ф squirrel cage induction motor are carried out based on fuzzy set theory. The proposed fuzzy logic controller is compared with PI controller with no load and some load conditions. The results shows robustness and effectiveness of proposed feed forward control by fuzzy logic controller for 3фSsquirrel cage Induction motor.

Key Words**:** *forward control, fuzzy logic controller, PI controller, 3ф Squirrel cage Induction motor, speed control.*

I. INTRODUCTION

The usages of induction motors in industrial applications are growing drastically. But the characteristics are also varying for different applications like speed,torque,power consumption,losses,slip etc. Earlier to achieve high performance speed control , field-oriented control of induction motor drive is employed[2], however the control design of such a system plays a role in system performance. The decoupling characteristics of vector-controlled induction motor are adversely affected the parameter changes in the motor. The speed control **Of induction motor** can be achieved by stator side and rotor side controlling techniques such as pole changing, frequency control, voltage control,v/f control, rotor resistance control etc. but these are conventional methods .due to advancement in technical areas these techniques can be improved to control the speed as per requirements. The speed control of IM issues are traditionally handled by fixed gain PI and PID controllers. However the fixed gain controllers are very sensitive to parameter variations, load disturbances etc. Thus, the controller parameters have to be continuously adapted. The problem can be solved by several adaptive control techniques such as model reference adaptive control, sliding mode control smc,variable structure control VSC and self tuning PI controller etc. The design of the entire above controller depends on the exact system mathematical model. However it is often difficult to develop an accurate mathematical model due to unknown load variation and unavoidable parameter variations due to saturation, temperature variations and system disturbance. . To overcome the above problems, Fuzzy logic controller (FLC) is being used for motor control purpose. There is some advantage of fuzzy logic controller as compared to conventional PI, PID and adaptive controller such as

- It doesn't need any exact system mathematical model
- It can handle non linearity of arbitrary complexity
- It is based on the linguistic rules with an IF-THEN general structure which is the basis of human logic[3]
- Proposed fuzzy logic controller is insensitive to load variations and sudden changes in speed command

This paper presents the feed forward control by using fuzzy logic controller for squirrel cage induction motor have been applied and it is successfully compared with PI controller**.**

II. FIELD ORIENTED OR VECTOR CONTROL

As The Name Indicates, Is Due To Magnitude Variations And Phase Alignment Of The Vector Variables Are To Be Controlled. Due to Inherent Coupling Effect in The Scalar Control Gives Sluggish Response and system goes in to instability higher order system effect. For example torque is increased by incrementing the slip (i.e. frequency) therefore results flux tends to decrease therefore flux variation is always sluggish. These problems can be solved by vector control in this the induction motor can be controlled like a separately excited dc motor. Vector control is also known as decoupling, orthogonal or transe vector control. Vector control can be applied to induction and synchronous motor drives.dc machines like performance can be extended to an induction motor if the machine control is considered in a synchronously rotating reference frame (d^e-q^e) where the sinusoidal variable appears as dc quantitys in steady state.dc machine like performance is only possible if i_{ds} is align in the ditection of φ_r and i_{qs} is perpendicular to it.

Feed forward control

It is same as field oriented control or vector control except the unit vector signals are generated in feed forward manner .in this $d^s_{-q}{}^s$ axes are fixed on the rotor and d^r-q^r axes are fixed on the rotor moving at a speed □r and synchronously rotating axes d^e-q^e are rotating ahead of d^r-qr axes by positive slip angle $□_{sl}$ related to slip speed $□_{sl}$ .for decoupling control i_{ds} on d^e axis is represented as flux component and i_{qs} is onq^e axis represented as torque component.

$$\theta_e = \int \omega e dt = \int(\omega r + \omega sl) = \theta r + \theta sl \qquad (1)$$

The Rotor Circuit Equation

$$\frac{d\Psi_{dr}}{dt} + \frac{R_r}{L_r}\Psi_{dr} - \frac{L_m}{L_r} Rr\ ids - \omega sl\ \Psi_{qr} = 0 \qquad (2)$$

$$\frac{d\Psi_{qr}}{dt} + \frac{R_r}{L_r}\Psi_{qr} - \frac{L_m}{L_r} R_r\ iqs + \omega sl\ \Psi_{dr} = 0 \qquad (3)$$

For decoupling control Ψqr=0, so the total flux $\hat{\Psi}_r$ directs on the de axis.

Now equations (1)and (2) we get

$$\frac{L_r}{R_r}\frac{d\hat{\Psi}_r}{dt} + \hat{\Psi}_r = L_m i_{ds} \qquad (4)$$

Slip frequency can be calculated as

$$\omega_{sl} = \frac{L_m\ R_r}{\hat{\Psi}_r\ L_r} i_{qs} \qquad (5)$$

For constant rotor flux Ψr and dΨr/dt=0,substituting in equation (4) yields the rotor flux set as

$$\hat{\Psi}_r = L_m \quad i_{ds} \qquad (6)$$

The electromechanical torque developed is given by

$$T_e = \frac{3}{2}\frac{p}{2}\frac{L_m}{L_r}\hat{\Psi}_r\ i_{qs} \qquad (7)$$

III. DESIGN OF PROPOSED FEED FORWARD METHOD OF SQUIRREL CAGE INDUCTION MOTOR BY USING FUZZY LOGIC CONTROLLER

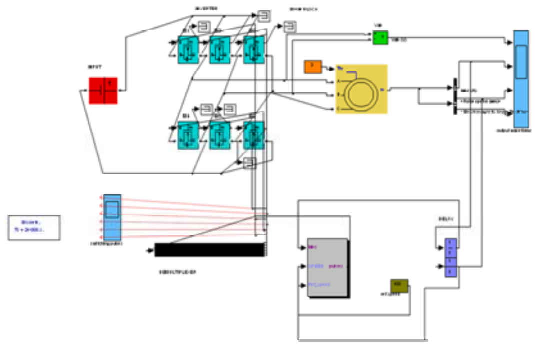

Fig 1 : Proposed feed forward based squirrel cage induction motor by using fuzzy logic controller

The Basic configuration Of The Drive Consists Of Induction Motor Fed By A MOSFET Based Inverter .The Speed Error And Rate Of Change Of Speed Error Are Processed By The Fuzzy Logic Controller To Generate The Torque Producing Current component command $i_q^*(n)$ the phase current commands i_a^* i_b^* i_c^* are compared with the actual currents $i_{a,}$ i_b i_c to generate PWM signals which acts as A switching pulses to fire the power semiconductor devices of three phase inverter to produce the actual voltages to the induction motor.

IV. DESIGN OF FUZZY LOGIC CONTROLLER FOR SQUIRREL CAGE INDUCTION MOTOR DRIVE

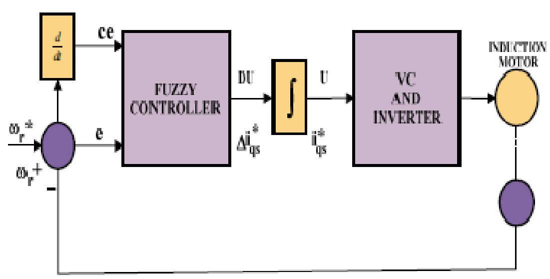

Fig 2: functional block diagram of fuzzy logic control

The functional block diagram represents the speed control of squirrel cage induction motor by using fuzzy logic controller . Here the inputs are speed error e and change in speed error ce these two inputs variables $e(t_s)$ and $ce(t_s)$ are calculated at Sampling time t_s and these input variables can be represented as From the fig:1 & 2, represents the change of error e, $\omega_r^*(t_s)$ is the reference rotor speed $\omega_r(t_s)$ is the actual speed,$e(t_s - 1)$ is the error value at previous sampling time, output is the change in torque ΔT which is integrated to get the reference torque.i.e represented as in the equation.

$$T^*(t_S)= T^*(t_s - 1) +\Delta T \quad (9)$$

From the figure 2, the internal structure of fuzzy logic controller consists of 3 stages such as

- Fuzzification
- Knowledge base inference system
- Defuzzification

Fuzzification: In this stage the crisp variables of input e(ts) and ce(ts)are converted into fuzzy variables. The fuzzification maps the error and change in error to linguistic labels of fuzzy sets. Membership function is associated to each label with triangular shape which consists of two inputs and one output. The proposed controller uses following linguistic labels NB, NM, NS, ZE, PS, PM, PB. Each of the inputs and output contain membership function with all these seven linguistics.

In this inference stage the input variables e(ts) ,ce(t_s) are processed by the inference machanism that executes 7*7 rules represented in the rule table as shown belowfor example from the table 1 IF change in speed error is nagative NM and change in speed is NB .here mumdhani algorithm is used.

Knowledge base inference system : a fuzzy inference system or fuzzy system basically consists of a formulation of the mapping from a given input set to output set using fuzzylogic .this mapping process provides the bases from from which the inference are conclusion can be made.a fuzzy inference process consists of the following 5 steps

1. fuzzification of input variables
2. application of fuzzy operator(AND ,OR,NOT) in the IF (antecedent)part of the rule
3. implication from the antecedent to the consequent (THEN part of the rule)
4. aggregation if the consequents across he rules
5. defuzzification

Defuzzification:

Defuzzification means coversion of the fuzzy output to crisp output ,here the fuzzy output variable is ΔT.as we know that thw defuzzification having many methods among them centre of gravity method or centre of area method is used to calculate the resultant fuzzy value ΔT (t_s). Defuzzification using COA method means that crisp output of ΔT*(ts) is obtained by using centre of gravity, in which the crisp output ΔT(ts) variable i taken to be the geometric centre of the output fuzzy variables value μout(ΔT)area, where μout(ΔT) is formed by taking the union of all the contributions of rules with the degree of fulfilment greater than zero. Then the COA expression with discretised universe of discourse can be written as

$$\Delta T=\sum_{i=1}^{n} \Delta T_i\ \mu_{out}(T_i) \ / \ \sum_{i=1}^{n} \mu_{out}(\Delta T_i) \quad (10)$$

Then T_{e^*} obtained by integration which is used to calculate i^*_{Qs}

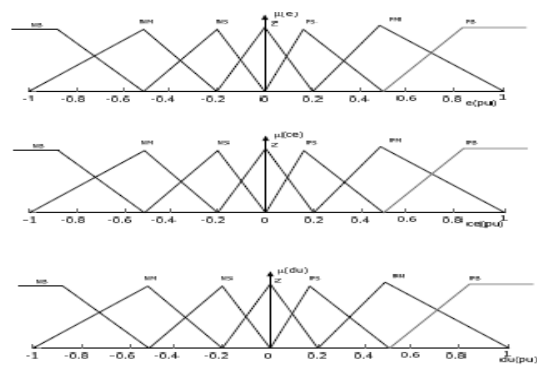

Fig:4 membership function of fuzzy variables $\mu_{e,}\mu_{ce,}\mu(du)$

e(pu) / ce(pu)	NB	NM	NS	ZE	PS	PM	PB
NB	NB	NB	NB	NB	NM	NS	Z
NM	NB	NB	NB	NM	NS	Z	PS
NS	NB	NB	NM	NS	Z	PS	PM
ZE	NB	NM	NS	Z	PS	PM	PB
PS	NM	NS	Z	PS	PM	PB	PB
PM	NS	Z	PS	PM	PB	PB	PB
PB	Z	PS	PM	PB	PB	PB	PB

Table:1 rule matrix for fuzzy speed control

IV. SIMULATION RESULTS AND DISCUSSION

The machine is initially at stand still with no load. The reference speed is linearly increased from zero its rated value 100rpm with fuzzy logic controller and PI controller. Different simulations were carried out on feed forward control of squirrel cage induction motor by using fuzzy logic controller and PI controller.

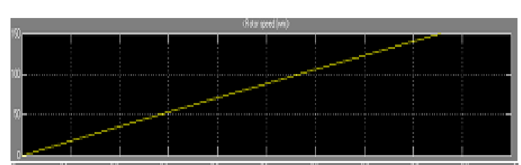

Fig 5 :Speed Curve Using Pi Controller

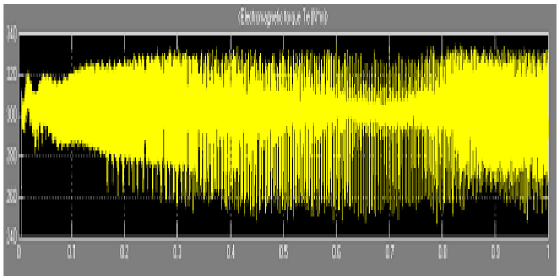

Fig 6 :Torque Curve Using Pi Controller

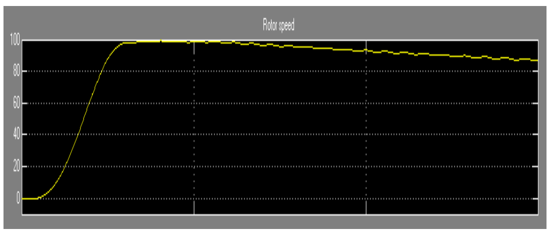

Fig 7 : speed curve using fuzzy logic controller

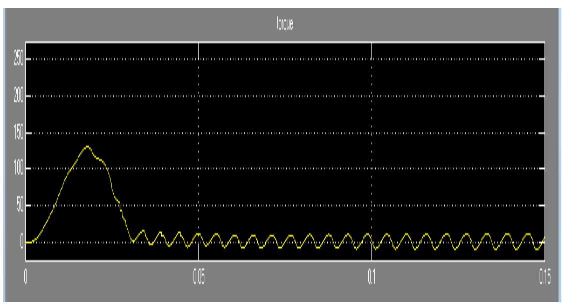

Fig 8: Torque Curve Using Fuzzy Logic Controller

fig.5 & 7 shows The PI and FLC with a step command of Speed are applied with load condition. In case of PI Controller the rise time is in between ts=0.7 to ts=0.8 , but in case of FLC rise time is in between ts=0.03 to ts=0.04 .It is conclude that FLC offers faster response as compare to PI. Hence FLC based drive system is superior to PI based drive system in all respect rise time, settling time and overshoot. From the fig: 6&8 shows PI and FLC with a step/constant command of Torque are applied with load condition. In PI controller the torque is varying with disturbances where as in FLC the torque is maintained constant and more robust to load disturbance as compared to PI controller.

V. CONCLUSION:

In this paper fuzzy logic controller for the control of a feed forward control for a squirrel cage induction motor was described. The drive system was simulated with fuzzy logic controller and PI controller and their performance was compared. Here simulation results shows that the designed fuzzy logic controller realises a good dynamic behaviour of the motor with a rapid settling time, no overshoot and has better performance than PI controller. Fuzzy logic control has more robust during change in load condition.

APPENDIX

Specification of Induction Motor:

Machine type-3 phase induction motor

Rotor type-squirrel cage

Reference type-Stationary

50HP, 460V,60 hz,4 poles,Ns =1800 rpm,

Rs=0.087Ω,Rr=0.228Ω,

Ls=0.8mH, Lr=0.8mH, Lm=34.7mH

J=1..662Kg.m^2,B=0.1kg.m/s

REFERENCES:

[1] B.K Bose "modern power electronics and ac drives "Prentice-Hall Publication,Englewood Cliffs,New Jersey,1986

[2] F.BLASCHKE, "The principle of field orientation as applied to the new transvector closed-loop control system for rotating-field machine," Siemens Rev., Vol.34,no.3,pp.217-220,May1972.

[3] M Nasir Udin,Tawfik S.Radwan,and M.Azizur Rahman," Performance of Fuzzy-Logic-Based Indirect vector control for induction motor drive,"IEEE Transaction on Industry Applications,vol.38,no.5,September/October 2002.

[4] Z Ibrahim and E.Levi, "A comparative analysis of Fuzzy Logic and PI controller in High-Performance AC machine drives using Experimental Approach,"IEEE Trans.Industry Application,vol.38,no.5,pp1210-1218,Sep/Oct 2002.

[5] Gilberto C.D.Sousa,Bimal K.Bose and John G.Cleland "FuzzyLogic Based On-Line Efficiency Optimisation Vector-Controlled Induction Motor Drives,"IEEE Trans.Industrial Electronics,Vol.42,pp.192-198,April 1995.

[6] Mariun,N.; Noor,S.B.M.;Jasni,J.;Bennanes,O.S. "A fuzzy logic based controller for an indirect controlled three-phase induction motor,"TENCON 2004,2004 IEEE Region 10 Conference,Publication Year: 2004,Page(s) :1-4,Vol-4.

[7] MinhTa-Cao, J.L. Silva Neto,Houng Le-Huy, "Fuzzy logic based controller for induction motor

drives,"Canadian conference, Publication Year,1996,Pages631-634,Vol-2.

[8] L.Zhen and L.Xu, "Fuzzy learning enhanced speed control of an indirected field-oriented induction machine drives,"IEEE Trans.Control System Technology, Vol-8,no-2,pp.270-278,March 2000.

[9]. Biranchi Narayan Kar, K.B. Mohanty, Madhu Singh "Indirect Vector Control of Induction Motor Using Fuzzy Logic Controller",2011

◈◈◈

Three-Level Boost Inverter Based Wind Energy Conversion System Using PMSG

J Karthick & S Vijayalakshmi

Department of electrical and electronics engg, SRM University, Chennai,India

Abstract - The proposed work deals with the topology of a boost three level (TL) chopper on the front of a TL diode-clamped multi level inverter is used for direct driven WECSs. With the increase of wind energy conversion system (WECS) ,conventional two-level voltage source converters tend to be replaced gradually by diode-clamped multi level converters. The concept of the proposed control system is based on Voltage Oriented Control with Sinusoidal Pulse Width Modulation (SPWM) The controller with dual PI regulators is designed for the boost chopper. When wind speed is beyond the rating, the rotating speed is limited by regulating β to keep output power constant. These elements have been modelled by using MATLAB/Simulink interface.

Keywords*— Boost three-level (TL) chopper, neutral-point (NP) potential balancing.*

I. INTRODUCTION

In worldwide, wind energy has been the fastest growing energy technology within the last several years, and all factors indicate that the growth will continue for many years in the future. Among the various types of wind turbines, the variable speed wind turbines based on the doubly fed induction generator (DFIG), which has many disadvantages and hence DFIG tends to gradually replaced by permanent magnet synchronous generator.

With the increase of WECS capacity, the high-power and multilevel techniques have come to be the development trend of power conversion devices. Especially, three-level diode-clamped converters have been adopted for the WECS and other high power applications. Compared with the other two strategies, the hysteresis type control scheme is the most robust, but it suffers current ripple at half-switching frequency.

There are a limited number of topologies that provide multilevel voltages and are suitable for medium voltage applications. The most known topologies are the neutral-point clamped ,flying capacitor, and the cascaded H-bridge multilevel converters.

The current gearbox-systems can do the job reliably, direct drive mechanisms that use about half as many parts should be even more reliable and thus reduce operating costs.

II. THREE LEVEL DIODE-CLAMPED MULTI LEVEL INVERTER

In this study, a Three level diode-clamped converter is used as the grid-side-connected inverter in a wind energy conversion system, and a boost TL chopper is set on the front of it to provide enough dc-link voltage for inversion at low commutating voltage, which results from low rotating speed.

In a multilevel inverter three levels of output voltages are possible compared to two in a two level inverter. The various levels of output voltages are Vp0,Vn. Due to three voltage levels output waveforms are more sinusoidal with less ripple content. This reduces the filter requirement at the output. The voltage applied to the inverter is half the voltage applied to the conventional inverter and no of IGBT used is 4 in each leg with 3 legs for 3 phases.

The switching loss is very less as the switching frequency to produce the same output is almost half the switching frequency required for a conventional two level inverterThe multilevel voltage source inverters unique structure allows them to reach high voltages with low harmonics without the use of transformers or series connected synchronized switching devices, a benefit that many contributors have been trying to appropriate for high voltage, high power applications. The waveform obtained from the three level converters is a quasi-square wave output.

The commutation of the power switches aggregate these multiple dc sources in order to achieve high voltage at the output; however, the rated voltage of the power semiconductor switches depends only upon the rating of the dc voltage sources to which they are connected. However, the elementary concept of a multilevel converter to achieve higher power is to use a series of power semiconductor switches with several lower voltage dc sources to perform the power conversion by synthesizing a staircase voltage waveform. Capacitors, batteries, and renewable energy voltage sources can be used as the multiple dc voltage sources.

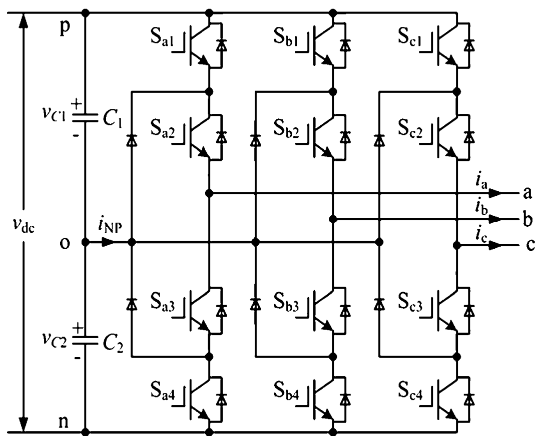

Fig. 1. Topology of TL diode-clamped inverter

IGBT	Vout=Vp	Vout=Vo	Vout=Vn
Q1	ON	OFF	OFF
Q2	ON	ON	OFF
Q3	OFF	ON	ON
Q4	OFF	OFF	ON

Table 1. switching sequence of diode clamped multi level inverter

III . OPERATING PRINCIPLE OF BOOST TL CHOPPER

The mechanism of NP potential is discussed briefly below and the topology of TL diode-clamped inverter is shown in Fig. 2.Supposing that NP potential remains balance (vC1 = vC2 =vdc/2). The chopper controls are also described in detail. This paper also presents the control strategy of the overall wind-power unit. Performance of the overall wind power unit, including the NPC converter system. A sinusoidal PWM switching is adopted for the NPC converters. The PWM carrier signals of both NPC converters and the buck converter are synchronized to the grid voltage Vsabc at the low voltage side of the interface transformer.

A key problem with diode-clamped topology is to control the neutral-point voltage at one half of the dc-link voltage . In fact, under certain operating conditions , a low frequency voltage oscillation appears in the neutral point. Therefore current is drawn from neutral point, causing one dc link capacitor to be charged, while the other is discharged. Several methods to balance the neutral point voltage have been proposed. The basic procedure is to measure the error between the capacitor voltages and use a simple controller to calculate an offset to be added to each of the PWM modulation waves, which modifies the neutral point current and produce a charge balancing on the capacitor.

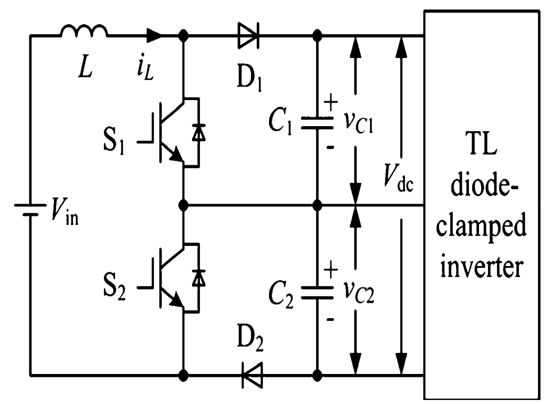

Fig 2. Topology of boost TL chopper.

The power switches S1 and S2 are turned on or off alternately, and the phase delay Θ between two switching signals is usually equal to π. Assuming that the inductance L is large enough to maintain the continuity of the current iL. From Figs. 3 and 4(a), the operating principles when D>0.5 can be summarized as follows.

1) From *t*0 to *t*1 and from t2 to t3, S1 and S2 are both on, and the inductance current flows in the circuit. The energy is stored in the inductance and the charge or discharge of capacitorsC1 and C2 is dependent on the operating state of the TL inverter. Case 1) only occurs when D >0.5.

2) From t1 to t2 , S1 is on and S2 is off, and the inductance current flows through the circuit. The energy stored in the inductance transfers to capacitor C2. Consequently voltage vC2 rises and iL gradually drops from ILmax to ILmin.

3) From t3 to t4 , S1 is off and S2 is on, and the current flows through the circuit . C1 is charged by the boost

chopper, and voltage vC1 increases. The current decay is the same as in case 2.

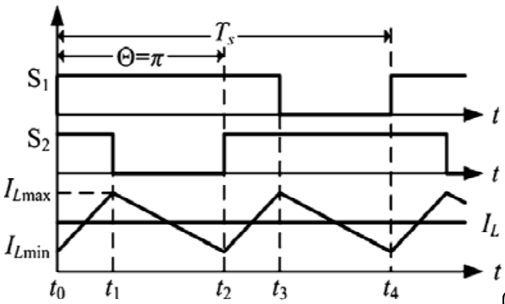

(a)

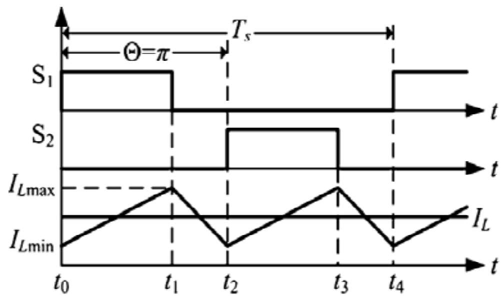

(b)

Fig3. Switching signals and inductance currentwaves of boost TL chopper

With Θ = π. (a)D > 0.5. (b)D < 0.5

The case of $D < 0.5$ can be analyzed in a similar way. It can be seen from the earlier that capacitors $C1$ and $C2$ are charged or discharged equally during one sampling period in the case of $\Theta = \pi$, so the NP potential is not affected by the boost TL chopper. The SSPDC is adopted for the boost TL chopper to balance the NP potential of TL inverter.

IV. MAXIMUM POWER POINT TRACKING CONTROL OF WECS

The maximum power point tracking (MPPT) control is introduced briefly as the boost TL chopper is used for NP potential balancing and MPPT simultaneously. According to the aerodynamic model, the wind power captured by turbine can be calculated as follows

$$\text{Pcap} = \frac{1}{2}\,\pi\,\text{p}\,\text{R}^2\,\text{v}^3 \qquad (1)$$

The power coefficient Cp can be written as a function of λ and β

$$(\tau, \beta) = 0.22\left(\frac{116}{\tau i} - 0.4\beta - 5\right)e^{\frac{-12.5}{\tau i}} \qquad (2)$$

Where

$$\frac{1}{\tau \text{i}} = \frac{1}{\tau + 0.08\beta} - \frac{0.035}{\beta^3 + 1},\ \tau = \frac{\square R}{V}$$

When the wind speed is below the rating, the pitch angle β is always equal to 0 and the MPPT can be achieved by controlling the generator-side converter. When wind speed is beyond the rating, the rotating speed is limited by regulating β to keep output power constant .From (1) and (2), the maximum captured power can be obtained when p = 0.438 or λ = 6.325. The optimal rotating speed, as the reference value, can be calculated when Rand v are given. In steady state, induced voltage, generator and generator torque are given as follows

$$\text{E} = \text{Ke}\ \Omega \qquad (3)$$

$$\text{Te} = \text{K}\square\ \text{I}\square \qquad (4)$$

The dc-link voltage Vdc can be written as

$$\text{Vdc} = \frac{3\sqrt{6}}{1 - \text{D}}\sqrt{\text{Ke}^2} - \sqrt{\left(\frac{\text{Pn Ls Te}}{\text{Kt}}\right)^2} \qquad (5)$$

The dc-link current of inverter is characterized as average value by this equivalence. Taking the total losses of generator, diode rectifier, and boost TL chopper into account, the equation of equivalent resistive loads can be expressed as

$$\text{n Pcap max} = \frac{\text{Vdc}^2}{4}\left(\frac{1}{\text{R1}} + \frac{1}{\text{R2}}\right) \qquad (6)$$

Supposing that disturbances of vin and θ are small enough to be ignored and Θ=π, R1 = R2 = R, VC1 = VC2 = Vdc/2 in steady state, the transfer function between duty ratio and rotor speed disturbances in s-domain can be written as

V. VOLTAGE ORIENTED CONTROL OF PWM RECTIFIERS

The Voltage Oriented Control technique for the AC/DC line-side converters originates from Field Oriented Control for the induction motors. It provides the fast dynamic response since the current control loops are applied. The properties of the control systems based on the VOC strategy are different depending on the involved PWM technique. The hysteresis pulse-width modulation method provides the on-line current tracking thus the influence of any disturbances is minimized and the better robustness of the control system is achieved. On the other hand the varying switching frequency introduces an additional stress in the power switches and requires the higher values of the parameters of the input filter.

The Voltage Oriented Control-based system for the PWM rectifier has the cascaded structure. The line current control is realized in the inner loop while the DC-link voltage control proceeds in the outer loop. Referring to the control system is coupled and the performance of the PI control may not be satisfactory. The power balance equation represents the nonlinear differential equation and reveals the nonlinearity included in the formal description of the PWM rectifier.

The control strategies for the AC/DC line-side converters have been adapted from the methods elaborated for the vector control of the induction motors. The classical control techniques require the strict knowledge of the values of the line and load parameters since the PI control performance is strictly dependent on the proper identification of the line chokes inductance and the DC-link capacitance.

VI . SIMULATION RESULTS AND ANALYSIS

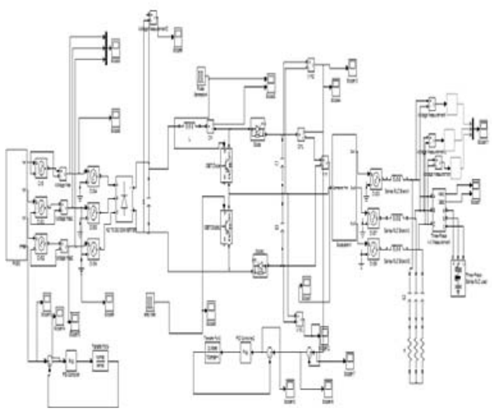

fig.4 simulation diagram of of multi level inverter in WECS using PMSG

The WEC, is simulated to evaluate the proposed control strategy. Some typical parameters of the WECS used in the simulation are listed in Table II.

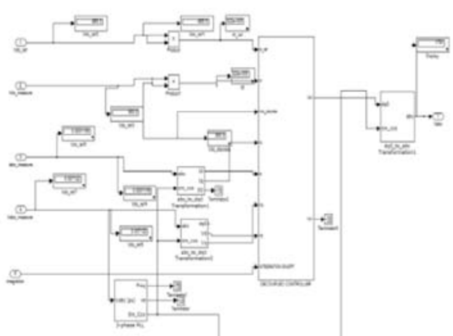

fig 5 simulation diagram of of voltage oriented controller

Rating of wind speed(m/s)	12
Air density(kg/m3)	1.225
Wind turbine radius(m)	28
Generator moment of inertia(kgm2)	7*10^4
Number of pole pairs	48
Rating generator line voltage(v)	690
Dc link voltage of TL inverter(v)	1500
Dc link capacitor of rectifier(µF)	1*10^4
Inductance of boost TL chopper(mH)	0.2
Dc link capacitor of inverter(μF)	1*10^5
Inductance of LCR filter(mH)	1.75

Table II parameters of simulation system

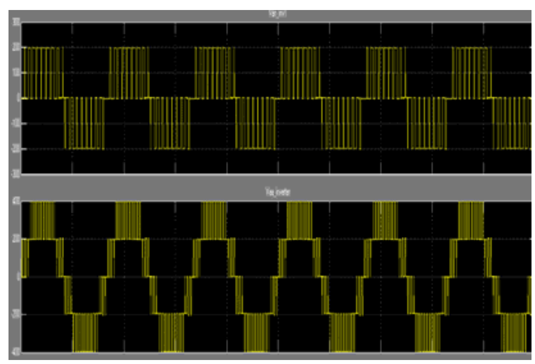

(a)

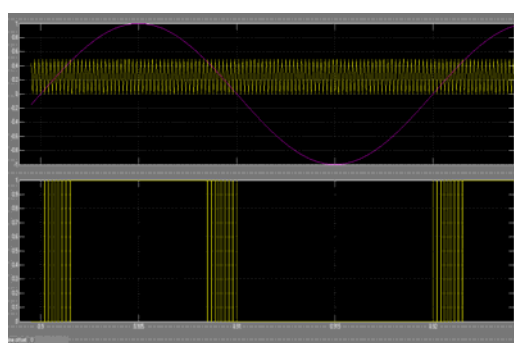

(b)

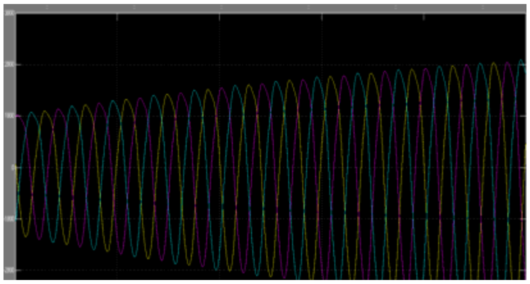

(c)

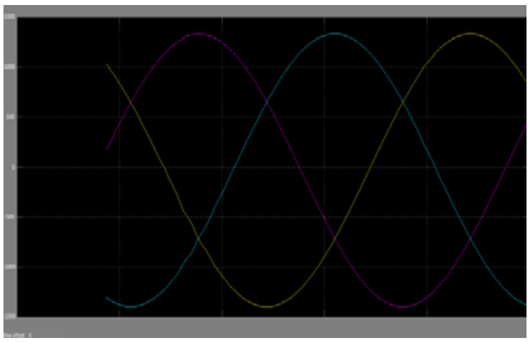

(d)

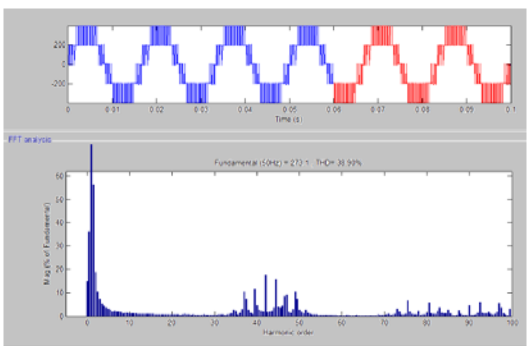

(e)

Fig 6. (a) shows the step output waveform of line voltage of three level inverter when the input gate pulse generated by the pwm generator. (b) Output waveform of SPWM (c) grid voltage without voltage oriented controller. (d) grid voltage with voltage oriented controller(e) FFT analysis and total harmonic distorsion for three level inverter

VII. CONCLUSION

In this paper, a power converter topology using diode rectifier, three-level boost converter based wind energy conversion system using PMSG has been proposed. In this study wind turbine is directly coupled with PMSG and connected to the grid through multi level inverter.By increasing the number of levels, the THD will be decreased but on the other hand cost and weight will be increased as well. The proposed model has been implemented in MATLAB.

REFERENCES

[1] N. Celanovic and D. Boroyevich, “A comprehensive study of neutral-point voltage balancing problem in three-level neutral-point-clamped voltage source PWM inverters,” IEEE Trans. Power Electron., vol. 15, no. 2,pp. 242–249, Mar. 2011.

[2] S. M. Dehghan, M. Mohamadian, and A.Y.Varjani, “A newvariable-speed wind energy conversion system using permanent-magnet synchronous generator and Z-source inverter,” IEEE Trans. Eergy Conv., vol. 24, no. 3, pp. 714–724, Sep. 2009.

[3] B. P. Schmitt and R. Sommer, “Retrofit of fixed speed induction motors with medium voltage drive converters using NPC three-level inverter high-voltage IGBT based topology,” in Proc. IEEE Int. Symp. IndustrialElectronics, vol. 2, 2008, pp. 746–751.

[4] A. Bendre and G. Venkataramanan, “Modeling and design of a neutral point regulator for a three level diode clamped rectifier,” in Conf. Rec.IEEE-IAS Annu. Meeting, vol. 3, 2007, pp. 1758–1765.

[5] G. Ramtharan and N. Jenkins. "Modelling and Control of Synchronous Generators for Wide-Range Variable-speed Wind Turbines".Wind Energy,Wiley Interscience, vol. 10, pp. 231-246, March 2007.

[6] M. Chinchilla, S. Arnaltes and 1. C. Burgos. "Control of Permanent Magnet Generators Applied to Variable-Speed Wind-Energy Systems Connected to the Grid". IEEE Transactions on Energy Conversion,vol. 21, no. 1,2006.

[7] G. Cvetkovski, L. Petkovska and S. Gair, "Performance Analysis of a Permanent Magnet Disc Motor for Direct Electric Vehicle Drive", Journal,Vol. 10, No. 3, July-September 2003, pp. 353-358

A ZigBee Based Hot Axle Monitoring System For Rolling Stock

N K Kulshrestha, M L Dewal & H K Verma

***Abstract* -** Wireless technology is making its impact felt in almost all walks of life. Be it Home automation, Building Automation, street light control, utility metering or patient health care systems, all areas have begun to utilize wireless technology to advantage.

The ZigBee technology has been developed specifically to target large adhoc wireless networks that have low intermittent data rates, low power/battery operation and a small physical footprint.

The technology has admirably targeted wireless sensor networks and is emerging as the technology of choice for these applications.

An area where the adoption of this technology has not been as pervasive is rolling stock or railway vehicles. A train occupies a large geographical area and need for communication of information throughout the train can be immediately felt. This paper puts forth certain areas of application of ZigBee technology in the area of rolling stock. A system for monitoring of hot axles on railway coaches/wagons is designed and other applications in the same area are outlined.

The paper concludes that adoption of ZigBee technology on rolling stock would be a meaningful exercise with a diverse range of applications, limited only by the imagination of the designer.

I. INTRODUCTION

A wireless sensor network differs in several respects from a conventional wireless network such as 802.11 type networks. Generally in a typical sensor network topology the arrangement is such that a number of sensors/actuators referred to as nodes direct/receive their traffic from a single master node. This is in sharp contrast to conventional wireless networks, where a route or path can be required between any two nodes that might desire to exchange data. Other key differences are:

- Data requirement ranges from few bits to a maximum of few kilobits.
- Reliability requirements are usually very stringent.
- Certain applications require real time low latency data.
- Power available at the nodes is usually limited; hence it should be possible for nodes to conserve power whenever necessary.

This work was carried out at Indian Institute of Technology, Roorkee.

N.K.Kulshrestha is currently pursuing a Master Of Technology degree in Electrical Engineering at IIT Roorkee,.

Dr. M.L. Dewal is currently Professor of Electrical Engineering at IIT Roorkee.

Dr. H.K. Verma is currently Professor of Electrical Engineering at IIT Roorkee.

Keeping in view the above differences it is observed that the overheads associated with a conventional TCP/IP scheme are too expensive for such applications. Here ZigBee technology comes to the rescue.

The ZigBee specification provides for data transmission rates of up to 250 Kbps and a range of up to 30 meters. Power requirements are significantly reduced. Main features of ZigBee are [10][11]:

- PHY and MAC based on IEEE802.15.4.
- NWK and APS defined by ZigBee alliance.
- Low cost and Low power.
- Multi Hop capability extends range.
- Self configuring battery power operation possible.
- Mesh topology allows self healing capabilities and improved reliability.

- Sleep mode possible where a device periodically wakes up, carries out the assigned tasks and goes back to sleep again.

II. ZIGBEE FEATURES [10][11]

The ZigBee has been designed to provide the following features:

i) Low power Consumption implemented by providing sleep mode. A ZigBee device can have two states: Sleep and active (transmit/receive).

ii) The addressing mechanism of IEEE 802.15.4 PHY allows the network to handle an extremely large number of devices. Devices can have 64 bit addresses allowing up to 2^{64} addresses and 16 bit network addresses.

iii) Low cost per node as a simple microcontroller with modest amount of ROM/RAM can be used. The stack implementation has a small foot print.

iv) PHY layer supports 2.4GHz and 868/915 MHz

v) Data rates of 250 Kbps @2.4GHZ

vi) Optimized for low latency, low duty cycle devices like sensors and controls

vii) Fully handshaked data transfers for reliability.

viii) Allows periodic, intermittent and repetitive low latency data.

III. CONVENTIONAL ZIGBEE APPLICATIONS

Up to now ZigBee has been successfully and gainfully employed in following application areas:

Heating, Ventilation and Air Conditioning [1]

- Pump configuration and control
- Thermostat control
- Fan Speed control
- Dehumidifier control

Lighting [1] [2]

- On/Off Control
- Brightness Control
- Color control
- Ballast configuration

Measurement & sensing [1] [2]

- Iluminance measurement
- Iluminance level sensing
- Temperature measurement
- Pressure measurement
- Flow measurement
- Relative humidity measurement
- Occupancy sensing

Advanced Metering Infrastructure (AMI) [8]

- Bidirectional communications of energy metering data
- Energy management to provide more efficient and reliable use of energy usage.
- Real-time pricing information for voluntary load shedding.

Commercial Building Automation (CBA) [7]

- Applications targeted at a commercial building environment.

Home Automation (HA) [1]

- Applications for the residential automation market

Personal, Home and Hospital Care (PHHC) [7]

Non-invasive health care applications such as

- Chronic disease monitoring
- Personal wellness monitoring (ensuring an individual's wellness and safety)
- Physical fitness

Wireless Sensor Applications (WSA) [6]

Wireless sensor network (WSN) applications include

- Environmental Monitoring of either indoor or outdoor areas
- Asset Tracking of mobile tagged-things or persons
- Structural or Machine Monitoring

IV. ZIGBEE APPLICATIONS IN ROLLING STOCK

The above are some of the conventional areas of application of ZigBee technology. An area where this technology, though not commonly applied till now can be very gainfully employed is rolling stock. A train by its very nature presents a very distributed environment for monitoring and control applications. It would be very advantageous if certain information could be made available at a central point that could be the locomotive or the guard’s cabin. Similarly it would be very advantageous if certain operations in the coaches could be carried out by the driver. Based on this following application areas immediately emerge:

- Alarm Chain pulling.

- ❖ Automatic opening/closing of doors throughout the chain.
- ❖ Air conditioning set-point control and monitoring of A/C coaches
- ❖ Fire Detection and Alarm in coaches.
- ❖ Detection of train parting.
- ❖ Updating of passenger Information Display in coaches.
- ❖ Battery and alternator voltage monitoring in coaches...
- ❖ Tracking of coaches and wagons in yard and relaying of this information to the Yard master.

In the next section a somewhat non conventional area for application of ZigBee technology for rolling stock is presented.

V. ZIGBEE BASED HOT AXLE MONITORING SYSTEM

The term “Hot axle” refers to the development of high temperatures due to friction between axle and bearing when there is improper lubrication. This problem can occur on both passenger coaches as well as goods wagons. It is more common in wagons owing to longer maintenance schedules. Hot axles can lead to seizures of wheels and can ultimately lead to derailment of train. Currently monitoring is done manually with a person standing and viewing the axles for signs of overheating , as the train passes a station. Needless to say the system is ineffective and very prone to human error. Since this is a safety related issue, railways have been looking for ways to automate this monitoring.

A previous attempt to automate this system was carried out using temperature sensors provided in the axles. The signals from each axle were led into the wagon body by means of slip rings. The signals were suitably conditioned and transmitted for monitoring to the front of the train using a wired communication link. The system as implemented above was very cumbersome and was not successful owing to following reasons:

- ❖ The slip rings were difficult to maintain.
- ❖ The problem of running a wired link through the wagons was severe. Not only were links unreliable but provisioning of couplers on wagons was also difficult. They had to be uncoupled and re-coupled each time a wagon was changed.
- ❖ Wagons do not have any battery or provision for charging thereof.

In view of these the system was abandoned.

A ZigBee based hot axle monitoring system is proposed to overcome these disadvantages. Such a system should be able to:

- ❖ Send data of axle temperatures to the locomotive periodically.
- ❖ Should not require slip rings.
- ❖ There should not be any couplers/wiring running throughout the length of the train.
- ❖ Power requirement should be sufficiently low, so as to allow operation off a small battery for years.

Figure 1: Arrangement of sensors and modules on the axle

This is discussed in the next section.

VI. GENERAL DESIGN DESCRIPTION

The requirements for a hot axle monitoring system were defined in the previous section. A ZigBee based design for the hot axle monitoring system is now presented. A prototype system based on this design, for four axles is developed and it is demonstrated, how this overcomes the drawbacks of the earlier proposed slip ring based system.

The system has been designed with the following objectives:

- ❖ Display of axle temperatures, directly in the locomotive.
- ❖ No requirement for slip rings.
- ❖ AA cell battery operation with life of at least one year.
- ❖ Reporting of battery condition on display in the locomotive.
- ❖ Fully wireless operation.
- ❖ Fault tolerance against any node going defective, by

establishing communication through adjacent node.

- ❖ No requirement for inter-wagon couplers for signal transmission.

The system proposed, comprises of the CC2530 System on chip (SoC) from Texas instruments, based ZigBee compliant modules, powered by a 2xAA cell, 3 Volts alkaline battery, mounted individually on each axle, that rotate along with the axle. Each module interfaces to the two TMP36 temperature sensors, mounted, at the two axle ends, so that direct reading of axle temperatures is obtained. Each module communicates directly with the module on the adjacent axle, and thus relays its own data as well as that received from its predecessors to the next, till the data reaches from one wagon to the other and finally to the locomotive, where it is displayed. The overall scheme is demonstrated in fig. 1 and fig. 2. The hardware of the system comprises of the following modules:

1) CC2530 based ZigBee Module [13].

2) Sensor and battery board.

3) LCD and keyboard display module.

The CC2530 based ZigBee module plugs into the sensor and battery board. One such unit is provided on each axle. A TMP36 temperature sensor from Analog Devices is attached at each end of the axle at the point, where the temperature is to be monitored. This is wired to sensor and the battery board. The CC2530 on each module remains in low power sleep mode. It wakes up periodically and carries out the A/D conversion on the two temperature channels. It also carries out an A/D conversion on the battery voltage. It then transmits this data to its parent, along with the data received from its child and goes back to sleep mode again until the next cycle, thereby conserving battery power. Once this data reaches the coordinator, the coordinator sends out this data on the serial link to the LCD and keyboard Module, where it is displayed.

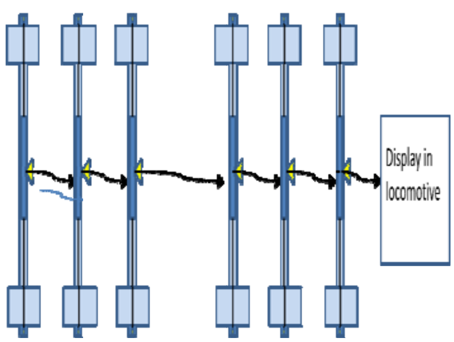

Figure 2: Communication scheme and transmission of Data

VII.HARDWARE DESCRIPTION

The hardware comprises of:

i) ZigBee Module

The block diagram of the ZigBee module is shown in fig 3. The module comprises of the CC2530 SoC from Texas Instruments. Except for the RF pins all other pins of the SoC are brought out on board interconnect, connectors P1 and P2 thereby allowing the module to be plugged into the main board. The RF pins lead to the antenna through the impedance matching network.

The module is designed to operate off 3-3.6 V power supply that may be obtained from a dry cell battery, or a rechargeable battery. The module consists of a 32MHz primary oscillator, and a 32.768 KHz secondary oscillator for real time clock implementation. The CC2530 module provides a microcomputer board with a ZigBee radio that can be used to implement many standalone systems.

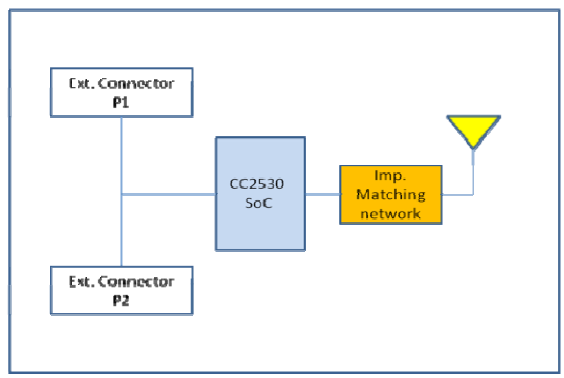

Figure 3: CC2530 ZigBee Module

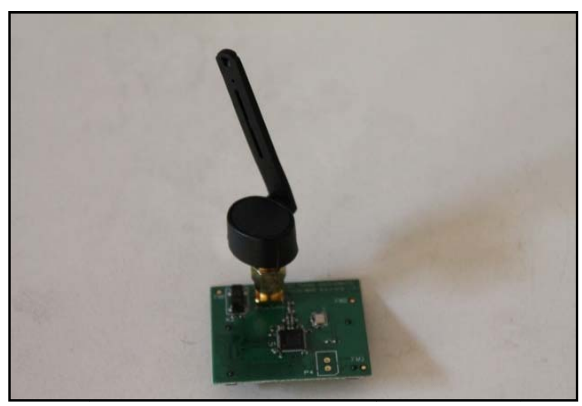

Figure 4: CC2530 ZigBee Module Photograph

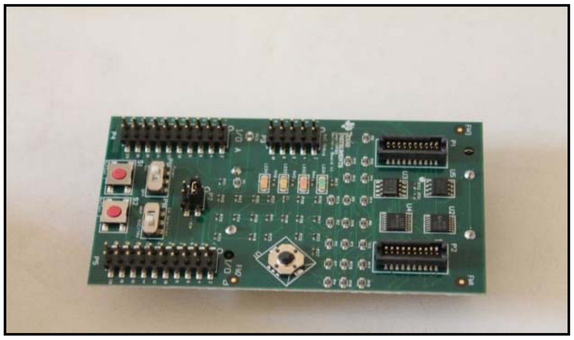

Figure 5: Sensor and Battery board Photograph

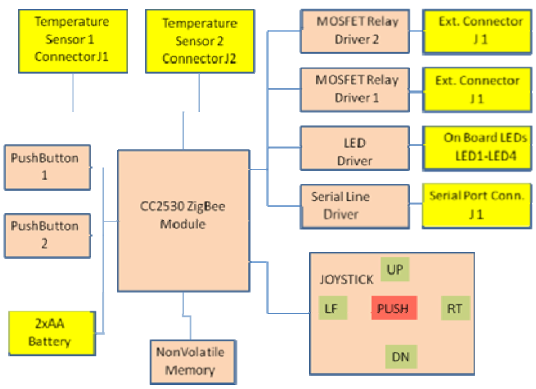

Figure 6: Sensor and Battery board Block Diagram

ii) Sensor and Battery board.

The block diagram of the sensor and battery board is shown in

Fig. 6. The ZigBee module plugs into the sensor and battery board which provides it with external connections. This board provides the following:

- A PCB mounting joystick used to configure the module as a coordinator, router or end device.
- Four status LEDs.
- Two nos. Push button switches to act as inputs.
- Battery case for 2x AA cells to power the module.
- Interface connectors to temperature sensors mounted at the point of interest.
- Line receiver and driver for RS232 interface.
- Drain outputs of two uncommitted Mosfets, to act as relay drivers.
- A serial flash memory, for Non volatile storage.
- All the pins of the ZigBee module are brought out on bergstik connectors P3 and P4 for accessibility.

iii) LCD Display and Keyboard Interface

In order to display the temperature data received by the network coordinator a 16x2 LCD display and a 16 key membrane type keyboard is provided. The network coordinator periodically transmits the temperature data received ,alongwith the end device identifier over the serial port. The LCD/Keyboard interface module , receives this data, processes it, and displays the same on the LCD display. The keyboard is used to for set up purposes, like entering real time, transmission interval and retrieving stored data. A real time non volatile clock is also provided on this module. The block diagram of this module is given in fig. 7.

Figure 7: LCD Display/Keyboard Interface Block Diagram

The module is built around the MCS-51 compatible device AT89C52 from Atmel corporation. The dot matrix LCD module requires, 8 bit lines for communication and these are Connected to Port 2 of the microcontroller. Apart from these the module requires an Enable signal, a Read/-Write signal and a command/data signal. These are provided by lines P3.7, P3.6 and P3.4 of the microcontroller respectively. The keyboard is a 4x4, scanned matrix keyboard, that interfaces with Port0. Lines P0.0 to P0.3 form the keyboard scan lines, whereas lines P0.4 to P0.7 form the keyboard return lines. The serial port lines TxD and RxD of the microcontroller are buffered by the level translator MAX232 and brought out on an external connector. A DS1307 real time clock IC along with a CR1302 lithium battery is provided for real time information. The AT89C52 is clocked by an 8 MHz crystal whereas the DS1307 is clocked by a 32.768 KHz crystal.

VIII.DEMONSTRATION APPLICATION

For the purpose of demonstration, five ZigBee modules, five sensor and battery boards and one

LCD/Keyboard interface module is used. A ZigBee node is built up by plugging the ZigBee module and two TMP36 type temperature sensors into their respective connectors into the sensor and battery board. One of these is set up as the PAN coordinator whereas others are set up as routers. The Coordinator also acts as a gateway and interfaces with the LCD and Keyboard module over the serial link. The coordinator receives data from the routers and sends periodic reports to the LCD/Keyboard module for visual display of data received. Since all the nodes are identical, selection as router/coordinator is done by the Joystick switch provided. The network is illustrated in fig 8. All the nodes, startup as routers and try to locate and join a ZigBee network, by scanning the different channels in the 2.4 GHz band. If the Joystick switch is moved up on any node, its configuration changes to that of a PAN coordinator and it starts up its own network with a unique PAN identifier. This node should be chosen to be the one that is connected to the LCD keyboard interface. Now if the Joystick switch is moved right, this node will allow binding and accept binding requests from the other nodes. Only one device in the network should be in this mode, so that all data is directed towards it. Other nodes while collecting data from their own sensors, also act as routers and help to extend the range of the network by providing hops for routing of messages. The periodic sending of data is started by moving Joystick switch down on each node.

While powering on any node, if the joystick is held pressed in centre position, it causes the node to ignore previous configuration stored in Non Volatile memory and search for a new network. The Joystick should be released only after lapse of a two seconds from power on. Normally basic information such as PAN id, node short address etc. are restored from Non volatile memory when device is powered up.

The application software (firmware) is developed in the C/C++ language and is divided into two categories:

1) The ZigBee module firmware developed using Z-Stack[14][17] which is ZigBee specification's implementation by Texas Instruments for their CC25XX series SoC's. Z- Stack's simplified API's [15][16][18][19]are used to develop the software for the ZigBee modules. These are compiled using IAR's embedded workbench for C51 family.

2) LCD Display and Keyboard monitor firmware, which allows communication with the Coordinator over serial port

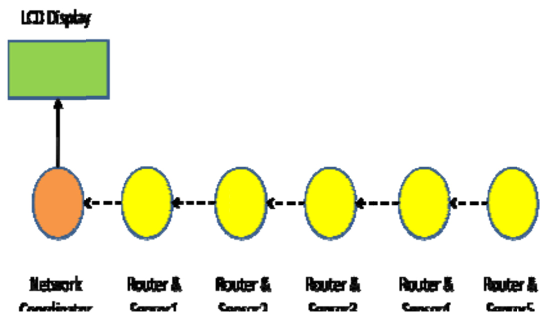

Figure 8: The Demonstration network

and then displays data on the LCD. It also incorporates code for scanned matrix keyboard that is required for screen selection.

The overall objective of the application program running on the routers is to select the A/D conversion channels for the two temperature sensors and the battery voltage channel, carry out an A/D conversion on the selected channels organize them in form of a report and then transmit them over the air. The over the air report is five bytes in following format:

Temperature1 1 byte	Temperature2 1 byte	Battery voltage 1 byte	Parent address Hi byte	Parent address Lo byte

The coordinator is required to send out the over the air received report, over the serial port to the LCD/Keyboard display module where it can be displayed. The payload structure of this message is exactly the same as that of the OTA report above.

The LCD Display and Keyboard Monitor software provides functions for

- initializing and controlling the LCD display.
- scanning the keyboard and reporting key presses.
- initializing and receiving data from serial port.
- parsing the received data and displaying it as per current selection.

IX. TESTING AND RESULTS

For testing the nodes were placed 10m apart and the network was setup as outlined in the previous selection. Keys 0, 1, 2, 3, 4 were used to select the node the data for which was displayed on the LCD. The change in temperatures was simulated by varying the voltage on the ADC input channels using a potentiometer in place of TMP36. Self healing features of the network were observed by switching of a node and the communication resumed through the preceding node. The distance in between the nodes was increased to 30 meters and then 50 meters. Satisfactory communication was observed in both the cases. However in the latter case when an intermediate node was switched off, data from succeeding nodes could not be received.

Accelerated battery life test was conducted by programming the nodes to send data every 2 seconds and keeping the system in operation for 24 hrs. This corresponds to 30x60x24 readings ,i.e. a total of 43200 readings. Actual rate will be around 6 readings per hour or 144 readings in a 24 hr. period. Hence system could safely be concluded to work for 300 days.

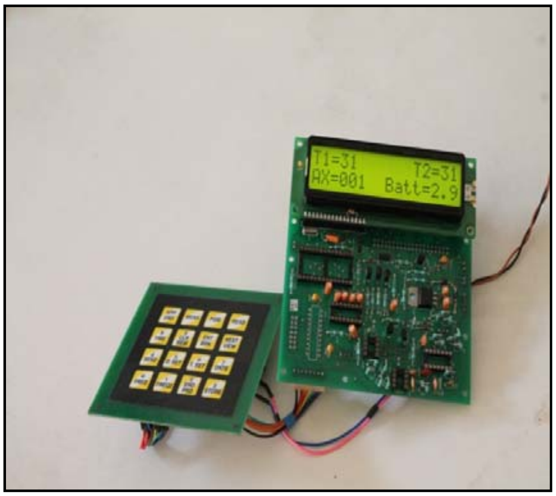

Figure 9: Photograph of readings on display

X. CONCLUSIONS AND FURTHER WORK

It was seen that the system worked efficiently and suffered from non of the drawbacks of the earlier wired systems. It also met the design objectives outlined in section VI. Hence it can be safely concluded that ZigBee technology can be expected to find its way into rolling stock applications in the future. However the network size was small. A real world system would require at least 200 nodes since a train may have upto 200 axles. This would require re-programming of the display system to generate an alarm whenever an increasing trend of temperature that crossed a threshold limit, was detected, since it would not be possible to display all temperatures and then display only that temperature that exceeds the limit.

REFERENCES

1. Theodore B. Zahariadis, “End to End Reference Architecture” in “Home Networking Technologies and Standards” (Book), Artech House, Inc. 2003.
2 .“Corporate Brochure”, http:// www.digihome.co.in/ corpbrochure.pdf
3. “Intelligent Buildings Design and building management systems”, http://www.businessballs.com/intelligentbuilding designs.htm
4. T.Nikolau,D.Kolokotsa,G.Stavrakakis,” Introduction to intelligent buildings”
5. http://en.wikipedia.org/wiki/Sensor_Networks
6. Daniele Puccinelli and Martin Haenggi-Wireless Sensor Networks: Applications and Challenges of ubiquitous Sensing ,IEEE Circuits And Systems Magazine, Third Quarter 2005
7. https://docs.zigbee.org/zigbee-docs/dcn/09-4962.pdf
8. https://docs.zigbee.org/zigbee-docs/dcn/07-5021.pdf
9. http://en.wikipedia.org/wiki/ZigBee
10. IEEE802.15.4-2006 , IEEE Computer Society
11. ZigBee Specification ZigBee Alliance Document 053474r17
12. http://www.daintree.net/learning- Understanding the ZigBee Application FrameWork
13. http://www.ti.com-CC2530XX data sheet
14. http://www.ti.com-HAL Drivers Application Programming Interface Document Number: SWRA193
15. http://www.ti.com-OS Abstraction Layer Application Programming Interface Document Number: SWRA194
16. http://www.ti.com-802.15.4 MAC Application Programming Interface Document Number: SWRA192
17. http://www.ti.com-Z-Stack Application Programming Interface Document Number: SWRA195
18. http://www.ti.com-Z-Stack Monitor and Test API Document Number: SWRA198
19. http://www.ti.com-Simple API for Z-Stack Document Number: SWRA196

SIB Converter with Reduced Harmonic Distortion using Fuzzy Logic Controller

N. Karthik

Dept. of EEE: Hindustan University, Chennai, India.

***Abstract* -** An integrated conventional boost converter and a single ended primary inductor converter (SEPIC) using Fuzzy Logic Controller is presented on this paper. By use of classical boost converter, it contains insufficient step-up ratio, distribution of voltage stress is complex. It needs snubber circuit for additional protection. However, it is very difficult to satisfy both high voltage conversion ratio and high efficiency at once. As a solution to supplement the insufficient step-up ratio and distribute a voltage stress of a classical boost converter, a Sepic-integrated boost (SIB) converter, which provides an additional step-up gain with the help of an isolated Sepic converter using Fuzzy Logic Controller, is proposed. The main advantages a simple structure, continuous input current, and clamped switch voltage stress to the output voltage.

Key Words: Boost converter, Sepic converter. Sepic integrated Boost (SIB) converter, harmonic reduction, fuzzy logic controller.

I. INTRODUCTION

The boost converter is the usual structure utilized in high-power-factor (HPF) rectifiers in order to improve power factor (PF) and reduce the total current harmonic distortion (THD). However, for universal input voltage application, the efficiency can be reduced mainly in the lowest input voltage, and the worst operation condition must be considered in the power converter design procedure [1]. The improvement of the efficiency at lower line voltage is important because the thermal design and heat sinks size are defined considering the worst operation point. Many works were developed in order to improve the operation characteristics of the power converter utilized in HPF universal input rectifiers.

The non-isolated high step-up conversion technique finds increasing necessities in applications, such as electric vehicles, uninterrupted power supplies (UPS), high-intensity discharge (HID) lamp, fuel cell system, and photovoltaic systems.

II. CONVERTER DESCRIPTION

The basic converter topologies such as the Buck, Boost, Fly back, SEPIC, Cuk, and others, have long been attractive and are often chosen for implementing simple, low cost, and low power converters. The use of a single active switch with relatively simple control circuitry is a strong reason for this choice [2].The buck and the boost converters with an input or output filter results in a more bulky converter when compared to the Cuk converter. This is because the input and output inductor cannot be coupled into a single magnetic core as in the Cuk converter ,hence, it increases the overall cost and board area required, which is an undesirable for many applications[1].

For applications which require low ripple current at the input and output port of the converter, the Cuk converter seems to be a potential candidate in the basic converter topologies. The fly back converter requires an additional input and output L–C filter to reduce the switching ripple and noise level at both terminals. The major disadvantage of the Cuk topology besides its inverting output polarity is that both the power switch and the output diode must carry significantly higher currents than typically encountered in other topologies. The potential voltage and current stresses imposed on both the power switch and the diode force the circuit designer to use overrated components [2].

On the other hand, the SEPIC converter was developed primarily to have step up/down capability without inverting the polarity of the regulated output voltage. Actually, both SEPIC and Cuk converters present very similar characteristics and they have the same semiconductor voltage and current stresses [4]. Both configurations offer easy implementation of transformer isolation. It has also been shown that both converters have advantages over the boost converter in terms of the conducted electromagnetic interference noise[1].

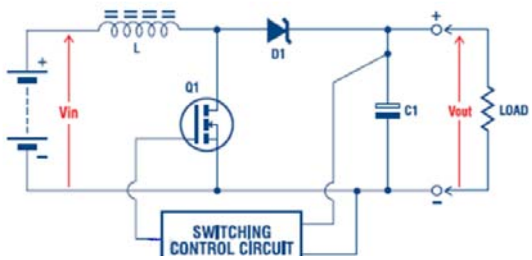

Fig.1 Conventional Boost converter

The power circuit of the classical SEPIC converter is presented in Fig. 2. Moreover, in high output voltage applications, a high-voltage rating diode causes a severe reverse recovery problem,

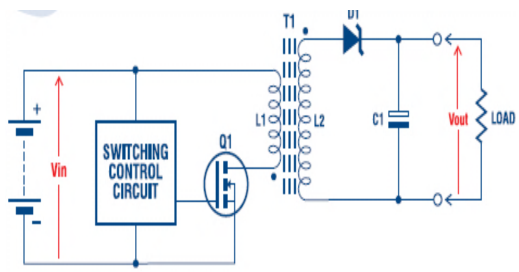

Fig.2 Conventional SEPIC converter

which requires a snubber circuit. As a result, a general boost converter would not be acceptable for high step-up applications. To overcome these limitations, various types of step-up converters, utilizing the voltage conversion ability of a transformer, a coupled-inductor, and a multiplier cell, can be adopted [1].

III. PROPOSED CONVERTER

The step-up and step-down static gain of the SEPIC converter is an interesting operation characteristic for a wide input voltage range application. However, as the switch voltage is equal to the sum of the input and output voltages, this topology is not used for a universal input HPF rectifier.

Current-fed type converters, which easily offer a high step-up ratio using a transformer, are attractive for high power step-up applications with multiple switches [2]. However, they require snubber to limit the voltage spike across switches caused by the existence of transformer leakage inductance, resulting in an additional loss. Moreover, an auxiliary circuit is needed for below 0.5 duty operation and the input current is no longer continuous in this operation [5]. Active clamp approaches release these problems and reduce switching losses, but lead to complex structures with increased number of switches.

A coupled-inductor-employed boost converter is also a favorable candidate in low-to-medium power applications for its simple structure; though the input current is not continuous as in a general boost converter and an auxiliary circuit is also required to suppress the switch voltage spike [1], [2].As the output voltage is increased, however, the number of stage is increased, requiring more capacitors and diodes. Besides, the current snubber is required to reduce the reverse recovery on diode.

To simplify the circuit, a boost converter and a Sepic converter, as a series output module can be simply integrated, as shown in Fig. 2, because they can share common parts, i.e., a boost inductor LB and a switch Q. Since this series output module should have a floating output ground, an isolated-type Sepic converter is adopted.

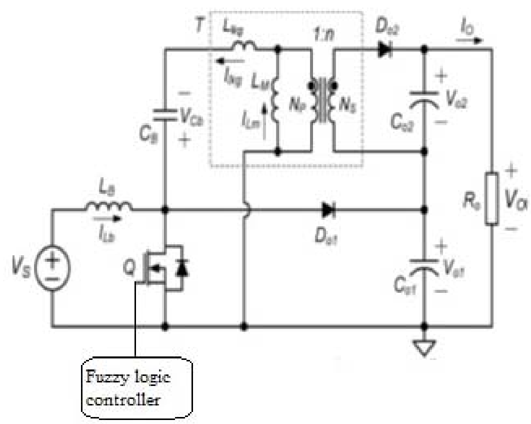

Fig.3 SEPIC Integrated Boost (SIB) converter using Fuzzy Logic Controller.

As a result, a Sepic-integrated boost (SIB) converter is derived, as shown in Fig. 3. This converter provides an additional step-up ratio and a distributed voltage stress on devices, while maintaining the advantages of the boost converter, such as continuous input current and clamped voltage stress on switch. Moreover, the transformer leakage inductance provides a current snubbing effect, which alleviates the reverse recovery problem on diodes.

III. OPERATION PRINCIPLES

SEPIC is a type of DC -DC converter that allows the electrical potential (voltage) at its output to be greater than, less than, or equal to that at its input; the output of the SEPIC is controlled by the duty cycle of the control transistor. A SEPIC is similar to a traditional buck-boost converter, but has advantages of having non-inverted output (the output voltage is of the same polarity as the input voltage), the isolation between its input and output (provided by a capacitor in series).

STATES	MODE-I	MODE-II	MODE-III	MODE-IV
ON	Q,Do2,1:n	Q	Do1,Do2,1:n	Do2,1:n
OFF	Do1	Do1,Do2,1:n	Q	Q,Do1

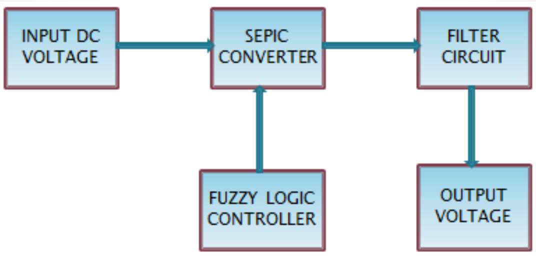

Fig.4 Block Diagram of SEPIC converter.

This paper has presented a modified SEPIC converter with a continuous output current. The principle of operation and the design-oriented analysis of the proposed converter have been presented. Normalized expressions for peak component stresses are also given, which allow the design optimization of the power stage.

A comparison between the proposed topology and the conventional SEPIC converter shows that the components current stresses are much lower in the presented topology.

Thus, in low-voltage high-current applications, the proposed topology can be more beneficial than a conventional SEPIC converter. Furthermore, this study also shows that the output capacitor current ripple is greatly reduced when compared to the conventional SEPIC, which in turn minimizes the converter's output capacitance requirements.

IV. MATHEMATICAL ANALYSIS

The SEPIC is a DC to DC topology similar to the Cuk converter. It is capable of stepping up or down the input voltage; it has an input inductor and a capacitor for an energy transfer device [2]. The difference is that the output of the converter is reconfigured so that the output voltage has the same polarity as the input voltage. The SEPIC topology is shown in Fig 2.

$$\frac{dIL_1}{dt} = \frac{Vin}{L_1} + \frac{Vc_1 + Vc_2}{L_2}(S-1)$$

$$\frac{dIL_1}{dt} = \frac{Vc_1}{L_2}S + \frac{V_0}{L_2}(S-1)$$

$$\frac{dVc_1}{dt} = \frac{IL_1}{C_1}.(1-S) - \frac{IL2}{C_1}S$$

$$\frac{dVc_2}{dt} = \frac{IL_1 + IL_2}{C_2}.(1-S) - \frac{I_0}{C_2}$$

Performing a similar procedure to find the relationship of input and output voltage of the Boost converter, the SEPIC relationship is:

$$\frac{V_0}{Vin} = \frac{D}{1-D}$$

V. SIMULATION RESULTS

To illustrate the design procedure for a 200-W prototype converter with 42 V input and 400 V output operating at 60 kHz, an example is presented as follows. The required input–output voltage gain Mis 9.52 (=400/42), i.e., about 10.

To distribute and limit the voltage stress across the diode in the Sepic converter by Vo2 with a non-dissipative way, the secondary side is substituted by the clamp diode structure. Therefore, the nominal duty cycle Dnom should be selected as above 0.5. In the converter design, a selection of the switch Q, which is burdened by the large input current ILb and ILm as well, is primarily considered with respect to the cost and the efficiency. Therefore, a D should be selected to accommodate as a low voltage stress as possible, while still having a low rms value of a switch current. To utilize a 200 V switch with a sufficient margin, therefore, the Dnom is selected as about 0.6.

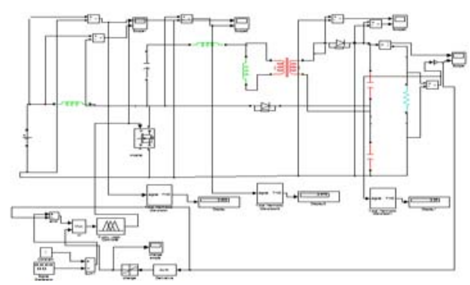

Fig.5 Simulation circuit for Sepic Integrated Boost (SIB) converter using Fuzzy Logic Controller.

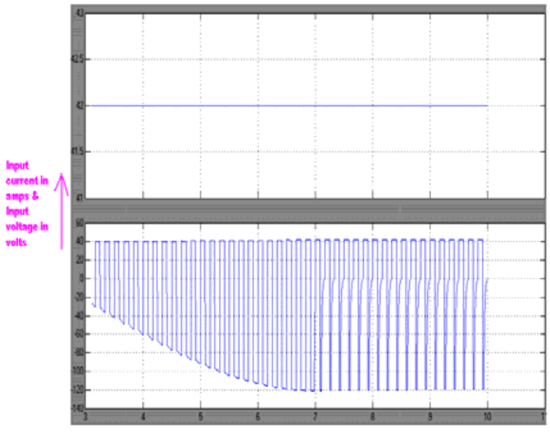

Fig.6 Input voltage and input current of SIB converter using Fuzzy Logic Controller.

An rms value of switch current is decreased as D is increased. That is, a larger D is of benefit for reducing a switch conduction loss. However, a switch voltage stress $VS / (1-D)$, is increased in return, which lead to a use of higher voltage switch having larger ON-resistance.

The SIB converter can achieve a high-voltage gain with the additional step-up ability of the isolated Sepic converter and distributed voltage stress, while maintaining the advantages of the boost converter, such as a continuous input current and a clamped voltage stress on switch.

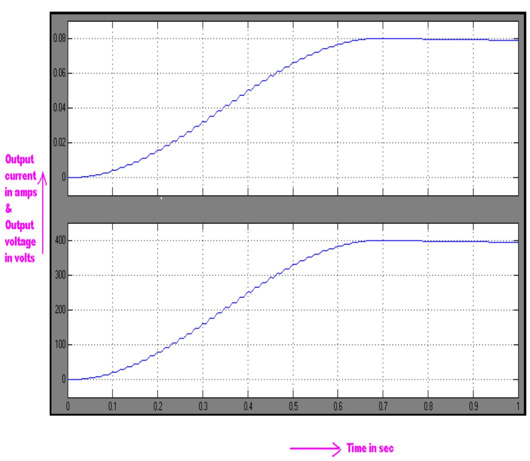

Fig.7 Output voltage and output current of SIB converter using Fuzzy Logic Controller.

TABLE-I

SPECIFICATION USED IN SIMULATION

To verify the performance of the proposed control strategy, a MATLAB-SIMULINK prototype of the SEPIC Integrated Boost (SIB) converter is developed. To illustrate the design feasibility of the proposed converter, a prototype with the following specifications is chosen.

DESCRIPTION	VALUE
Input Voltage Vs	42V
Switch Q	Rd=0.06Ohm
Transformation Ratio n	5
Output Voltage Vo	400V
Output Current Io	0.5A
Switching Frequency Fs	60Khz
Output Power Po	200W
Boost Inductor Lb	618uH
Balance Capacitance Cb	11uF
Gain	2.5
Main Diode	Do1 (Vf=1.2V), Do2 (Vf=1.4V)

TABLE-II

TOTAL HARMONIC DISTROTION ANALYSIS

Total Harmonic Distortion (or Distortion Factor) of voltage or current is the ratio of the RMS value of harmonics above fundamental, divided by the RMS value of the fundamental.

The THD value in this table is expressed as a function of the nominal system RMS voltage rather than of the fundamental frequency voltage magnitude at the time of the measurement.

The performance of the modified SEPIC converter is compared with the classical boost converter. The experimental waveforms are obtained with the experimental prototype operating with the nominal output power Po = 200 W and THD=28.31%.The output voltage is regulated in Vo = 400 Vdc.

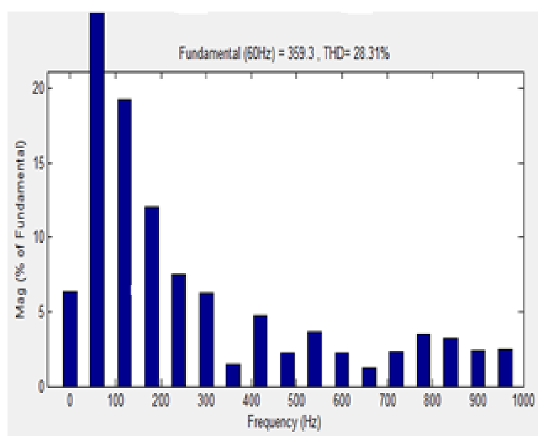

Fig.7 The presence of Total Harmonic Distortion in the Output voltage using Fuzzy Logic Controller.

VI. CONCLUSION

For non-isolated high step-up applications, the SIB converter, which combines a boost converter and an isolated sepic converter with one switch, is introduced in this paper. The SIB converter can achieve a high-voltage gain with the additional step-up ability of the isolated sepic converter and distributed voltage stress, while maintaining the advantages of the boost converter, such as a continuous input current and a clamped voltage stress on switch and maintain the low THD value on the output voltage waveform using fuzzy logic controller compared with the PWM gate pulse given to the switch Q.

Moreover, the reverse recovery problem is well suppressed, since the transformer leakage inductance alleviates a di/dt ratio of the turn-off diode current without additional snubber and the voltage stress on the secondary diode is limited by the clamp diodes. It is noted that other converters, which have a boost inductor and a switch as an input stage, can also be integrated with the boost converter similar to the SIB converter. By using the PWM controller gate pulse the presence of THD on the output side will be THD=31.07%, and by use of Fuzzy logic controller as the pulse of the switch Q, the presence of THD on the output side will be THD=28.31%.

REFERENCES

[1]. M. A. Al-Saffar, "An improved topology of SEPIC converter with reduced output voltage ripple," IEEE Trans. Power Electron., vol. 23, no. 5, pp. 2377–2386, Sep. 2008.

[2]. Paolo Mattavelli" General-Purpose Fuzzy Controller for DC–DC Converters", IEEE Trans. Power Electron. vol. 12, no. 1, pp. 79-86, May. 1995.

[3]. Henry Shu-Hung Chung" A Novel Maximum Power Point Tracking Technique for Solar Panels Using a SEPIC or Cuk Converter," IEEE Trans. Power Electron. vol. 18, no. 3, pp. 717-724, May. 2003.

[4]. Edy E. Jiménez-Toribio" Sensorless Control of SEPIC and Cuk Converters for DC Motors using Solar Panels," IEEE Trans. Power Electron.2009.

[5]. Simone Buso" Simplified Control Technique for High-Power-Factor Flyback Cuk and Sepic Rectifiers Operating in CCM," IEEE Trans. Power Electron. vol. 36, no.5, pp. 1413–2000, Sep. 2000.

An Efficient High Voltage Full-Bridge DC-DC Converter for High Voltage DC Applications

Benny K.K. & J.T. Kuncheria

Rajagiri School of Engineering & Technology, Cochin, India

Abstract - This paper proposes a zero current switched current-driven high power DC-DC converter for high voltage applications. In this circuit a snubber capacitor is connected in parallel with the primary winding of the coupling transformer. The special feature of the proposed circuit is the splitting of the resonant inductor to decrease the power loss and to increase the efficiency. The proposed converter has the following key features. First, by splitting the resonant inductor the circulating resonant energy is reduced to a minimum value so as to switch the inverter switches at zero current. Second, the value of one part of the resonant inductor can be customized with the available leakage inductance from the transformer. Third, there is no extra voltage or current stress expected on the inverter switches. The maximum voltage expected across any component is limited to the primary voltage of the transformer and maximum current is limited to the input current of the inverter. The DC supply is first converted into high frequency (20 kHz) AC. This high frequency AC can be stepped up to the desired level (15 kV) using a high frequency transformer which will be very small in size compared to the low frequency transformer. The output of the transformer can be converted to high voltage DC using a simple bridge rectifier and a filter capacitor. The switching operation of the inverter is symmetrical in both the half cycles. Therefore one half cycle is explained in five modes. By considering the energy equivalence between the inductor and capacitor, the design of the resonant circuit components are carried out. A simulation file was created using PSIM software for a 5 kW, 15 kV Converter. The simulation results assured the soft switching of the inverter switches, current and voltage stress within the limits, and much higher efficiency than the hard switched converters.

Keywords— *high voltage converter, zero current switching, energy efficiency.*

I. INTRODUCTION

FOR high power dc-dc conversion mostly full-bridge(FB) converters are used. To increase the efficiency of the converters, the major concerns are power loss reduction and increased switching frequency. So in-order to increase the efficiency of full-bridge dc-dc converters with high switching frequency, soft switching is necessary. Otherwise as switching frequency is increased switching losses also will be increased.

A number of technical papers are available, where zero-voltage switching (ZVS) is established for PWM-FB converters [1]-[10].The zero voltage switching technique is more suitable for MOSFETs which are majority carrier type devices. Here the capacitive turn on and turn off minimizes the overlap between current and voltage by slowing down the voltage rise across the switch, and thus minimizes the switching losses. But nowadays insulated gate bipolar transistors (IGBT) are preferred for high voltage and high power applications. Because IGBT is a combination of BJT and MOSFET, it is a minority carrier type device and has low on state conduction loss and needs only a simple gate drive circuit. Since IGBT is a minority carrier device, it has slightly longer tail current at turn off. This turn off tail current may cause high switching losses. Therefore for IGBT, zero current switching would be more effective than the zero voltage switching.

For non-isolated PWM converters, different zero-current transition (ZCT) switching schemes have been proposed [11]–[19]. The majority concepts used in these techniques are based on placing an active switch and passive components in parallel to the main switch. The circuit is activated just before turning the main switch off to divert the switch current away. Although the main switch is soft-switched, the advantage is offset by some drawbacks, such as hard switching of the auxiliary switch [11], extra current stress on the main switch [12]–[14] or auxiliary switch [14], [17], high circulating current [12], [13], [16], and extra voltage stress on the auxiliary switch [19].

By applying the concept of ZCT directly for PWM-FB converters, two ZCT auxiliary circuits are placed on the primary side of the bridge circuit [19]–[21]. The concept is extended in [22]–[24] for current-driven PWM-FB converters, in which the auxiliary circuit is placed on the primary side. The current driven converter has the advantage of having continuous input current without using large input filter. Moreover, the lack of the output inductor in converters with a very high output voltage is highly preferred. In [22] and [23], the auxiliary circuit is a resonant capacitor and is designed for achieving ZCS at full-load condition, so it introduces unnecessary duty cycle loss, peak resonant current, and conduction loss at other loading conditions.

With further improvement, some ZCS-FB converters utilize Snubbers on the secondary side [25]–[27]. In [25], all the switches are soft-switched, but the resonant inductor causes voltage ringing across the output rectifier diodes. The solution in [26] tackles the aforementioned problem, but it suffers from the reverse recovery problem of the anti-parallel diode in the auxiliary circuit. In [27] and [28], the reverse recovery problem of the anti-parallel diode of the auxiliary switch is solved. As the resonant inductor current has to surpass the output current in order to bring the primary current to zero, the secondary resonant current peak implies a high peak in the primary current, which leads to extra conduction loss in the primary-side switches.

Finally, the majority switching methods seldom handle the energy flow for soft switching. Non-optimal usage of the soft-switching energy causes undesired current and/or voltage resonant peaks and thus leads to additional conduction loss. This paper proposes splitting of the resonant inductor into two parts to minimize the circulating resonant energy loss. The second part of the inductor can be customized with the available leakage inductance of the coupling transformer. So the resonant energy will be circulated only through the first part of the resonant inductor which is kept at a minimum value. Therefore the efficiency of the proposed converter should be much better than the hard switched counterpart.

II. CIRCUIT STRUCTURE OF THE CONVERTER

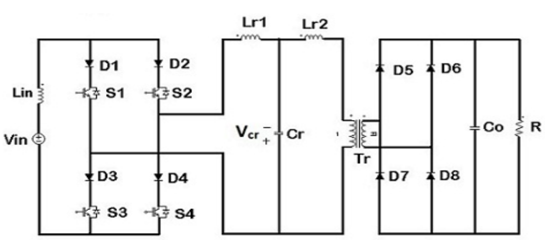

Fig.1 Proposed circuit Structure of the Converter

Fig. 1 shows the circuit details of the proposed current- driven FB converter. The switches S_1 -S_4 and the diodes D_1-D_4 forms the front stage dc to ac converter and the diodes D_5- D_8 forms an output stage rectifier. The front stage rectifier formed by the combinations of S_1 -D_1, S_2 -D_2, S_3-D_3, and S_4-D_4 which are four unidirectional switches ensure zero current switching. The two stages are interconnected by a coupling transformer T_r with the turns ratio *n*: 1. The input side of the converter is supplied through an inductor L_{in}. The resonant inductor L_r is split into two as L_{r1} and L_{r2}. L_{r1} and L_{r2} together with resonant Capacitor C_r forms a snubber circuit and is connected across the primary of the coupling transformer. This snubber circuit is able to make the switches S_1 – S_4 switch at zero current.

III. PREDICTED TIMING DIAGRAM OF THE CONVERTER

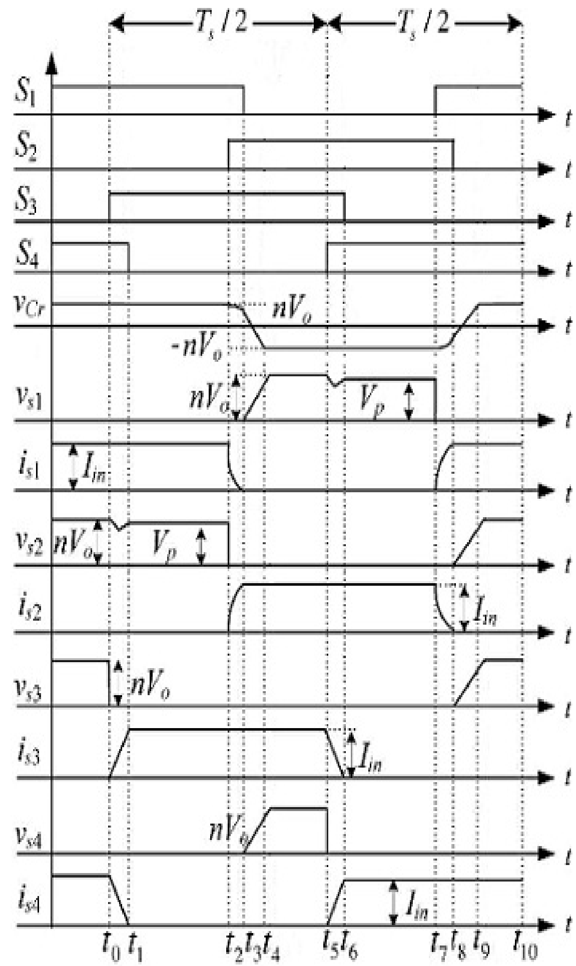

Fig. 2. Timing diagrams and key waveforms of the converter

Fig.2 shows the predicted signal timings of the converter switches and the expected voltage and current waveforms. The switch pair concept is quite different from the conventional phase-shifted **FB** converter where each leg in the bridge is a switch pair. Here the switches *S*1 and *S*2 are switched in antiphase, while *S*3 and *S*4 are also switched in antiphase. Therefore switches *S*1 and

*S*2 form one switch pair, as well as switches *S*3 and *S*4 form another switch pair. The average output voltage of the converter can be controlled by adjusting the phase angle between the switches *S*1 and *S*4.

IV. MODES OF OPERATION

While starting the explanation of the modes of operation, let the circuit topology be as shown in Fig.3.

A. Mode 0 [Before t_0]

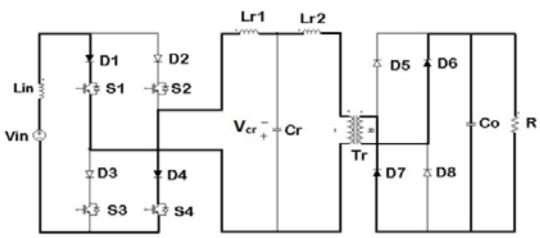

Fig.3 Mode 0 operation

Now the energy is being transferred from input to the output through L_{in}, S_1, Tr, D_6, D_7, Lr_2, Lr_1 and S_4. By analyzing the circuit the variable parameters can be estimated as follows,

$$v_p(t_0) = nV_{out} \tag{1}$$

$$v_{Cr}(t_o) = nV_{out} \tag{2}$$

$$i_{Lr1(t_o)} = i_{Lr2}(t_0) = I_{in} \tag{3}$$

Where v_p is the voltage across the primary of the transformer, Vout is the output voltage of the load; v_{Cr} is the voltage across C_r, i_{Lr1} and i_{Lr2} are the resonant inductor currents.

B. Mode I [$t_0 - t_1$]

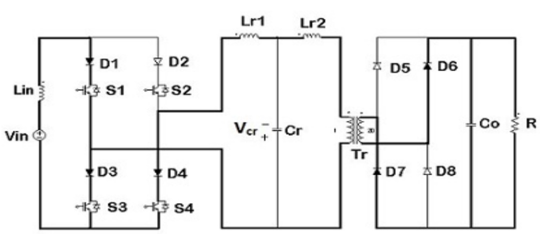

Fig.4 Mode I operation

To attain the next half cycle S_2 & S_3 has to be switched on and S_1 & S_4 has to be switched off at zero current. Now at t_0 since S_3 carries no current, it can be switched on at zero current. Then the presence of Lr_1 and Lr_2 in the current path will allow only a soft increase in the current. The primary voltage of the transformer is fairly constant, since the diodes D_6 and D_7 are conducting. As Lr_1 and Lr_2 releases energy through S_4 the current through S_4, i_{S4}, decreases while the current through S_3, i_{S3}, increases. Thus the analysis will be as follows.

$$V_{Cr}(t) \cong nV_{out} \tag{4}$$

$$i_{Lr1}(t) = i_{Lr2}(t) = I_{in} - \frac{nV_{out}}{L_{r1}+L_{r2}}t \tag{5}$$

The current through S_4 which is equal to i_{Lr1} decreases as per the above equation (5) and reaches to zero when the stored energy in the inductor is fully released. At the end of this mode S_4 is turned off with zero current. At this point (t_1),

$$i_{Lr1}(t_1) = i_{s4}(t_1) = 0 \tag{6}$$

$$t_{01} = t_1 - t_0 \cong I_{in}\frac{L_{r1}+L_{r2}}{nV_{out}} \tag{7}$$

$$i_{s3}(t_1) = I_{in} \tag{8}$$

C. Mode 2 [$t_1 - t_2$]

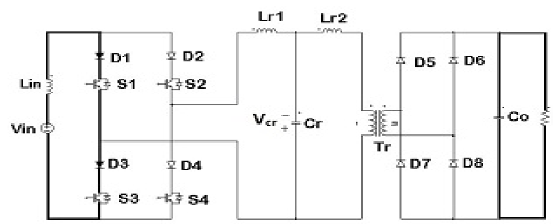

Fig.5 Mode 2 operation

In this mode L_{in} undergoes charging. The parameters can seen as follows,

$$v_{s4}(t) = 0 \tag{9}$$

$$v_{s2}(t) \approx nV_{out} \tag{10}$$

$$i_{s1}(t) = i_{s3}(t) = I_{in} \tag{11}$$

$$v_{Cr}(t) = nV_{out} \tag{12}$$

$$i_{Lr1} = i_{Lr2} = 0 \tag{13}$$

At the end of this mode S_2 is switched on for regulating the output voltage.

D. Mode 3 [$t_2 - t_3$]

At t_2 , S_2 is turned on. A resonant path is created by Cr, S_3, Source, S_2 and L_{r1}.

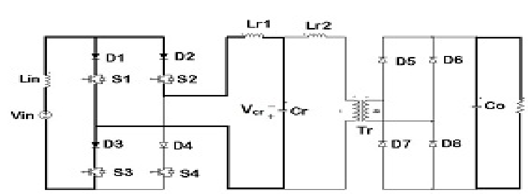

Fig.6 Mode 3 operation

The circuit equations in this mode will be as follows,

$v_{Cr}\,(t) = nV_{out}\ \cos\omega_1\ (t - t_2)$ (14)

$i_{s2}(t) = -i_{Lr1}(t) = \frac{V_{Cr}}{z_1} sin\omega_1(t - t_2)$ (15)

$i_{s1}(t) = I_{in} - i_{s2}(t)$ (16)

$i_{Lr2}(t) = 0$ (17)

Where $\omega_1 = 1/\sqrt{L_r C_r}$ and $z_1 = \sqrt{L_r/C_r}$

At t_3, $i_{Lr1}\,(t_3) = -I_{in}$ and $i_{S1}\,(t_3) = 0$ and this mode ends when S_1 is turned off with zero current. Thus,

$$t_{23} = t_3 - t_2 = \frac{1}{\omega_1} sin^{-1} \frac{I_{in}Z_1}{nV_{out}} \qquad (18)$$

If i_{Lr1} has to reach $-I_{in}$ as per the equation (15), V_{Cr} / Z_1 should be greater than I_{in}. This would mean that there should be enough energy in the capacitor to charge the inductor L_{r1}.

E. Mode 4 [$t_3 - t_4$]

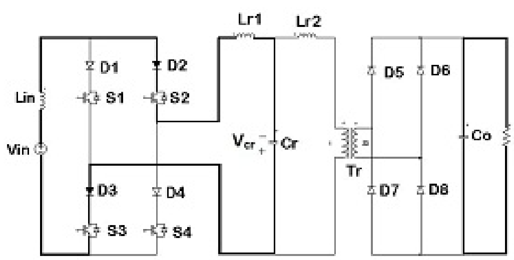

Fig.7 Mode 4 operation

The Capacitor continues to discharge with constant current I_{in} and then charge in the reverse direction to $-v_{Cr}$. The analysis of the circuit gives:-

$v_{Cr}\,(t) = v_{Cr}\,(t_3) - \frac{I_{in}}{C_r}(t - t_3)$ (19)

$i_{Lr1}(t) = -\,i_{s2}(t) = -\,i_{s3}(t) = -\,I_{in}$ (20)

$i_{Lr2}(t) = 0$ (21)

$t_{34} = t_4 - t_3 = \frac{C_r}{I_{in}}[V_{cr}(t_3) + nV_{out}]$ (22)

At t_4 when this mode ends the voltage on the capacitor will be $-V_{Cr}$.

F. Mode 5 [$t_4 - t_5$]

When the voltage of the capacitor C_r reaches nv_{out} the energy is transferred from input to the load through D_2, S_2, Lr_1, Lr_2, Tr, D_3, S_3, D_5 and D_8.

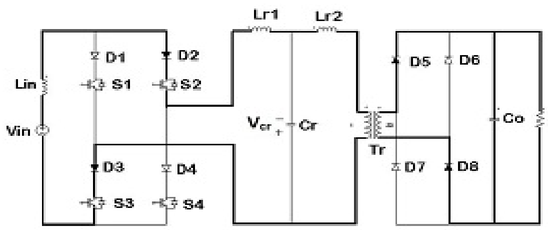

Fig.8 Mode 5 operation

The analysis of the circuit gives:-

$v_p(t) = -nV_{out}$ (23)

$v_{Cr}\,(t) = -nV_{out}$ (24)

$i_{Lr1}\,(t) = i_{Lr2}(t) = -\,I_{in}$ (25)

One half cycle of the switching period is completed. All the converter switches are soft switched. Minimum resonant energy is used for circulation. There is no extra current or voltage stress experienced on any of the switches.

V. DSIGN CONSIDERATIONS OF THE CONVERTER

A. ZCS Conditions

1. For the Leading switches: If the switch pairs do not *have sufficient dead time $t_{d,lead}$ to carryout current transfer, soft switching may not take place properly. In the first mode $t_{d,lead}$ should be long enough for the current through S_3 to increase from zero to I_{in} and the current through S_4 to decrease from I_{in} to zero. Thus, based on (7), $t_{d,lead}$ should satisfy the following criterion.*

$$t_{d,lead} > \frac{I_{in}(L_{r1}+L_{r2})}{nV_{out}} \qquad (26)$$

For the Lagging switches: The capacitor provides the required energy for ensuring zero-current switching of the lagging switches. Thus as per the equation (18), the dead time of the lagging switches should satisfy the following criterion

$$t_{d,lag} > \frac{1}{\omega_1} \sin^{-1} \frac{I_{in}Z_1}{nV_{out}} \qquad (27)$$

B. Component Design

Value of Resonant inductors: As per the equation (26), it should be ensured that the leading switches complete the current transfer process within t_{01}. Therefore maximum value of total inductance should be limited to a value;

$$L_{r\,,max} = \frac{nV_{out}}{I_{in}} t_{01} - L_{lk} \qquad (28)$$

$L_{r,\,\max}$ is designed at the rated load condition

Value of Resonant Capacitor: By equating the energy stored in the inductor and capacitor we get:

$$\frac{1}{2}C_r{V_{Cr}}^2 \geq \frac{1}{2}L_{r1}{I_{in}}^2 \quad (29)$$

Then,

$$V_{Cr} \geq \sqrt{\frac{L_{r1}}{C_r}}I_{in} \quad (30)$$

Since $V_{Cr} = nV_{out}$ we get,

$$C_r \geq \frac{L_{r1}{I_{in}}^2}{n^2{V_{out}}^2} \quad (31)$$

VI. DESIGN PROCEDURE AND SIMULATION RESULTS

A Simulation file of the proposed converter has been created using PSIM software with the following specifications:

1) input voltage, V_{in} : 530 V;

2) Output voltage, V_{out}: 15 kV;

3) Maximum output power,: 5 kW;

4) Switching frequency, f_s : 20 kHz;

5) Transformer turns ratio: 1:20.

The main design procedure is as follows

1) The chosen value for the lead time (t_{01}) is 0.14µs. The discharge time for the capacitor is chosen to be 0.75µs.

2) The value of the input inductor L_{in} is chosen to limit the current ripple to 2.5%. Thus,

$$L_{in} \geq \frac{nD(1-2D)V_{out}}{f_s\Delta i_L} \quad (32)$$

3) The value of the output capacitor is chosen to limit the voltage ripple, ΔV_{out}

$$C_0 \geq \frac{2D_{max}I_0}{f_s\Delta V_{out}} \quad (33)$$

TABLE I MAIN COMPONENTS OF THE SIMULATION

Component	Value
Resonant capacitor , C_r	100nF
Resonant inductor , L_{r1}	1.5µH
Resonant inductor , L_{r2}	8.5µH
Output capacitor, C_o	220nF
Transformer, T_r	1:20

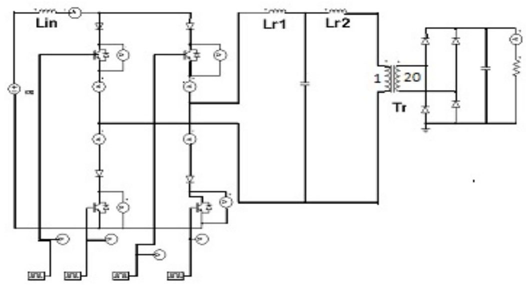

Fig.9 Simulation Circuit

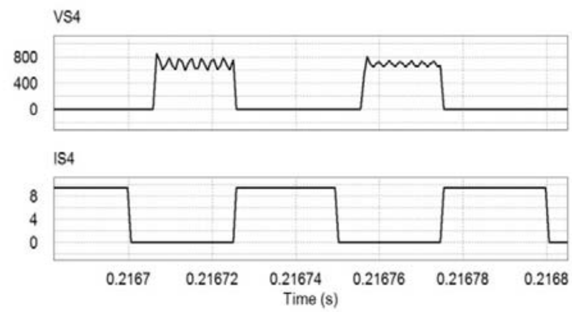

Fig.10 Voltage and Current waveforms of switch S_4

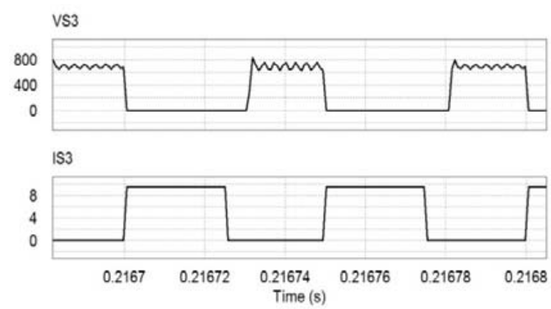

Fig.11 Voltage and Current waveforms of switch S_3

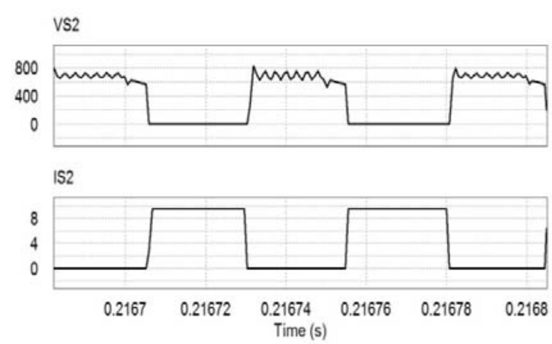

Fig.12 Voltage and Current waveforms of switch S_2

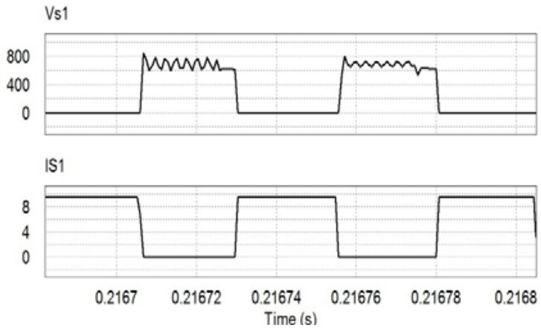

Fig.13 Voltage and Current waveforms of switch S_1

VII.CONCLUSION

A high voltage current driven full bridge converter was proposed in this paper. The zero current switching for the main switches of the converter could be realized using a simple snubber circuit. The resonant energy used for achieving zero current switching is minimized by splitting the resonant inductor into two parts. Thus less circulating energy is used for the resonance process. Moreover none of the components in the circuit experiences over current or over voltage stress. The current flowing through all the switches never exceeds the input current and the voltage across any switch never exceeds the primary voltage of the transformer. Though the conduction losses are same as that of the hard switched converter the switching losses are considerably reduced. The simulation results show almost complete elimination of turn-off switching loss and an efficiency of 96% is obtainable. The total efficiency is much better than the hard switched converter.

REFERENCES

[1] X. Ruan and Y. Yan, “A novel zero-voltage and zero-current-switching PWM full bridge converters using two diodes in series with the lagging leg,” IEEE Trans. Ind. Electron., vol. 48, no. 4, pp. 777–785, Aug. 2001.

[2] X. Ruan and J. Wang, “Calculation of the resonant capacitor of the improved current-doubler-rectifier ZVS PWM full-bridge converter,” IEEE Trans. Ind. Electron., vol. 51, no. 2, pp. 518–520, Apr. 2004.

[3] M. Borage, S. Tiwari, and S. Kotaiah, “A passive auxiliary circuit achieves zero-voltage-switching in full-bridge converter over entire conversion range,” IEEE Power Electron. Lett., vol. 3, no. 4, pp. 141–143, Dec. 2005.

[4] Y. Jang and M. Jovanovic, “A new PWM ZVS full-bridge converter,”IEEE Trans. Power Electron., vol. 22, no. 3, pp. 987–994, May 2007.

[5] W. Chen, X. Ruan, and R. Zhang, “A novel zero-voltage-switching PWM full bridge converter,” IEEE Trans. Power Electron., vol. 23, no. 2, pp. 793–801, Mar. 2008.

[6] A. Mason, D. Tschirhart, and P. Jain, “New ZVS phase shift modulated full-bridge converter topologies with adaptive energy storage for SOFC application,” IEEE Trans. Power Electron., vol. 23, no. 1, pp. 332–342, Jan. 2008.

[7] R. Watson and F. C. Lee, “A soft-switched full-bridge boost converter employing an active clamp circuit,” in Proc. IEEE Power Electron. Spec. Conf., Baveno, Italy, Jun. 1996, pp. 1948–1954.

[8] J. G. Cho, C. H. Jeong, H. S. Lee, and G. H. Rim, “Novel zero voltage transition current fed full bridge PWM converter for single stage power factor correction,” IEEE Trans. Power Electron., vol. 13, no. 6, pp. 1005 – 1012, Nov. 1998.

[9] G. Moschopolous and P. Jain, “Single stage ZVS PWM full bridge converter,” IEEE Trans. Aerosp. Electron. Syst., vol. 39, no. 4, pp. 1122–1133,Oct. 2003.

[10] E. Adib and H. Farzanehfard, “Zero-voltage transition current-fed full bridge PWM converter,” IEEE Trans. Power Electron., vol. 24, no. 4, pp. 1041–1047, Apr. 2009.

[11] G. Hua, E. X. Yang, Y. Jiang, and F. C. Lee, “Novel zero-current-transition PWM converters,” IEEE Trans. Power Electron., vol. 9, no. 6, pp. 601– 606, Nov. 1994

[12] G. Ivensky, D. Sidi, and S. B. Yaakov, “A soft-switcher optimized for IGBTs in PWM topologies,” in Proc. IEEE Appl. Power Electron. Conf. Expo., 1995, pp. 900–906.

[13] R. C. Fuentes and H. L. Hey, “An improved ZCS-PWM commutation cell for IGBT’s application,” IEEE Trans. Power Electron., vol. 14, no. 5, pp. 939–948, Sep. 1999.

[14] H.-S. Choi and B. H. Cho, “Novel zero-current switching (ZCS) PWM switch cell minimizing additional conduction losses,” in Proc. IEEE Power Electron. Spec. Conf., 2001, pp. 872–877.

[15] R. C. Fuentes and H. L. Hey, “A comparative analysis of the behavior iand of the switching losses for a group of ZCS-PWM converters using IGBTs,” in Proc. IEEE Power Electron. Spec. Conf., 1997, pp. 972–977.

[16] C.-M.Wang, “A novel ZCS-PWM power-factor preregulator with reduced conduction losses,”

IEEE Trans. Ind. Electron., vol. 52, no. 3, pp. 689–700, Jun. 2004.

[17] P. Das and G. Moschopoulos, "A comparative study of zero-current transition PWM converters," IEEE Trans. Ind. Electron., vol. 54, no. 3, pp. 1319–1328, Jun. 2007.

[18] E. Adib and H. Farzanehfard, "Family of zero-current transition PWM converters," IEEE Trans. Ind. Electron., vol. 55, no. 8, pp. 3055–3063, Aug. 2008.

[19] D.Y. Lee, M. K. Lee, D. S. Hyun, and I. Choy, "New zero-current transition PWM dc/dc converters without current stress," IEEE Trans. Power Electron., vol. 18, no. 1, pp. 95–104, Jan. 2003.

[20] X. H.Wu, D. M. Xu, J. H. Kong, C. Yang, and Z. Qian, "High power high frequency zero current transition full bridge dc/dc converter," in Proc. Appl. Power Electron. Conf. Expo., 1998, pp. 823–827.

[21] M. Marx andD. Schroder, "A novel zero-current-transition full-bridge dc–dc converter," in Proc. IEEE Power Electron. Spec. Conf., 1996, pp. 664–669.

[22] C. Iannello, S. Luo, and I. Batarseh, "Small-signal and transient analysis of a full-bridge, zero-current-switched PWM converter using an average model," IEEE Trans. Power Electron., vol. 18, no. 3, pp. 793–801, May 2003.

[23] J. Chen, R. Chen, and T. Liang, "Study and implementation of a single stage current-fed boost PFC converter with ZCS for high voltage applications," IEEE Trans. Power Electron., vol. 23, no. 1, pp. 379–386, Jan.2008.

[24] A. Leung, H. Chung, and K. Chan, "A ZCS isolated full-bridge boost converter with multiple inputs," in Proc. IEEE Power Electron. Spec. Conf., 2007, pp. 2542–2548.

[25] S. Atoh and H. Yoshike, "PWM dc–dc converter with a resonant commutation means," in Proc. INTELEC 1991 Conf., pp. 308–313.

[26] D. M. Xu,X.H.Wu, J. M. Zhang, andZ.Qian, "High power high frequency half-wave-mode ZCT-PWM full bridge dc/dc converter," in Proc. IEEE Appl. Power Electron. Conf., 2000, pp. 99–103.

[27] J. Zhang, X. Xie, X. Wu, G. Wu, and Z. Qian, "A novel zero-current transition full bridge dc/dc converter," IEEE Trans. Power Electron., vol. 21, no. 2, pp. 354–360, Mar. 2006.

[28] L. Qin, S. Xie, and H. Zhou, "A novel family ofPWMconverters based on improved ZCS switch cell," in Proc. IEEE Power Electron. Spec. Conf., 2007, pp. 2725–2730.

[29] N. Mohan, T. M. Undeland, and W. P. Robbins, Power Electronics: Converters, Applications and Design. Hoboken, NJ: Wiley, 2003.

[30] Q. Sun, H.Wang, R. Li, H. Chung, S. Tapuchi, N. Huang, and A. Ioinovici, "A ZCS full-bridge PWM converter with self-adaptable soft-switching snubber energy," in Proc. IEEE Power Electron. Spec. Conf., Jun. 2008, pp. 3001–3007.

[31] T. Song, H. Chung, andA. Ioinovici, "A high-voltage dc–dc converter with Vin/3—Voltage stress on the primary's switches," IEEE Trans. Power Electron., vol. 22, no. 6, pp. 2124–2137, Nov. 2007.

[32] T. Song, H.Wang, H. Chung, S. Tapuhi, and A. Ioinovici, "A high-voltage ZVZCS dc–dc converter with low voltage stress," IEEE Trans. Power Electron., vol. 23, no. 6, pp. 2630–2647, Nov. 2008.

◈◈◈

Dual Output DC-DC Forward Converter

Kusuma .R & Jaipal.R

Department of Electrical and Electronics Engineering, VTU Belgaum, RVCE Bangalore, India

Abstract - The purpose of this project is to implement MOSFET based high precision low size dual output DC-DC forward converter with current mode control and operating at a switching frequency of 500khz. The proposed design also has added feature of over temperature protection. Input voltage in this design can be from 18V to 36V which provides dual output of +15V and -15V with a output current of 0.75A with a power rating of 22.5W. In this design in addition to providing with the voltage feedback it also senses MOSFET current which is fed back for faster response.

Keywords—*DC-DC converter, Converter, Dual Converter.*

I. INTRODUCTION

DC-DC converters are used to convert the output of DC power source, such as batteries and other unregulated voltage levels to a required stable voltage level for various applications.

In general there are two categories of power supplies:

- Linear regulated power supply
- Switched mode power supply

In this design, choice made is Switched mode power supply over linear regulated power supply due to following drawbacks of linear regulated power supply: In linear regulator circuits the excess voltage from the unregulated dc input supply drops across a series element, whereas in switched mode circuit the unregulated portion of the voltage is removed by modulating the switch duty ratio.

In most of the switched mode power supplies it is possible to insert a high frequency transformer to isolate the output and to scale the output voltage magnitude. In linear power supply the isolation and voltage-scaling transformer can be put only across the low frequency utility supply. The low frequency transformer is very heavy and bulky in comparison to the high frequency transformer of similar VA rating. Similarly the output voltage filtering circuit, in case of low frequency ripples is much bulkier than if the ripple is of high frequency. The switched mode circuit produces ripple of high frequency that can be filtered easily using smaller volume of filtering elements.

II. METHOD OF CONTROL

Next important design consideration is method of control

All switching converter output voltage is a function of the input voltage, duty cycle and load current, as well as converter circuit component values. The output voltage should be constant regardless of variation in input voltage, load current and converter circuit parameter values. Despite variation, it is desired that the output voltage be within a certain limit. This is not practical to achieve without negative feedback, and setting the duty cycle to a single value. There are two basic methods to control the duty cycle to keep the output voltage within the specified limit: voltage mode control and current mode control.

Voltage Mode Control

In voltage mode control, the output voltage is measured and then compared with the reference value (desired output voltage). The error is then processed by the compensation block to generate the next duty cycle value, as shown in Figure 1.1.

This mode has only one control loop, so it is easy to design and analyze. However, in this control method, any change in the line or the load must be first sensed as an output voltage change and then corrected by the feedback loop. Therefore, the response is slow and the transient response (step load change) is not favorable.

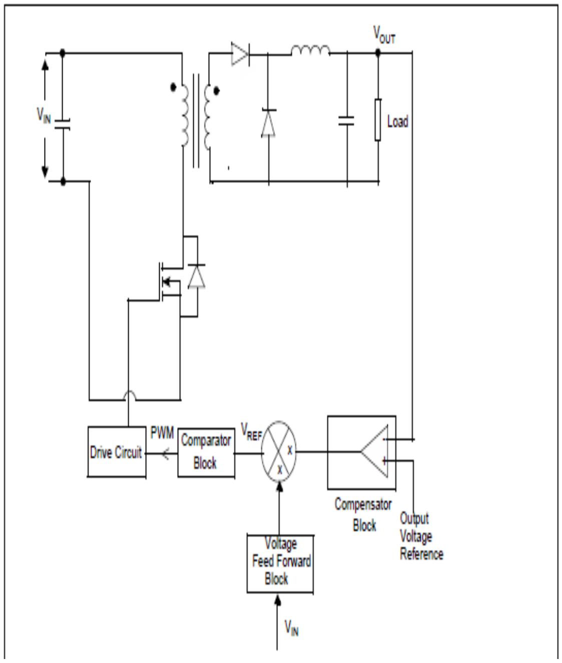

Figure 1.1: Voltage Mode Control

Current Mode Control

The current mode control technique requires two feedback loops, as shown in Figure 1.2. In this mode, two parameters are measured for control purposes. The output voltage is measured at the output capacitor or at the load end (known as remote sensing). The output inductor/primary switch current is also measured.

In current mode control, the output voltage is first compared with the reference voltage (desired output voltage). This error is then processed by the compensation block to generate the reference signal for the current loop. This current reference is compared to the measured current. Any error generated by the comparison of the reference generated by the voltage compensation block and the actual current drawn from the input is processed by the current compensation block. This generates the required duty cycle to maintain the output voltage within the specified limit. As current mode control senses the circuit current, any change in output load current or the input voltage can be corrected before it affects the output voltage.

Sensing the input current, which depends on input voltage, provides the inherent feed-forward feature. It also improves step load response and transient response because of the inner current loop

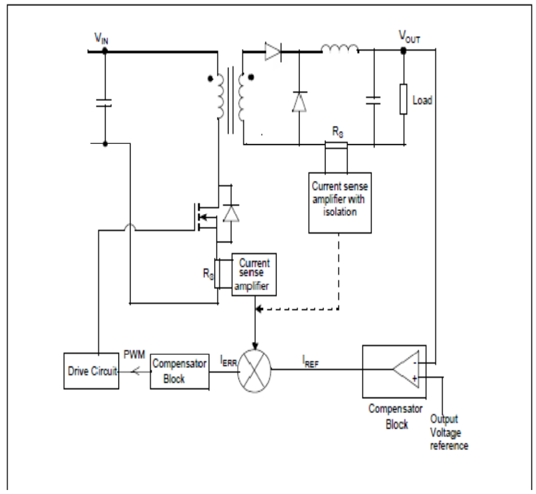

Figure 1.2: Current Mode Control

III. DESIGN CONSIDERATIONS

The block diagram in fig 1.4 below shows the dual output DC-DC Converter. As shown in the fig below input varies from 18V to 36V and designed to operate at a switching frequency of 500 kHz. It has input to output isolation provided by transformer TX2. Closed loop control is provided by a voltage feedback and current sense circuits. Voltage feedback is provided by a optocoupler and current is sensed using current sense transformer for faster response. The design also provides with over temperature protection circuit provided by Quad Comparator LM139.

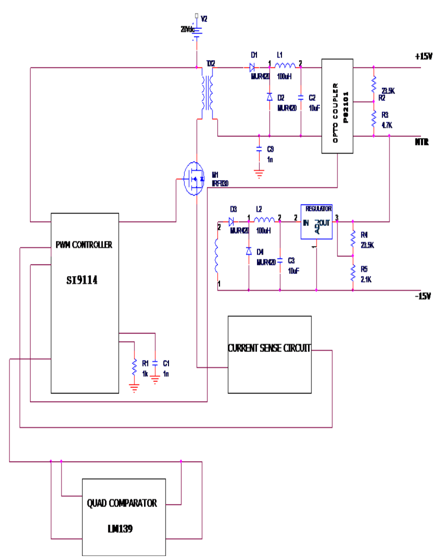

Figure 1.3: Block Diagram of Dual Output DC DC Converter

The equivalent circuit of the forward DC-DC Converter is as shown in fig 1.5 below. It consists of high frequency switch mode PWM controller Si9114A which drives the MOSFET and is designed to operate at a frequency of 500 kHz. For voltage feedback an optocoupler PS2101 used, current sense transformer TX1 is used to sense the MOSFET current which is fed back to the current sense input of the PWM controller for faster response. A LDO regulator is used at the output of the power stage. An over protection circuit is provided by the Quad Comparator LM139 using a thermistor.

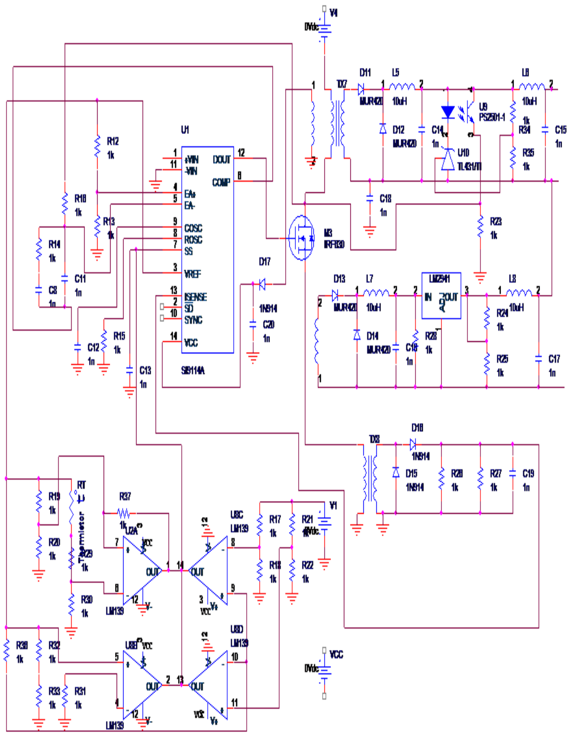

Figure 1.4: Equivalent circuit of Dual Output DC-DC Forward Converter

IV. COMPONENT SELECTION

The PWM Controller used in the design is Si9114A. The Si9114A is a BiC/DMOS current-mode pulse width modulation (PWM) controller IC for high-frequency dc/dc converters. Single-ended topologies (forward and fly back) can be implemented at frequencies up to 1 MHz the oscillator has an internal divide-by-two that limits the duty ratio to 50%. An oscillator sync output allows converters to be synchronized in phase as well as in frequency, in a master/slave configuration.

Other features include a 1.5% accurate voltage reference, error amplifier, shutdown logic control, soft-start and under voltage lockout circuits. Functional block diagram of Si9114A is as shown in fig 1.5 below.

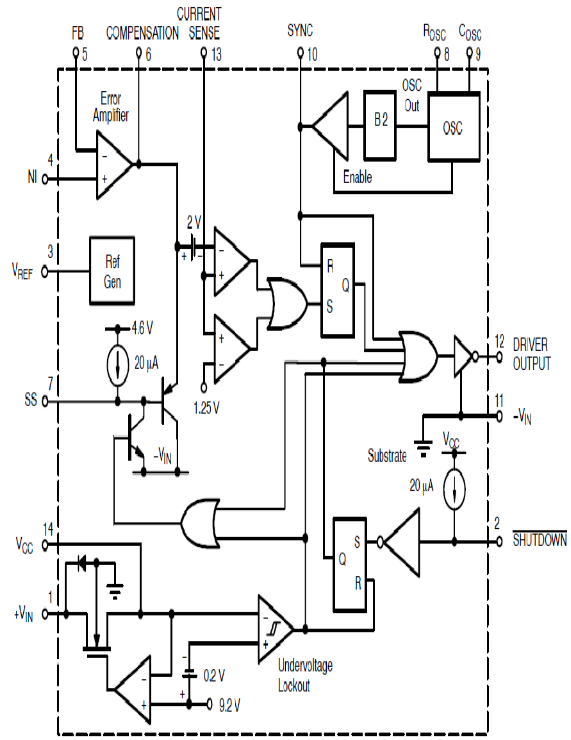

Figure 1.5: Functional block diagram of Si9114A

Where

Pin 1-High Voltage Pre Regulator

Pin 2-Shutdown

Pin 3-Reference

Pin 4, 5 & 6-Non Inverting, Voltage Feedback and Compensation inputs of Error amplifier respectively

Pin 7-Soft Start

Pin 8 & 9- Oscillator

Pin 10-Synchronization

Pin 11 & 14- V_{IN} &V_{DD}

Pin 13-Current S

Low power low offset Quad Comparator

Quad Comparator in this design is mainly used for over temperature protection, wherein if the temperature crosses certain limit output of the quad comparator goes low. And also if input voltage goes below certain level, output of quad comparator goes low.

In this design all four comparator are ANDed and given as input to the soft start of the PWM controller Si9114A, such that if even one of the outputs of any one of the four comparators goes low, input to the soft start is held low.

Calculation of switching frequency

$T_{ON} = (1.025 \text{ X } R_T \text{ X } C_T) / 8$

$T_{OFF} = 5 \text{ X } R_{ql} \text{ X } C_T$; Where $R_{ql} = 25$ ohms

$F_{OSC} = 1/2(T_{ON} + T_{OFF})$

Selecting R_T=68k ohms & C_T=100pF and

substituting these values in the above equations yields:

$T_{ON} = (1.025 \text{ X } R_T \text{ X } C_T) / 8$

$T_{ON} = (1.025 \text{ X } 68 \text{ X } 10^3 \text{ X } 100 \text{ X } 10^{-12}) / 8$

$T_{ON} = 0.87125 \text{ X } 10^{-6}$ sec

$T_{OFF} = 5 \text{ X } R_{ql} \text{ X } C_T$; Where $R_{ql} = 25$ ohms

$T_{OFF} = 5 \text{ X } 25 \text{ X } 100 \text{ X } 10^{-12}$

$T_{OFF} = 0.0125 \text{ X } 10^{-6}$ sec

$F_{OSC} = 1/2(T_{ON} + T_{OFF})$

$F_{OSC} = 1/2((0.87125 \text{ X } 10^{-6}) + (0.0125 \text{ X } 10^{-6}))$

$F_{OSC} = 565.77 \text{ X } 10^3$ Hz

$F_{OSC} = 565.77$K Hz

Design of Capacitor and Inductor for Forward Converter

$P_{out} = V_{out} * Io = 15*0.75 = 11.25$W

$P_{in} = P_{out}/eff = 11.25/0.8 = 14.0625$

$I_{dc} = P_{in}/V_{in} = 14.0625/28 = 0.502$

$I_A = P_{in}/(V_{in*}d) = 14.0625/(28*0.4929) = 1.0189$A

$I_{RMS} = I_A/2 = 1.0189/2 = 0.4948$A

$V_{RIPPLE} = 20$mV

$C_{MIN} = I_{RMS}/(8*f_{SW}*V_{RIPPLE}) = 0.4948/(8*500*10^3*10^{-3}) = 6.185$uf

Practically C of value larger than the calculated value is chosen. Hence C=10uF

$V_L = Ldi/dt$

$V_L = E_{IN} - E_{OUT} - E_{SW} = 28-15-1.5 = 11.5$V

$t_{off} = 1/(2*f_{sw}) = 1/(2*500*10^3)$

Del $I_l = 0.1*I_{out} = 0.1*0.75 = 0.075$A

$L = (V_L * t_{off}) / \text{Del } I_l = (11.5*1*10^{-6})/0.075 = 153.3$uH

Practically inductance of lower value than the calculated value is chosen. Hence L= 100uH to 110uH.

Design of Transformer Turns for Transformer TX2

$N_p = (V_{min} * t_{onmax})/(B_{max} * A_{eff}) =$

$(18*1*10^{-6})/(100*10^{-3}*24.5*10^{-6}) = 7.3 = 7$turns

$V_{sec} = (V_{out} + V_{Loss})/D_{max} = (15+1)/0.5 = 32$V

Turns Ratio = TR= $V_{min}/V_{sec} = 18/32 = 0.5625$

$N_s = N_p/TR = 7/0.5625 = 12.44 = 12$turns

V. SIMULATIONS AND RESULTS

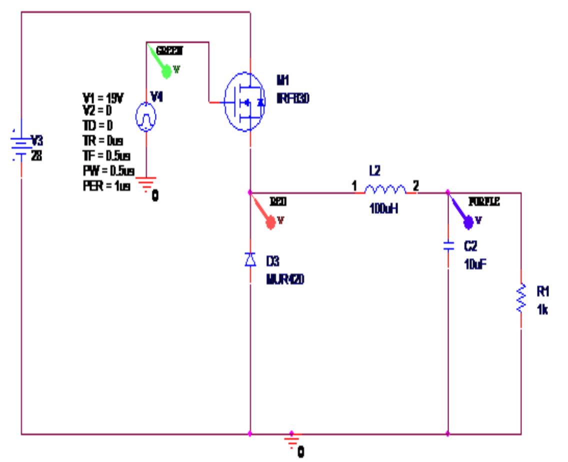

Figure 1.6: Buck converter

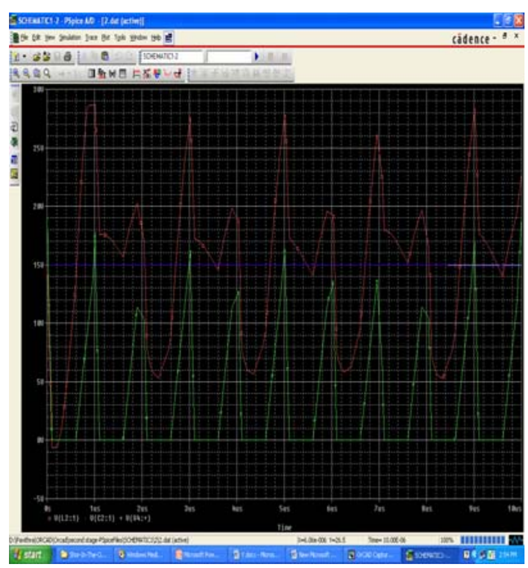

Figure 1.7: simulated result of Buck converter

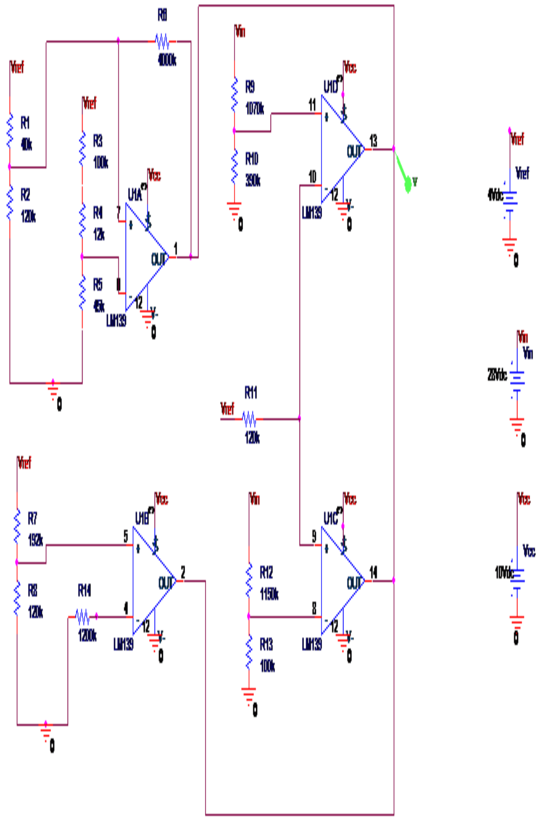

Figure 1.8: quad comparator

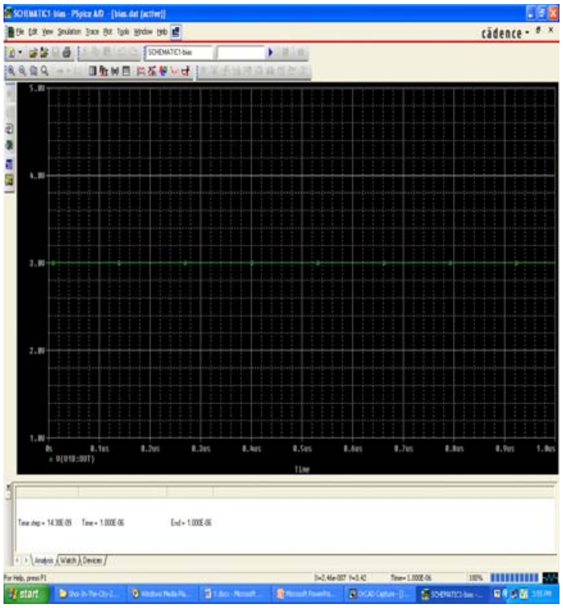

Figure 1.9: simulated result of quad comparator

Results for No Load Regulation

Input voltage(v)	Output voltage1(v)	Output voltage2(V)
18	15.019	-15.034
20	15.019	-15.034
22	15.020	-15.036
24	15.021	-15.038
28	15.022	-15.038
30	15.022	-15.040
36	15.023	-15.043

VI. CONCLUSIONS

In this paper, a Dual Output DC-DC Forward Converteris implemented which has superior characteristics over traditional converter, control requirements and reliability. Simulation results illustrate was rigged up in PCB and tested for no load condition, The result shown in above figure1.6, 1.7, 1.8, 1.9 performance and effectiveness of the resistive types of load and found to work satisfactorily. The converter also works satisfactorily

REFERENCES

1. http://ecourses.vtu.ac.in/nptel/courses/Webcourse-contents/IIT%20Kharagpur/Power%20Electronics/PDF/L21%28DP%29%28PE%29%20%28%28EE%29NPTEL%29.pdf
2. http://books.google.co.in/books?id=NXMJNAVXkzoC&pg=PA17&dq=factors+affecting+the+choice+of+appropriate+topology&hl=en&sa=X&ei=1yaVT_5ohNatB4GT4foE&ved=0CDUQ6AEwAA#v=onepage&q=factors%20affecting%20the%20choice%20of%20appropriate%20topology&f=false
3. http://ww1.microchip.com/downloads/en/AppNotes/01114A.pdf
4. *Forward Type Switch Mode Power Supply*, Version 2 EE IIT , Kharagpur.

◈◈◈

Cast Shadow Removal For A Single Texture Images

M. Sivagami & T.Revathi

School of Computer science, VIT, Chennai, India

Abstract - Shadow removal is an important pre-processing step for computer vision algorithms and image enhancement. Color based shadow detection is one of the commonly used method for shadow detection. In this paper we present a novel method for shadow detection and cast shadow removal for single texture image using color based shadow detection and pixel mapping based shadow removal. The color based shadow detection uses the LAB color space. Experimental results show that the proposed method reduces the computation and the execution time.

Keywords-*component; shadow detection; shadow removal; image enhancement; pixel mapping.*

I. INTRODUCTION

The shadow is areas where direct light from a light source cannot reach due to obstruction by an object .In computer vision the shadows degrade the visual quality of images. So shadow Removal is therefore a vital pre-processing step for computer vision algorithms and image enhancement [2]. The shadows can be divided into hard shadows and soft shadows. Hard shadows: shadows created by light from a single source, causing shadows with a solid interior and sharp distinct edges, cast by the umbra ,contrast with soft shadows. Soft shadows: shadows created by light from multiple sources, causing multiple overlapping shadows and a region of intermediate grey values with fuzzy edges cast by the penumbra, contrast with hard shadows .For the removal of shadows, shadow detection is the pre-processing step .There are various methods for the shadow detection and it is based on intensity, chromaticity, physical properties, Geometry and texture. Intensity based shadow detection assume that the regions under shadow will be darker, that is the regions are blocked from the source of illumination.

The chromacity based shadow detection detects shadows using the color information. The physical properties based shadow detection detects shadows using the illumination sources .In geometry based shadow detection the size orientation and shape of the shadows are estimated using the illumination source, object shape and the ground plane[1].

II. PREVIOUS WORK

Many approaches have been proposed to address the problem of the shadow removal in real images. Finlayson [10, 17, 18] presented the automated methods that detect the shadow edge by entropy minimization. Using entropy minimization the intrinsic images are formed. Intrinsic Image: an image which records the variation in only one physical quantity (e.g.-reflectance or illumination). Using that intrinsic image the shadow in the color image was removed by the following steps. First the intrinsic image is formed and using that image together with the original image shadow edges was detected. Secondly, applying shadow edges to zero in the edge representation of the original image. Thirdly, using the Poisson equation shadow free color image was recovered. Baba et al. [14] proposed a method that can estimate gradually changing shadow opacities, assuming that the scene does not contain complex textures. Nielsen and Madsen estimated gradually changing shadow opacities from complex textured images. Eli Arbeland and Hagit [3] removed the curved surfaces while retaining the textural information in the penumbra. Here the shadow region is classified to umbra and penumbra region. Umbra: the darkest central portion of a shadow.

Penumbra: the portion of a shadow in semi-shade between the umbra and un-shaded zone. Recently interactive methods are used for the shadow removal.Wu and Tang's [15,16] methods remove shadows by the user specified shadow and un-shadowed region. Shadows are also removed by using retinex algorithm[19].

III. PROPOSED METHOD

The proposed method is concerned with single texture images. Color based shadow detection method is used to detect the shadows. After the detection of shadows it is removed by our algorithm .The proposed algorithm is given below:

i) Apply color transform CIELAB to the input rgb image. (i.e. convert rgb to lab image.)

RI=T (rgb) (1)

Where RI=Reference Image

ii) The RI is converted to binary or grey level image based on the contrast of the image to identify the shadow edges.

GI=T(RI) or BI=T(RI) (2)

Where, GI=Grey Image,

BI=Binary Image

iii) Apply canny edge detection algorithm to detect edges in grey level or binary image and compare the edge values in the RI with binary or grey level image to detect the shadow edges. Then the shadow mask is produced using the shadow edges.

iv) The pixels in the un-shadowed regions are mapped to the shadowed region in the RI image using shadow mask.

v) After mapping, the lab color space is converted to rgb color space.

Rgb=T(Lab) (3)

vi) The final obtained image is rgb image without shadows.

IV. STUDY AREAS

The study areas used single texture shadow images which were taken from the Google.

A. Shadow images without objects

Figure-1

Figure-2

Figure-3

Figure-4

B. Shadow Images with Object

Figure-5

Figure-6

Figure-7

V. RESULTS

The proposed algorithm is implemented in mat lab version 7.13 on windows XP platform. The results of the cast shadow removal algorithm for single texture images were efficient.

A. Figures of Shadow Removal without Objects

Figure-8

Figure-9

Figure-10

Figure-11

B. Figure of Shadow Removal with Objects

Figure-12

Figure-13

Figure-14

The figure1 to figure7 shows the input Shadow image. Figure6 to figure 11 shows the shadow removal of the single texture cast shadow image without object. The figure12 to figure14 shows the shadow removal result of the single texture image with object. This algorithm works for both single texture shadows with objects and without objects. This gives an efficient result for shadow removal of a single texture image.

Figure 15: Original Image

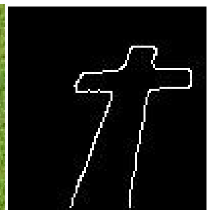

Figure 16: Shadow Edge

Figure 17: Shadow free image

D. Tables

TABLE I: CHROMATICITY BASED METHODS

Paper	Color space	Level
Cucchiara et al. 2003 [6]	HSV	pixel
Salvador et al.2004 [7]	C1C2C3	window
Cavallaro et al .2005 [8]	Normalized RGB	pixel
Chen et. Al 2010 [9]	YUV	pixel
Sun and li 2010 [10]	HSV and C1C2C3	pixel
Our approach	LAB	pixel

VI. CONCLUSION AND FUTURE ENHANCEMENTS

The proposed system gives the efficient result for cast shadow removal for single texture images with and without objects. The proposed system uses the Lab color space and canny edge detection algorithm for the efficient shadow removal in the image. The proposed system reduces the complexity of computation when compared to other methods. Finlayson [10, 17, 18] methods which require the physical properties of the camera. In our method no physical properties of the camera are needed. In future the same work can be extended for multiple texture images with form shadows.

ACKNOWLEDGEMENTS

This work has been funded by Department of Science and Technology, New Delhi, India.

REFERENCES

[1] A.Sanin, C.Sanderson, B.C. Lovell." Shadow Detection: A Survey and Comparative Evaluation of Recent Methods." Pattern recognition Vol.45, No. 4, pp.1684-1695, 2012.

[2] Daisuke Miyazaki, Yasuyuki Matsushita, Katsushi Ikeuchi" Interactive Shadow Removal from a Single Image Using Hierarchical Graph Cut". ACCV (1) 234-245, 2009

[3] Eli Arbel, Hagit Hel-Or:"Texture-Preserving Shadow Removal in Color Images Containing Curved Surfaces." CVPR 2007

[4] Y.Weiss,"DerivingIntrinsicImagesfromImage Sequences,"Proc.Int'lConf.ComputerVision,pp.II :68-75,2001.

[5] B.K.Horn,"DeterminingLightnessfromanImage, "ComputerGraphicsand ImageProcessing,vol.3,pp.277-299,1974.

[6] R. Cucchiara, C. Grana, M. Piccardi, and A. Prati. "Detecting moving objects, ghosts, and shadows in video streams." IEEE Transactions on Pattern Analysis and Machine Intelligence, 25(10):1337–1342, 2003.

[7] E. Salvador, A. Cavallaro, and T. Ebrahimi."Cast shadow segmentation using invariant color features." computer vision and image understanding 95(2):238–259, 2004.

[8] A. Cavallaro, E. Salvador, and T. Ebrahimi. "Shadow aware object based video processing "IEEE proceedings on vision, Image and signal processing, 152(4):398-406,2005.

[9] C.T. Chen, C.Y. Su, and W.C. Kao."An enhanced segmentation on vision based shadow removal for vehicle detection". In International Conference on Green Circuits and Systems, pages 679–682, 2010.

[10] Removing Shadows from Images, ECCV European Conference on Computer Vision. vol. 4, pp. 823-836, 2002

[11] B.V.FuntandG.D.Finlayson,“ColorConstant ColorIndexing,”IEEETrans.PatternAnalysisandMachineIntelligence,vol.17,no.5,pp.522-529,May1995.

[12] G.FinlaysonandS.Hordley,“ColorConstancyataPixel,”J.OpticalSoc.Am.A,vol.18,no.2,pp.253264,UKPatentapplicationno.0000682.5,underreview, BritishPatentOffice,2001.

[13] Y. Wang, K.F. Loe, and J.K. Wu.”A dynamic conditional random field model for foreground and shadow segmentation. “*IEEE Transactions on Pattern Analysis and Machine Intelligence*, 28(2):279–289, 2006.

[14]. Baba, M., Mukunoki, M., Asada, N.:”Shadow removal from a real image based on shadow density.” In: ACM SIGGRAPH Posters. (2004) .

[15] Wu, T.P., Tang, C.K.” A bayesian approach for shadow extraction from a single image.” In: Proc. of Int’l Conf. on Comp. Vis. (ICCV). Volume 1. 480–487, 2005

[16]. Wu, T.P., Tang, C.K., Brown, M.S., Shum, H.Y.” Natural shadow matting”. ACM Transactions on Graphics ,2007

[17] Graham D. Finlayson:” Simple Shadow Removal” ICPR:832-835,2006

[18] Graham D. Finlayson,” On the Removal of Shadows from Images” IEEE Trans. Pattern Anal. Mach. Intell. 28 (1): 59-68, 2006

[19] Graham D. Finlayson, S.D .Hordley” Removing Shadows from Images using Retinex” Sit/SID., 2007

◈◈◈

Direct Drive System Enabled Electric Car

M. Syed Abdul Kalam

Department of Electrical Engineering, R.V College of Engineering, Bangalore, India

***Abstract* -** To eliminate the deficiencies in the conventional electric cars, I have designed a new technique of obtaining optimum propulsion in a very efficient manner from the electric motor by incorporating a gearless drive system and also can achieve efficient regeneration of power while in motion and in deceleration keeping power to weight ratio into consideration. This design inevitably as an advantage transforms as a four wheel drive electric car and also has an option of interchanging to two wheel or four wheel drive depending upon the payload.

***Keywords* -** *conventional electric cars, efficient regeneration of power, four wheel drive, gearless drive system, power to weight ratio.*

I. INTRODUCTION

The electric cars available in the Indian market at present have limitations of initial pick up; achieving high speeds and the range of kilometers which it can travel per charge is also less. This project entitled direct drive System enabled Electric car uses four 3hp DC compound motor connected directly to the wheels of the car; it can also be called as “In-wheel drive system”.

Basically in a mechanical car the engine is coupled to a gear box; the output of these engines be it petrol or diesel engine is controlled via the gear box. In case of the Electrical motors we can control the speed and torque of the motor directly without the use of the gear box. The average weight of the gear box including the drive shafts and the differentials is around 200 Kg as per the necessity of the car. By eliminating it we can achieve a better power to weight ratio and in turn get high speed and better range per charge.

The Induction motor which is commonly used in the electric cars will be replaced here with DC compound motor for advantages of better initial pick up, smooth and easier control. Since the four motors are connected directly to each wheels of the car it inevitably forms “four wheel drive system”. At the time of starting the four motor will be utilized for forward propulsion of the vehicle, after attaining a stable speed any two motor can be used for regeneration. The entire working concept to be discussed in further segments and the explanations of the above are clearly described in the following segments and diagrams.

1.1 Speed control of DC compound motors.

The most common two methods for controlling the speed of the DC Compound motor.

1.1.1 Armature voltage control

The speed is directly proportional to the voltage applied across the armature of the motor. By varying this voltage from zero to rated armature voltage a range of speed is achieved. The field winding is excited by supply voltage and the field current is kept constant [1]. The variation in armature voltage here is achieved using a Full bridge converter working as a dc-dc converter [2].

1.1.2 Flux control

The speed is inversely proportional to the flux; this flux is dependant on the current through the shunt field winding. Thus flux can be controlled by controlling the amount of current in the shunt field winding in turn achieving range of speeds. In this technique the motor can run above rated speeds [1].

1.1.3 Advantages of using DC compound motor drive.

- Can employ easier control circuitry
- High initial torque
- Has qualities of both shunt and series motors
- Smooth speed control is possible [1] [5]

II. CONTROL SCHEME

In this particular project Armature voltage control technique is used to control the speed of all four motors. The speed of the motors is controlled by varying the armature voltage using a single bridge converter working as dc-dc converter. The armature of all four motor are connected to the converter terminals as shown in the below figures indicated as load [2].

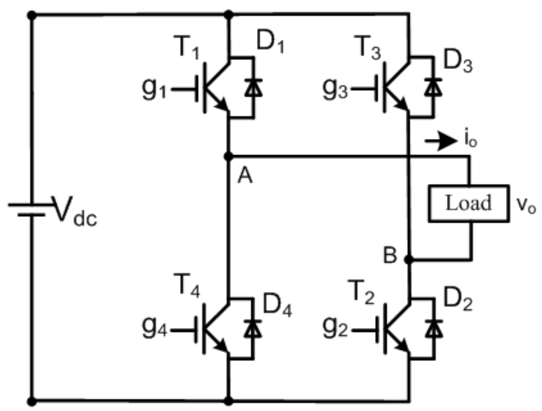

Fig. 1 : Bridge circuit used as dc-dc converter

2.1 Armature voltage Variation.

The voltage applied from the source to the armature circuit of the motors is via a bridge circuit as shown in Fig 1. The switches as triggered by a pulse of varying duty cycle. As the duty cycle of the triggering pulse is varied the output voltage of the converter circuit is also varied which is given by the equation.

$$Vdc= D*Vo$$

From the above equation it is clear that the armature voltage can be controlled by controlling the duty cycle of the triggering pulses generated. As speed is directly proportional to the voltage applied across the armature of the motor, the speed here is controlled by controlling the Armature voltage.

Speed is directly proportional to Armature voltage which is directly proportional to the triggering pulse duty cycle [2].

2.2 Forward motoring.

The switches T1 and T2 are triggered to achieve forward motion, in this the armature current flows from source→switch T1→load (armatures) → Switch T2 and back to the source providing forward propulsion [2].

2.3 Reverse motoring.

The switches T3 and T4 are triggered to achieve reverse motoring, in this the armature current flows from source→ switch T3→ load (armatures) → Switch T4 and back to the source, as we can see the direction of flow of current completely reverses which provides reverse propulsion [2].

2.4 Triggering circuit.

The triggering pulses are generated using Pulse width modulation technique where a simple comparator is used.

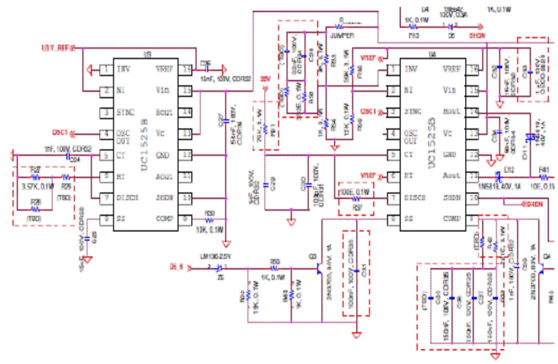

Fig. 2 : Triggering circuit.

The above circuit is which is been employed in this project to understand the concept [3] we will consider simpler figures and graphs which are shown below.

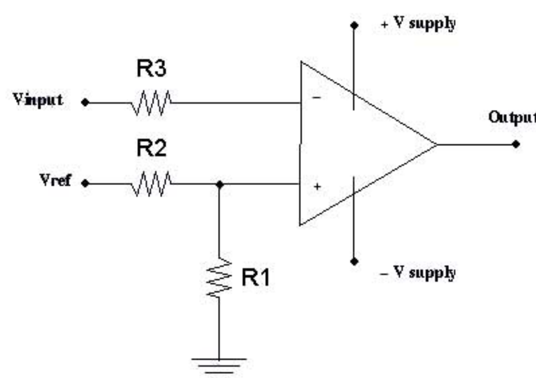

Fig. 3 : Basic comparator circuit.

The two inputs to be given to a comparator circuit are the reference voltage and repetitive waveform respectively. The comparator compares the two inputs and gives the pulses accordingly as the output. These pulses are given to the gate of the switches in the converter circuitry [2] [3].

2.4.1 Variation in duty cycle.

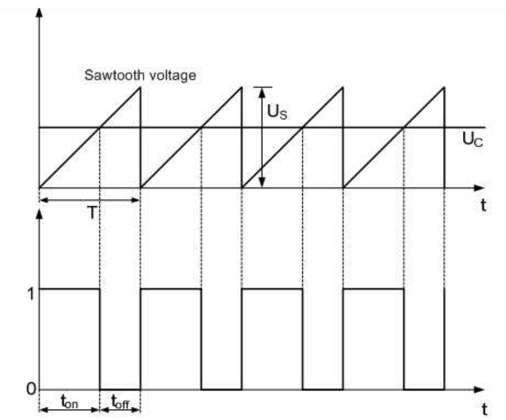

Fig. 4 : PWM Technique waveforms

The reference voltage Uc is given to the comparator from the potentiometer here a potentio-accelarator is used, this is compared with the repetitive saw tooth waveform, and depending upon the magnitude of the Reference voltage the pulse width varies which is shown in the above figure.

In this project the pedal force is directly proportional to the magnitude of the reference voltage and this is proportional to the pulse width obtained from the comparator output, this in turn decides the magnitude of the armature voltage which is solely responsible for the speed of the motors [2].

III. SELECTION OF CIRCUIT COMPONENTS AND ITS RATINGS.

3.1 Motor Ratings.

3 HP, 1500 rpm, 180V, DC compound motor [6] [7].

Fig 5. Eltek DC compound motor used.

3.2 Building of bridge Circuit.

As the peak current of Armature is 15A, the total of four motors becomes 60A [6]. Hence selection of switches to be done in a manner where if we go for current controlled switches it should be six times the rating of the load and if we go for the voltage controlled switches it should be somewhere around twice the rating of the load current. Since I am using a MOSFET, The current rating is twice the rated load voltage; therefore the following switch was selected.

Four MOSFETs (Irfp4242pbf) used in construction of the Bridge circuit [4].

3.2.1 MOSFET Ratings.

MOSFET (irfp4242pbf), N-channel, 300V, 130A [4].

3.3 Building of Triggering Circuit.

As the gate pulse of 12V is required to trigger the MOSFET, I had to select a PWM controller IC which can support this voltage.

The triggering circuit built up of two PWM controllers IC is shown in fig 2 [3].

3.3.1 PWM controller IC Ratings.

UC1525B, 8 to 35V Operation, 100Hz to 500 kHz Oscillator Range [3].

3.4 Power Source.

Each motor consume 15A of current while running at full speed condition, At present a battery source of minimum 180V,150AH is required for operation for minimum of five hours. Therefore the following Batteries are selected [8] [9].

50 Batteries of 12V, 17Ah used in series and parallel combinations making it up as an entire battery pack is constructed [10].

IV. MECHANICAL DESIGN.

A Maruthi 800 Chassis is used in the construction of this car. Every car has a system of drive shafts or Differentials to power either the front or the Back wheels of the car. In this project the engine, Gear box is completely removed leaving the car with steering column, Tires with the drive shaft, and the Chassis.

4.1 Front wheel drive shaft connection.

For the front wheels the drive shaft is connected directly to the motor, the image of the front drive shaft is shown below in the following figure.

Fig 6. Front wheel Drive Shaft.

4.1 Back wheel drive shaft connection.

To the back wheel the connection is made to the motors using the drive shaft fabricated separately and connected as shown in the following figures.

Fig 7. Back wheel Drive Shaft.

Fig 8. Back wheel drive shaft connected to the motor.

The Joint which is clearly seen in the shaft is connected to the shock absorbers directly. Once these connections to the wheels are made they are controlled as per the earlier description of the control schemes.

V. COMPARISON OF THIS CAR WITH REVA ELECTRIC CAR

5.1 Specifications of Reva Electric car.

Motor: High torque (52 Nm), AC Induction motor, 3 phase 13 kW peak.

Controller: 350A microprocessor based with regenerative braking.

Charger: 220 V, 2.2 kW, high Frequency switch mode type (optional 100-120V).

EMS: Microprocessor-based battery management system.

Power Pack: 48 V, 200 Amp-hr, EV lead acid batteries [13].

5.2 Specifications of My Electric car.

Motor: 4, 2.2KW, 1500 rpm, DC Compound motor.

Controller: PWM Controller IC based dc-dc converter.

Charger: 220V, Direct charging system.

EMS: Efficient regeneration while in motion and in deceleration.

Power Pack: 180 V, 150 Amp-hr, EV lead acid battery pack.

VI. CONCLUSION

This particular design has various advantages over its mechanical and electrical counter parts as a mean of transport which first and foremost is eco-friendly, Noise free, Highly efficient, Range of travel per charge is more, It can almost cope up with the initial pick up and speed when compared with low power mechanical cars, power which is developed is directly given to the wheels, At low battery stage power any two of the motors can be used as generators. The only Disadvantage is that as a service the brushes of the motors should be replaced once a year and this particular design is being implemented in a family car for daily travel, we can carry forward this design into Go kart racing cars, SUVs, and Mini trucks.

VII. ACKNOWLEDGEMENTS

I would like to thank my department and my college for all the support they gave to build this car, And I must thank my supportive guide Mrs. Sunanda, Assistant Professor, Electrical Department for giving me complete freedom for doing my project and also would like to thank my mentor Mr. Dinesh, Assistant Professor, Electrical Department for being there for me as moral support through out the course.

REFERENCES

Books:

[1] B.L Theraja, A.K Theraja, A textbook of electrical technology, Volume 2 (S.Chand & company ltd, 2006).

[2] Ned Mohan, Tore M. Undeland, William P. Robbins, Power Electronics - Converters, Application and Design (Wiley-India, 2007).

Datasheets:

[3] UC1525B PWM controller IC datasheet.

[4] IRFP4242PBF MOSFET Datasheet.

[5] Guide for users of VSD’s (Variable speed drives) by ABB.

Websites:

[6] www.eltekindia.com.

[7] www.gemotors.com.

[8] www.exideindia.com.

[9] www.amaron.in.

[10] www.electronics.howstuffswork.com/battery.htm.

[11] www.auto.howstuffswork.com/electric-car.htm.

[12] http://green.autoblog.com/2009/07/16/greenlings-whats-the-difference-between-ac-and-dc-which-is-be/.

[13] www.mahindrareva.com

Robot Automation Framework: A Brief Survey

Lakshman Priyatham Rallapally

Masters in Engineering (CS), Research & Development Engineer
Nokia Siemens Networks India Private Ltd., Bangalore, India

Abstract - Quality Assurance is immensely important in Software Projects with the three critical parameters time, cost & resources. Organizations are facing key challenges of improving quality and reducing time to market with limited resources. Here comes the concept of Test Automation. Test Automation in today's competitive environment is much needed than desired to keep operating efficiently and considerably cut down costs and efforts, without compromising on quality and security. To ensure maximum repeatability a framework is important. The paper gives a brief survey on Robot Automation Framework which is a Keyword driven scripting testing technique for quality assurance.

Keywords - *Robot Framework, Python, Keyword-Driven Scripting, Acceptance Testing, Libraries*

I. INTRODUCTION

Testing is a critical role in application development and maintenance. The high degree of customer interaction and increased competency of the systems magnifies the risk of failures with the software applications. Executing the test cases manually could be mundane and time consuming. With every feature loaded to an application it is difficult to run the entire gamut of testing. Organizations look at test automation as the medicine for all the problems in improving the test effort and quality.

Test Automation is the conclusion of repeated functional process. The goal of Automation is to find regression defects sooner than later, reduces test life cycle, increases the overall productivity and reduces the overall cost of the application development. Automated results reports with more accurate interpretation of test execution. With the disadvantage of manual testing where additional resources are deployed to have the run sequentially, automation run help in better test path coverage. Finally automation aims in increasing the application reliability while reducing the time and cost of software quality. Automation could be good only when it supports test efforts involving automated test tools and effective utilization of the automated test tool.

A Test Automation Framework which ensures maximum reusability results in higher efficiency is a set of assumptions, concepts and tools that provide support for automated software testing. The Test case file can be updated if there is a change in test case file. Keyword Driven Scripting or Table Driven Scripting or Action Driven Scripting is one of the scripting technique used for automated testing that separates the test creation process. Robot Framework is a generic test automation framework for acceptance testing and the acceptance test driven environment.

The paper is organized as follows: Basics of Robot Framework in section II followed by Test Case Preparation & Execution in Section III, Libraries in Section IV, Logs & Reports in Section VI.

II. BASICS OF ROBOT FRAMEWORK

Robot Framework [1] is a Python-based keyword-driven test automation framework for acceptance level testing and acceptance test driven development (ATDD). It has an easy to- use tabular syntax for creating test cases. Robot testing capabilities can be extended by test libraries implemented either in Python or Java. Users can also create new keywords from existing ones using the same simple syntax that is used for creating test cases. Test case results are stored in XML or easily readable HTML files.

A. Features of Robot Framework

- Enables easy-to-use tabular syntax for creating test cases in a uniform way.
- Allows using keyword-driven, data-driven and behavior-driven (BDD) approaches.
- Provides ability to create reusable higher-level keywords from the existing keywords.
- Provides easy-to-read reports and logs in HTML format.

- The modular architecture supports creating tests even for applications with several diverse interfaces.
- Provides a simple library API for creating customized test libraries.
- Provides a command line interface and XML based outputs for integration into existing build infrastructure (continuous integration systems).
- Provides support for Selenium for web testing, Java GUI testing, running processes, Telnet, SSH.
- Remote library interface enables distributed testing

III. TEST CASES PREPERATION & EXECUTION

In Robot, test cases are written in a tabular format. They can be saved either in HTML or tab separated value (TSV) files. These files can be created in any HTML/TSV editor. For users' ease, there is also a Robot Framework IDE [2], which was specially developed to make test case editing simple. Let's presume, we have a simple web application that we need to test. A 'E-mail Login' test case is presented in Figure 1.All entries in the 'Action' column are keywords (functions/procedures). These keywords can be implemented inside the 'Keyword' table, using other user-defined keywords or a wide range of built-in functions. For more complex functionalities, it is possible to use Python or Java-based libraries. Some already exist (Operating System, Selenium, Telnet, SSH, and Swing libraries), and others are under development.

Implementing own keywords in Robot is very simple. All we need to do is to describe the actions with arguments in the 'keyword' table, as in the example in Table 2. Simple and intuitive syntax allows for rapid keyword development, even by testers without programming experience. 'Open Browser' and 'Title should be' are internal keywords from the Robot web-testing library using Selenium. We can have test cases which have a unique procedure, or test cases that are similar to each other, where the procedure is always the same and only the input data changes. Robot also supports this data-driven approach. All one needs to do is to define a keyword which will take the input data and prepare a table with test cases.

A. *Test case Organization*

There are several ways of managing test cases in Robot. Test cases are organized into test suites, which are sets of test cases, taken either from single or multiple files. The simplest example of a test suite is a single HTML file containing multiple test cases. Another key feature of Robot is test case tagging. Each tag (e.g. critical, nightly, time-consuming, quick) assigns a test case to a separate set. When executing, tests can be selected based on tags, like "critical & nightly". Those tags are also included in the execution statistics later.

B. *Execution of Testcases*

When the test cases are written and ready, they can be executed using provided Python scripts. Robot Framework is system and platform independent - test cases can be executed on any platform where Python is available: be it Windows, Linux, Unix or Mac. The execution of test cases can done in the following steps.

- ✓ gathering test cases, reading and setting variables.
- ✓ executing all actions for every test case
- ✓ providing global statistics (test cases passed/failed)
- ✓ writing the log in xml format
- ✓ generating report and log in html format

IV. LIBRARIES

These test libraries are automatically installed with Robot Framework. They are always available for use but they need to be imported in the test data, expect for the BuiltIn library which is also imported automatically.

A. *Internal Libraries*

- ✓ BuiltIn
- ✓ OperatingSystem
- ✓ Screenshot
- ✓ Telnet
- ✓ Collections
- ✓ String
- ✓ Dialogs
- ✓ Remote

B. *External Libraries*

The list of publicly available test libraries from Table 1 that can be used with Robot Framework but need to be installed separately.

V. LOGS AND REPORTS

Another strong point of Robot are logs and reports. They are presented in a very readable format in HTML files. Reading logs is very intuitive: they are presented in a tabular/tree format, where green/red colors are used to mark passed and failed. Reports give an overview of the test cases executed: their names, execution time, duration, and final result. Logs provide more information on the execution, including all the keywords. One can easily trace the execution flow, which makes logs a perfect help for debugging. After executing the test cases, Robot saves the log into an XML file. This XML file can later be converted into an HTML file or processed further according to the tester's needs.

a) Tested Application Interface

There are three main domains where Robot can be applied command-line, web and GUI testing. Other interfaces can be tested using self-developed libraries. For command line testing, we have two useful libraries: OperatingSystem and SSHLibrary. OperatingSystem allows us to execute system commands, manipulate files, check files, read/set environment and manage processes. SSHLibrary allows us to connect to a remote host, execute commands and transfer files. Using those two libraries, we can create a powerful set of keywords for testing our application through the command line, whether it is installed locally or on a remote host. The example below shows a simple test case using command-line ping. It would also be possible to create a keyword 'Host should respond to ping' and just use it with a certain hostname/ip in the test case.

b) Real Browsers

The second interface type is the web using real browsers. In this case, we have a Robot Selenium library [3], which is a wrapper around Selenium Web application testing system [4]. The Robot Selenium library contains keywords to open a web page in the browser, input text, click button, submit, etc. It contains a lot of testing functions, like 'Location should be', 'Page should contain text field', 'List selection should be' and many others. A sample keyword implemented using the Selenium library is presented in Table 2 - all presented web application tests are running with Selenium.

c) Graphical User Interface

The third interface supported by Robot Framework is GUI. Currently the Swing GUI library exists. It provides keywords such as 'Dialog should be open', 'Push button', 'Menu item should be selected', 'Start application', 'Get selected table cell value', 'Close window' and many others. Figure 8 presents a sample user keyword implemented using Swing library.

Other interfaces can also be tested - it is possible to access the application using native libraries or standard/non-standard protocols. In this case, a wrapper must be written in Python or Java that will make user-level functions accessible to Robot. The user guide contains such examples.

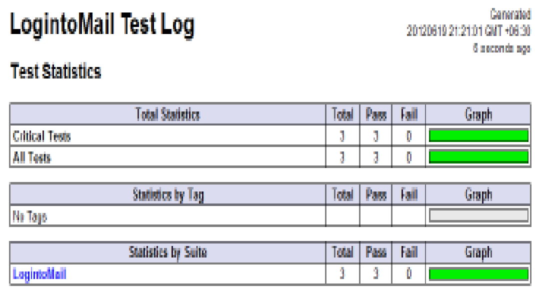

Fig. 1: Test Mail Statistics

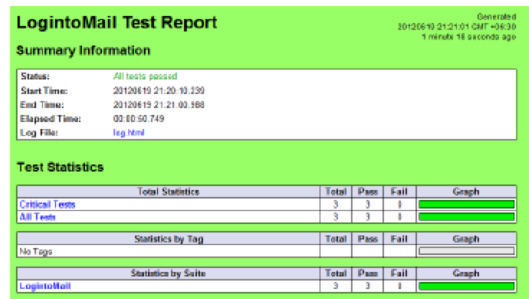

Fig. 2 : Test Case Report in Robot

VI. CONCLUSION

In this Paper a complete survey has been done on Robot Automation Framework which is very simple and easy-to-use, flexible, acceptance-level testing. It is system and platform independent and is extensible through Python and Java modules. Test cases can be written in a simple, tabular format, even by people without programming experience, using builtin or self-developed keywords. The logs and reports produced are easily readable and provide a perfect source for test case debugging. It is continuously developed and its base of keywords is growing.

TABLE I. EXTERNAL LIBRARIES

Library	Description
SeleniumLibrary	A web testing library that uses popular Selenium tool internally.
Selenium2Library	A drop in replacement for selenium Library using newer Selenium2WebDriverAPI
Waitr-robot	A web Testing Library that uses popular Watir tool via the remote library interface.
WatinLibrary	A web testing library that uses Watin tool (a .NET port of Watir) via the remote library interface.

SwingLibrary	A Swing GUI testing library
EclipseLibrary	A library for testing Eclipse RCP applications using SWT widgets.
AutoItLibrary	Windows GUI testing library that uses AutoIt freeware tool as a driver.
DatabaseLibrary (Java)	A test library that provides common functionality for testing database contents. Implemented using Java so works only with Jython.
DatabaseLibrary (Python)	Another library for database testing. Implemented with Python and works also on Jython.
SSHLibrary	A test library that enables SSH and SFTP.

TABLE II : USER KEYWORD IMPLEMENTATION

Keyword	**Action**	**Argument**
Open Login Page	Open Browser	www.mail.com
	Title Should be	Login Page

TABLE III : TESTCASE TABLE FOR LOGIN

Test Case	**Action**	**Argument**
E-mail Login	Open Login Page	
	Input Username	Demo
	Input Password	Mode
	Login	
	Welcome Mail	

REFERENCES

[1] http://robotframework.org: Robot Framework Main Page

[2] http://code.google.com/p/robotframework-ride - Robot Framework IDE

[3] http://robotframework-seleniumlibrary. googlecode.com - Robot Selenium Library

[4] http://selenium.openqa.org/ - Selenium Web Application Testing System.

◈◈◈

Facial Emotion Recognition from Video using SVM Classifier

Anand Rathod & Satyadhyan R Chickerur

Department of Information Science and Engineering, M S Ramaiah Institute of Technology, Bangalore, India

Abstract **-** Facial Expression analysis is one of the challenging problem in the field of Human Computer Interaction (HMI). The Facial Emotion Recognition (FER) system proposed in this paper consists of three stages: Face Detection, Feature Extraction and Emotion Recognition from Expression. The algorithm designed by Viola and Jones is used for face detection. Local Binary Pattern (LBP) is used for describing features from the expression. The classification of emotion is done by Support Vector Machine (SVM) classifier with RBF kernel function. The database used for training and testing contains the spontaneous emotions.

Keywords **-** *Expression recognition, Local binary patter, support vector machine, human computer interaction.*

I. INTRODUCTION

Facial expressions imply much information about human emotions and play an important role in human communications. The advancement in information technology, the wide spread use of Internet, mobile telephony and other inexpensive computer equipment has made human computer interaction (HCI) a usual activity in everyday life [1]. Mehrabian [2] conducted a psychological research, it shows that nonverbal part is most informative in social communication. The contribution of verbal part is about 7% of the message, vocal part is about 34% and facial expression contributes about 55%. This statistics shows that, face is a subject of study in many of science and technology The most expressive way humans display their emotional state is through facial expressions. Many applications, such as virtual reality, video-conferencing, synthetic face animation require efficient facial expression recognition in order to achieve the desired results. For examining the facial expressions psychologists were defined a set of six universal facial emotions including happiness, sadness, anger, disgust, fear, and surprise [3].

In this paper we propose new approach for facial emotion recognition which uses SVM classifier [4] for categorizing different emotions. SVMs gives good accuracy in classification even when we have modest amount of training database is available and SVM is the interactive approach for emotion recognition.

II. RELATED WORK

The three stages of facial emotion recognition are face detection, feature extraction and emotion recognition. For all these stages many people had proposed different approaches, however only major ones are explained in this paper. Zeng et al. [5] conducted a survey on comparison of all these related works.

In the stage of face detection the system will perform some image processing techniques on the input image in order to find face region. This technique is called face localization in image or tracking in videos. Huang and Huang [6] proposed a method which uses Point Distribution Model (PDM), it represents mean geometry of human face. Canny edge detector is applied in the beginning to find two symmetrical vertical edges which estimate the face position and then PDM is fitted. The methods used by Kimura and Yachida [7] processes input image with an integral projection algorithm to find position of eye and mouth corners by color and edge information. The position of eyes and mouth represents the Potential Net model from the face.

Based on how features are extracted from the input image, the facial emotion feature extraction can be categorized into three method such as- geometric-based, appearance-based, and hybrid-based approaches. In geometric based approach the face image is represented geometrically via fiducial points. The classification done by analyzing the distance between these fiducial points and facial component size. Pantic et al. [8] proposed a method for detecting facial actions by analyzing the bounded components of the face, which includes the eyes and the mouth. Geometric-based methods works well with all kind of skin patterns or dermatoglyphics. However this technique require accurate localization of fiducial points, this is difficult when the image contains complex background. In appearance-based methods the entire image is processed by applying a set of filters which extracts features from the face. Zhenet al.[9] used Gabor wavelets to represent changes in the appearance as a set of multi-scale and multi-orientation coefficients. This method works best with different people and illumination conditions. The recognition of emotions can be improved by combining features of appearance and geometric approaches. Zhang and Ji [10] proposed a multi-feature technique that is based on the detection of facial points, smile lines, and edges in the forehead area. In this method the extraction of feature is done by associating each Action Unit (AU) with a set of movements.

The last part is recognizing emotions, and this is based on machine learning theory, precisely this is known as classification task. There are many machine learning techniques for classification such as Artificial Neural Networks, Hidden Markov Models, Bayesian Networks, Support Vector Machines, K-Nearest Neighbors. Pantic and Rothkrantz [11] proposed the system with rule based classifier, which gives 89% accuracy to recognize 31 action units.

III. PROPOSED SYSTEM

Based on the study of different facial emotion recognition approaches we have divided the proposed into three stages : Face detection and tracking, Feature Extraction and emotion recognition (Fig.1).

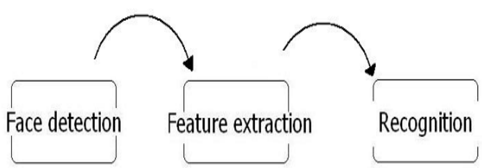

Fig.1 : Structure of FER system

This system operates both for static image and video. Static images are used for training and testing the database and interaction of the current system is designed only for video analysis.

A. Face detection and tracking

In the first part of this system is designing a module for detecting the face and localization of landmarks in the image. The algorithm used for face detection is based on work done by Viola and Jones [12]. In this approach a set of Haar-like features are generated from the input image. Possible types of features are two-, three- and four-rectangular features (Fig.2).

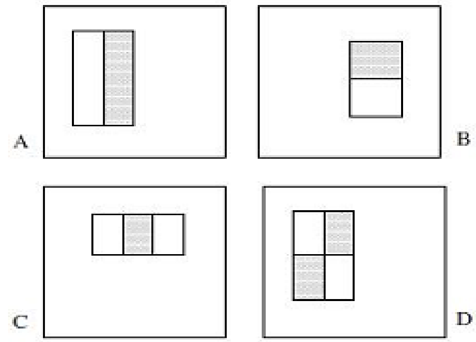

Fig. 2 : Haar-like feature

Rectangular features in the image needs to be trained using some classifier to decide if the image contains searched face or not. Adaboost algorithm was used for training when the number of features is much higher than the number of pixels in the original image. This algorithm is widely used in the area of face detection. However, this can be used to train for detecting any kind of object. Some steps are performed consecutively on the input image for face detection. The trained classifier searches for face in the image (Fig.3). If the face is not found in the image, further processing is omitted.

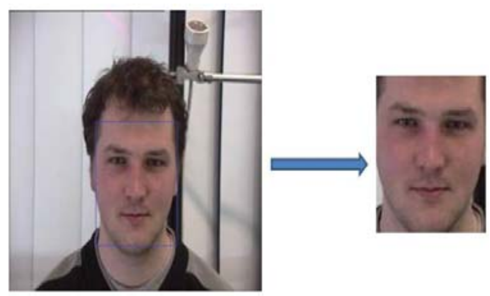

Fig. 3 : Face detection procedure

If the face is located, then upper part of the face is employed by the eye detection classifier. The left and right eyes are detected separately (Fig.4)

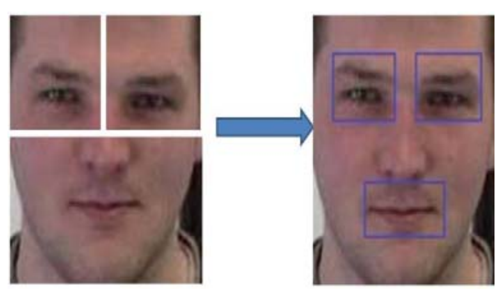

Fig. 4 : Face element localization

If the classifier finds more faces in the image then the algorithm takes the biggest one for processing.

B. Feature Extraction

In the proposed system Local Binary Patterns (LBP) are used for facial texture analysis. LBP were introduced by Olaja et al. [13] is an effective texture descriptor. Sliding window technique is used for transforming input image into LBP representation where value of each pixel in the neighborhood is thresholded with value of central pixel (Fig.5). Central pixel is encoded with LBP code (binary or decimal) in corresponding LBP image pixel.

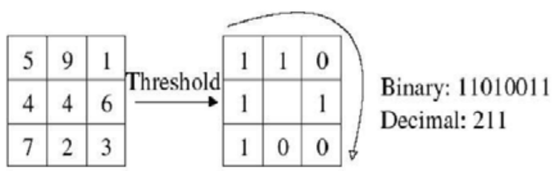

Fig.5 : LBP encoding

The two ways of encoding facial texture are holistic and analytic ways. Holistic way encodes whole face region with LBP features. This approach has a disadvantage, the spatial information about texture will get lost. In analytic approach the face region is divided into a grid of patches and then each of those patches are transformed to LBP histogram separately. This method may contain the patches which are not affected by emotion like hair or neck part. Because of this reason, in our system the LBP operator is applied only on two regions which are highly involved in face activity. Forehead-eyes area and chin-mouth-cheeks area (Fig.6) are involved much in face activity.

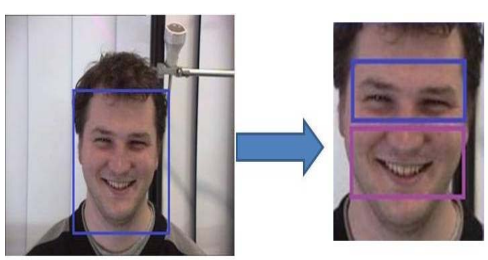

Fig. 6 : Regions involved in expressions analysis

The particular face region need to be normalized before we extract the features.

C. Emotion recognition

For this stage the classifier needs to be trained with a set of images with particular emotions displayed. For doing this we have obtained FG-NET Facial Expression and Emotion Database (FEED) [14] which consists of MPEG video files with spontaneous emotions recorded. The training set consists of 50,990 images of seven states including neutral and emotional (surprise, fear, disgust, sadness, happiness and anger).

In our system the Support Vector Machine with Radial Based Kernel Function is used as a classifier. The support Vector Machine is an adaptive machine learning system, it receives labeled training data and transforms it into higher dimensional feature space. The best separation between classes is determined by computing separating hyperplane with respect to margin maximization. The advantage of SVM is that it gives best results even if it is trained with small amount of database.

The work in this paper is still in progress. The system trained with FEED database gives the accuracy rate of 75% for recognizing the emotions. The emotions recognized are neutral, happiness and sadness, the future work will recognize other emotions surprise, fear, disgust, and anger. The emotion recognition results are also described in confusion matrix, which not only shows accuracy of emotion recognition, it also shows how a particular emotion can be confused with other. The confusion matrix can be obtained if all six emotions are recognized. The completed system will be tested in heterogeneous processing environment (in GPU) for performance improvement. The Table.1 shows the accuracy rate of each emotions in the current working system.

Emotion	**Rate of Accuracy (in %)**
Neutral	63
Happiness	79
Sadness	83

Table.1. Accuracy Rate

IV. CONCLUSION

The methods proposed in this paper is not only applicable to facial emotion recognition but also in hand gesture recognition, human action recognition and visual event analysis. This kind of applications can be used by psychologists to automate the manual face analysis. Even though the system cannot handle head rotations, head shifts are allowed. For future work we would like to improve the emotion recognition rate and efficiency by combining different algorithms. Increasing the number of training data may give the best accuracy rate and decrease confusion of one emotion with other.

REFERENCES

[1] George Votsis, Nikolaos Doulamis, Anastasios Doulais, NicolasTsapatsoulis and Steanos Kollias, "A Neural-Network-based Approach to

Adaptive Human Computer Interaction" Lecture Notes in Computer Science, Spinger-Verlang Press, Vol. 2130, pp. 1054-1059 2001.

[2] A. Mehrabian, "Communication without Words", Psychology Today, Vol. 2, No. 4, p. 53-56, 1968.

[3] P. Ekman and W. V. Friesen , Emotion in the Human Face . Englewood Cliffs, NJ: Prentice-Hall, 1975.

[4] Chih-Chung Chang and Chih-Jen Lin, LIBSVM : a library for support vector machines. ACM Transactions on Intelligent Systems and Technology, 2:27:1--27:27, 2011. Software available at http://www.csie.ntu.edu.tw/~cjlin/libsvm

[5] Z. Zeng, .M. Pantic, G. I. Roisman, T. S. Huang, "A Survey of Affect Recognition Methods: Audio,Visual, and Spontaneous Expressions", IEEE Transactions on Pattern Analysis and Machine Intelligence, Vol. 31, No. 1, 2009.

[6] C.L. Huang and Y.M. Huang, "Facial Expression Recognition Using Model-Based Feature Extraction and Action Parameters Classification," J. Visual Comm. and Image Representation, Vol. 8, No. 3, p. 278-290, 1997.

[7] S. Kimura and M. Yachida, "Facial Expression Recognition and Its Degree Estimation", Proc. Computer Vision and Pattern Recognition, p. 295-300, 1997.

[8] M. Pantic and L. J. M. Rothkrantz, “Facial action recognition for facial expression analysis from static face images,” IEEE Trans. SMC, Part B: Cybernetics, vol. 34, no. 3, pp. 1449–1461, 2004.

[9] W. Zhen and T. S. Huang, “Capturing subtle facial mo-tions in 3d face tracking,” in Proc. ICCV, 2003, pp.1343–1350.

[10] Y. Zhang and Q. Ji, “Active and dynamic information fusion for facial expression understanding from image sequences,” IEEE Trans. PAMI, vol. 27, no. 5, pp. 699–714, 2005.

[11] M.Pantic and L.Rothkrantz, "Expert System for Automatic Analysis of Facial Expression", Image and Vision Computing J.,Vol.18,No.11,p.881-905,2000.

[12] P. Viola and M. J. Jones, “Robust real-time object detection”, International Journal of Computer Vision, Vol. 57, No. 2, p.137–154,2004

[13] T. Ojala, M. Pietikainen, T. Maenpaa, “Multiresolution gray-scale and rotation invariant texture with local binary patterns”, IEEE Transactions on Pattern Analysis and Machine Intelligence Vol. 7, No. 7, p. 971-987, 2002.

[14] F. Wallhoff, "Facial Expressions and Emotion Database", Technische Universität München, 2006, http://www.mmk.ei.tum.de/~waf/fgnet/ feedtum.html.

◈◈◈

Extracting Maximum Power Optimization In Wind Turbine Using Neuro Fuzzy Logic Control

I. Arul[1], M. Karthikeyan[2], N. Krishnan[3] & K. Maniraj[4]

[1&3]Centre for Information Technology and Engineering, M.S University, Tirunelveli, India
[2]Department of ECE, Tamilnadu College of Engineering, Coimbatore, India
[4]Dept of CSC. M.S.P.V .L Polytechnic College Pavoorchatram, Tirunelveli Dist

Abstract **-** Wind energy has steadily established itself as one of the most reliable and affordable renewable energy resources. Of the country's wind energy generation capacity of around 14,000MW per year, TN accounts for 6,547MW. Tamil Nadu has an installed wind energy capacity of 6,696 MW, which is 41 per cent that of the country.

The paper presents an advanced prediction system that integrates models based on fuzzy-neural networks. The main objective of this paper is to fully control the wind turbine system with induction generator to maximize the power generation. The output power of a wind turbine is function of wind velocity cubed. The system has been optimized for operating around 15 m/s, and though the wind power continues to increase above this point.

The advanced method to introduce the new ability of estimating variable speed control . By using the controller, the speed can be tuned until it get similar to the desired output that user need. In this paper, neural networks are used in a novel way to solve the problem of tuning a fuzzy logic controller. The neuron fuzzy controller uses the neural network learning techniques to tune the membership function.

The aim is to ensure that by 2030, wind energy will be the most cost-efficient energy source on the market. However, with the growing demand for green electricity worldwide, rising turbine costs and increased competition to supply green electricity to the grid, wind farm operators must improve their existing power output. In India, the total installed capacity of wind power generation is 8754 MW in the year 2008.By the end of 2012, the total installed capacity is going to be reached to 12000 MW according to ministry of new and renewable energy, India and total installed capacity of wind energy is estimated to be more than 160 GW [WWEA] all around the world. The scopes include the simulation study, implementation of Neuron fuzzy logic controller to actual DC motor using MATLAB simulator.

I. INTRODUCTION

The aim of neuro- fuzzy controller is to establish maximum power delivery to the grid from available wind power. Nowadays doubly fed induction generator system are been used for controlling the excitation level and generator torque by which the speed of the induction generator is controlled according to the varies of the wind speed in order to control the maximum output power. Based on the simulation results, the effectiveness of the proposed neuro fuzzy controllers would be verified.

In this paper we present a neuro fuzzy controlled maximum power point tracking system suitable for the induction generator operating at variable speeds. The proposed system uses the generator speed and power output measurements to search for the optimum speed at which the turbine should operate for producing maximum power. The effectiveness of the proposed control scheme is validated through computer simulations under varying wind speeds.

Using neuro fuzzy control, we can produce controller outputs more reliable because the effect of other parameters such as noise and events due to wide range of control region and online changing of the controller parameters can be considered. More over without the need of a detailed mathematical model of the system and just using the knowledge of the total operation and behavior of system, tuning of parameters can be done more easily.

The aim of the project is to control the maximum wind generation system and maximum efficiency optimization approach. The wind generation system is highly non linear process since it is involved power electronic equipment. So non linear controller is necessary for controlling non-linear process. So we are using intelligent controller.

The combination of fuzzy system and neural network allows the increase computational efficiency of the software products. Neuro-fuzzy system combines the learning capabilities of neural networks with the linguistic rule interpretation of fuzzy inference systems. The synthesis of neuro-fuzzy inference system includes the generation of knowledge base rules that have IF-THEN form. Here, the problem is to find the optimal definition of the premise and consequent part of fuzzy IF-THEN rules through the training capability of neural networks, evaluating the error response of the system. In the paper neuro-fuzzy structure is applied to solve electricity consumption prediction problem.

1.1. Neuro Fuzzy Controller

A block diagram of the neuro fuzzy-controlled wind-powered generating system is shown in Fig. 1. It is assumed that the turbine blades have a fixed pitch angle; A field-oriented control scheme is used to regulate the generator speed to the optimum value at which maximum power is obtained. The proposed fuzzy controller generates the optimum speed command, which is used to regulate the input current of the AC to DC converter. The output of the converter is inverted back to a constant frequency, constant voltage to supply AC loads.

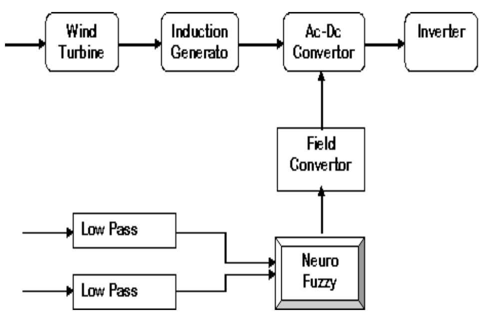

Fig. 1.1 Neuro Fuzzy Controller

1.2 Pitch Control

To produce a maximum energy, the blade angle must be tuned with wind straightforward using pitch angle control of wind turbine blades. It is worth noticing that we can use this characteristic in abnormal conditions such as grid faults to protect generator from over speeding. In two different cases, an increasing rotor speed may be occurred; a wind speed as input power and an abnormal case due to a fault existence. These must be distinguished first, before a control takes place. When the output terminal voltage falls under 0.9 p.u and the rotor speed is increased, it means a fault is happened.

Linearized system equations

If the system equations are linear (or have been linearized), the techniques of linear system analysis are used to study dynamic behavior. The most common method is to simulate each component by its transfer function. The various transfer function blocks are connected to represent the system under study. The system performance may then be analyzed by such methods as root-locus plots, frequency domain analysis (Nyquist criteria), and Routh's criterion.

Stability characteristics may be determined by examining the eigenvalues *o(* the A matrix, where A is defined by the equation

$$x. = Ax + Bu \qquad (1)$$

Where x is an *n* vector denoting the states of the system and A is a coefficient matrix. The system inputs are represented by the *r* vector u, and these inputs are related mathematically to differential equations by an *n* x *r* matrix B.

Large system with nonlinear equations

The system equations for a transient stability study are usually nonlinear. Here the system is described by a large set of coupled nonlinear differential equations of the form

$$x = f(x,u,/) \qquad (2)$$

where f is an *n* vector of nonlinear functions.

ANFIS structure for blade pitch angle control of VSWPGS is given in Figure below.

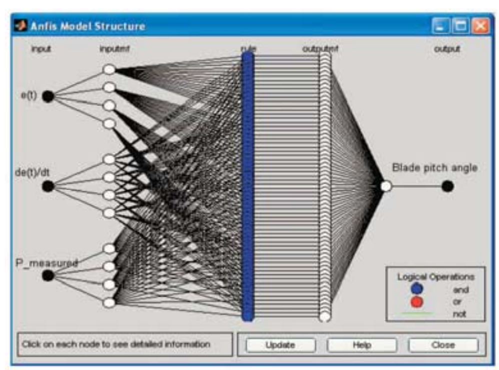

Fig. 1.2 : ANFIS

1.3 Doubly fed Induction Generator

A doubly fed induction generator is coupled to the grid through power electronic converter connected between the rotor windings of DFIG and the grid. The voltage drop at the terminals will result in large, oscillatory currents in the stator winding of DFIG. Because of magnetic coupling between stator and rotor winding, these currents will also flow through the converter and high current can cause its thermal breakdown.

During a fault, the rotor winding are short circuited by a set of resistors. The short circuit current will flow through this crow bar instead of the converter. This paper analyzes the behavior of a crow bar protected DFIG. Based upon this, approximate equations are derived that can be used to determine the short circuit current contribution of the turbine.

To construct a variable speed constant frequency system, an induction generator is considered attractive due to its flexible rotor speed characteristic with respect to the constant stator frequency. One solution to expand the speed range and reduce the slip power losses simultaneously is to doubly excite the stator and rotor windings. The power converters in the rotor circuit regenerate the majority of the slip power.

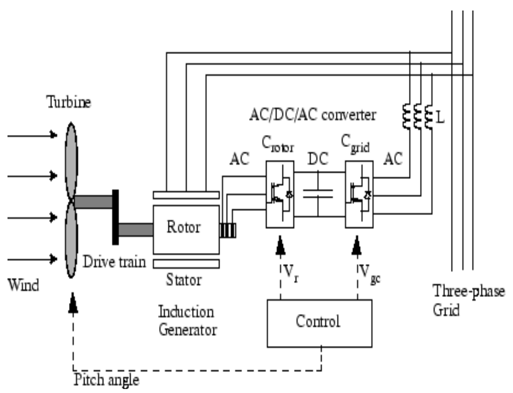

Fig.1.3: Doubly Fed Induction Generator In A Wind Turbine.

II. BACK PROPAGATION LEARNING ALGORITHM

Based on this algorithm, the networks learns a distributed associative map between the input and output layers. What makes this algorithm different than the others is the process by which the weights are calculated during the learning phase of the network. In general, difficulty with multilayer perceptions is calculating the weights of the hidden layers in an efficient way that results in the least (or zero) output error; the more hidden layers there are; the more difficult it becomes. To update the weights, one must calculate an error. At the output layer this error is easily measured; this is the difference between the actual and desired (target) outputs. At the hidden layers however, there is no direct observation of the error, hence some other technique must be used to calculate error, as this is the ultimate goal.

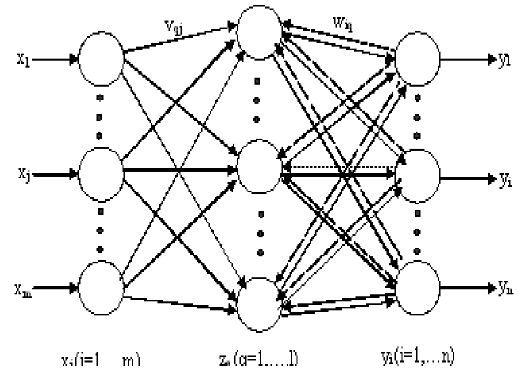

Fig. 2.1: Neuro-model

The basis for this weight update algorithm is simply the gradient – descent method as used for simple perceptrons with differentiable units. For a given input – output pair ($x_{k'}$, $d_{k'}$) the back – propagation algorithm performs two phase of data flow. First, the input pattern a_x' is propagated from the input layer to the output layer and, as a result of this forward flow of data, it produces an actual output y_k.

III. PROPOSED SIMULATION MODEL OF WIND TURBINE

In this wind power production system, variations in frequency, output voltage and drawn power curves of the system are obtained individually by means of the simulation study without any controller element. Different power demands of consumers are expressed as 120 kW, 150 and 180 kW. The controller element (PID controller and ANFIS) is put into operation depending on variations in electrical magnitudes of the wind power production system in such loading situations. Amplitude of the voltage obtained from the system must be within permitted limits whatever the electric energy production system is used. It is known that frequency of the system in other important magnitude is 50Hz in Turkey operating conditions. The system frequency in electric energy production stations is tried to be kept in 50Hz value. To obtain high quality power, the magnitude values of frequency and voltage must be kept in the desired range. The quality of obtained power may be brought to desired level by decreasing the undesired harmonic currents and voltages to minimum level. By considering the situation the wind power production system will operate with the network, the frequency and voltage value is adjusted according to the frequency and voltage values of the network.

Induction Generator

A 3-phase squirrel cage induction generator with a nominal power of 1.66MVA, 575V (φ-φ), 60 HZ is used for the above system with the parameters shown in Table 1.

Parameter	Unit
Stator Resistance	R1 0.004843 pu
Stator Leakage inductance	L1 0.1248 pu
Magnetizing Inductance	Lm 6.7 pu
Rotor inductance ref to Stator	L'2 0.1791 pu
Rotor Resistance ref to Stator	R'2 0.004347 pu

Table: 3.1 Parameter For Induction Generator

IV. EXPERIMENTAL SETUP AND RESULTS

4.1. Wind And Wind Turbine Model

This block implements a variable pitch wind turbine model. The performance co-efficient Cp of the turbine is the mechanical output power of the turbine divided with power and a function of wind speed, rotational speed and pitch angle. Cp reaches the maximum value of zero beta. The output is the torque applied to the generator shaft in per unit of the generator ratings. The turbine inertia must be added to the generator inertia.

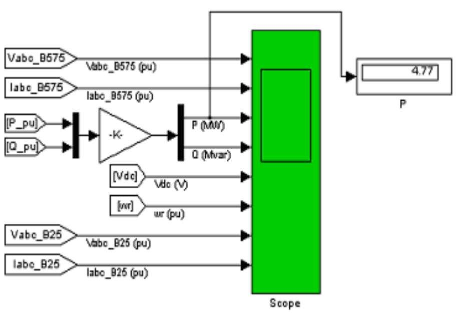

Fig. 4.1: Wind Turbine Model.

In the block diagram of the wind power production system given in Figure 4.1, the output of the wind speed model is defined as the kinetic energy or speed of wind. The wind speed is converted to mechanic power or moment by the wind turbine model. The obtained mechanic power or moment is the first input of the mechanic system (of drive system). The other second input of the mechanic system is the proportional speed of the asynchronous generator. Inputs of the asynchronous generator are: mechanical energy obtained from the wind turbine, voltage and frequency magnitudes at ends of the network or load. Outputs of the asynchronous generator are the active and reactive power values required for the network or load. In the wind power production systems that operate in isolated manner from electric networks, voltage and frequency of the asynchronous generator can be expressed as output magnitudes.

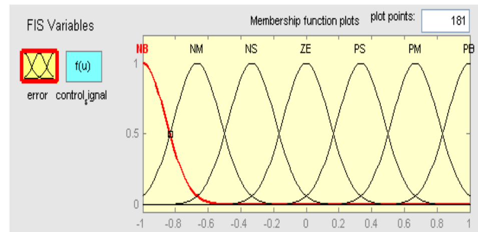

Fig. 4.2 : Membership Function

Parameter		Unit
Stator Resistance	R1	0.0045 Ω
Stator Leakage Reactance	X1	0.0513 Ω
Magnetizing Reactance	Xh	2.2633 Ω
Rotor Reactance(referred to Stator)	X'2	0.066 Ω
Rotor Resistance(referred to Stator)	R'	20.004 Ω
Magnetizing Resistance	Rfe	83.3 Ω

Table 2. Induction generator parameter

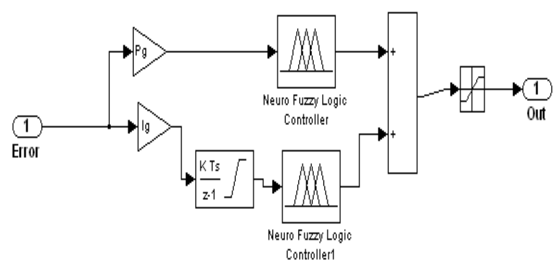

Fig.4.3: Neuro Fuzzy Architectural Design

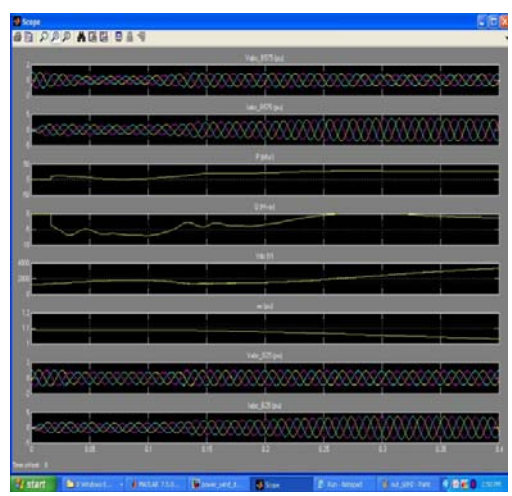

Fig. 4.4: Measured Current & Voltage in Matlab simulation

V. CONCLUSION

In this work, a neuro fuzzy control scheme for extracting maximum power from a variable speed wind turbine has been presented. It has been shown that the turbine power output depends nonlinearly on its angular speed and the wind speed. Neuro-Fuzzy control is well suited for searching the optimum speed at which the turbine should operate under varying wind conditions. The performance of the proposed scheme has been simulated under abrupt changes in wind. It has been shown that the Neuro-fuzzy controller adjusts the angular speed so that the turbine power coefficient converges to its maximum value in the steady state. The methodology used was simple and show step by step all the adjustments and calculations necessary for a satisfactory operation of the system.

For terminal voltage and frequency control of the variable speed wind power generation system, ANFIS is designed and is used in simulation block diagram of VSWPGS under the Matlab/Simulink program. To obtainin high quality power from the wind power generation system (VSWPGS), the effective value of output voltage must be at 400 volt and frequency in 50 Hz operational limit values. For this purpose, power limitation or speed control of the variable speed wind turbine is performed by means of controlling of turbine blade pitch angle. For controlling of blade pitch angle, the conventional PID controller and ANFIS are used separately.

As a result of controlling of the wind turbine blade pitch angle, it is determined from the simulation results that the output electrical magnitudes of VSWPGS (voltage, current, frequency and power) reach to desirable values within 1.5 seconds. When the simulation results are examined, it is observed that continuous situation error is close to zero in continuous operation. However, as the load of consumers fed from VSWPGS differs in every hour of a day, coefficients of the conventional PID controller must be readjusted depending on changing load situations. For this reason, in case of changing consumer load situations, the turbine blade pitch angle is adaptively adjusted to keep the terminal voltage and frequency within permitted tolerance values.

When simulation curves of electrical output magnitudes obtained as a result of controlling of blade pitch angle of VSWPGS with ANFIS are examined, it is seen that operational performance of the system is within a very good value. Meanwhile, no problem about compatibility of ANFIS with VSWPGS has been experienced.

REFERENCES

[1] B.Chitti Babu , K.B.Mohanty “Doubly-Fed Induction Generator for Variable Speed Wind Energy Conversion Systems- Modeling & Simulation “International Journal of Computer and Electrical Engineering,February, 2010.

[2] Quincy Wang, and Liuchen Chang, “An Intelligent Maximum Power Extraction Algorithm for Inverter-Based Variable Speed Wind Turbine Systems” IEEE Transactions On Power Electronics, September 2004.

[3] Whei-Min Lin, Chih-Ming Hong, and Chiung-Hsing Chen “Neural-Network-Based MPPT Control of a Stand-Alone Hybrid Power Generation System” IEEE Transactions On Power Electronics, December 2011.

[4] Pengwei Sun, Chuang Liu, Jih-Sheng Lai, Fellow, IEEE, and Chien-Liang Chen, “Grid-Tie Control of Cascade Dual-Buck Inverter With Wide-Range Power Flow Capability for Renewable Energy Applications” IEEE Transactions On Power Electronics, April 2012.

[5] Shuhui Li, Senior Member, IEEE, Timothy A. Haskew, Senior Member, IEEE, Richard P. Swatloski, and William Gathings “Optimal and Direct-Current Vector Control of Direct-Driven PMSG Wind Turbines “IEEE Transactions On Power Electronics, May 2012.

[6] Yu-Lin Juan, Member, IEEE “An Integrated-Controlled AC/DC Interface for Microscale Wind Power Generation Systems” IEEE Transactions On Power Electronics, May 2011.

[7] Xibo Yuan, Fei (Fred) Wang, Dushan Boroyevich, Fellow, Yongdong Li and Rolando Burgos, Member, IEEE “DC-link Voltage Control of a Full Power Converter for Wind Generator Operating in Weak-Grid Systems” IEEE Transactions On Power Electronics, September 2009.

[8] Wei Qiao, Wei Zhou, José M. Aller, and Ronald G. Harley, Fellow, IEEE “Wind Speed Estimation Based Sensorless Output Maximization Control for a Wind Turbine Driving a DFIG” IEEE transactions on power electronics, may 2008.

[9] Yuanye Xia, Khaled H. Ahmed, and Barry W. Williams “A New Maximum Power Point Tracking Technique for Permanent Magnet Synchronous Generator Based Wind Energy Conversion System” IEEE transactions on power Electronics, vol. 26, no. 12, december 2011.

[10] Kostyantyn Protsenko and Dewei Xu "Modeling and Control of Brushless Doubly-Fed Induction Generators in Wind Energy Applications" Department of Electrical and Computer Engineering Ryerson University, canada.

[11] Jon Are Suul, Marta Molinas, Member, IEEE, and Tore Undeland, Fellow, IEEE "STATCOM-Based Indirect Torque Control of Induction Machines During Voltage Recovery After Grid Faults" IEEE Transactions On Power Electronics, Vol. 25, No. 5, May 2010.

[12] Hans Øverseth Røstøen ,Tore M. Undeland,Terje Gjengedal "Doubly Fed Induction Generator In A Wind Turbine" Norwegian University of Science and Technology.

[13] D.Aouzellag , K.Ghedamsi, E.M.Berkouk " Power Control of a Variable Speed Wind Turbine Driving an DFIG" Electrical engineering Department, A.Mira University, Bejaïa, Algeria.

[14] Y¨uksel O˘GUZ1, ˙Irfan GUNEY2 "Adaptive neuro-fuzzy inference system to improve the power quality of variable-speed wind power generation system" Turk J Elec Eng & Comp Sci, Vol.18, No.4, 2010, _c TU¨BI˙TAK.

[15] Evgenije Adzic*, Zoran Ivanovic*, Milan Adzic**, Vladimir Katic "Maximum Power Search in Wind Turbine Based on Fuzzy Logic Control" Acta Polytechnica Hungarica Vol. 6, No. 1, 2009.

[16] Marcelo Godoy Sim˜oes, Member, IEEE, Bimal K. Bose, Life Fellow, IEEE, and Ronald J. Spiegel, Member, IEEE, "Design and Performance Evaluation of a Fuzzy-Logic-Based Variable-Speed Wind Generation System" , Ieee Transactions On Industry Applications, Vol. 33, No. 4, July/August 1997.

◈◈◈